HOST UNIVERSITY: Universitat Politècnica de Catalunya

FACULTY: Barcelona East School of Engineering

DEPARTMENT: Department of Chemical Engineering

Academic Year 2022-2023

Exploring the Feasibility of Using Fire Dynamics Simulator to Improve the Calculation of the Wildfire Available Safe Egress Time

Alfred El Haddad

Supervisors: Eulalia Planas, Enrico Ronchi

Master thesis submitted in the Erasmus+ Study Programme

International Master of Science in Fire Safety Engineering

Exploring the Feasibility of Using Fire Dynamics Simulator to Improve the Calculation of the Wildfire Available Safe Egress Time

Alfred El Haddad

Fire Safety Engineering
Lund University
Sweden

Report 5693, Lund 2023

Master Thesis in Fire Safety Engineering

Exploring the Feasibility of Using Fire Dynamics Simulator to Improve the Calculation of the Wildfire Available Safe Egress Time (WASET)

Alfred El Haddad

Report 5693
ISRN: LUTVDG/TVBB—5693--SE

Number of pages: 87
Illustrations: 37

Keywords
Wildfire, Trigger buffer, WUI, WASET, FDS, QGIS, Level set, WUI evacuation.

Abstract
Wildland-Urban Interface (WUI) fires pose a significant threat to public safety and property in areas where urban development encroaches upon natural landscapes. This thesis aims to investigate the effect of smoke from a WUI fire on the tenability conditions of a small village and to establish a worst-case-scenario trigger boundary around it as an improved basis for the WUI available safe egress time (WASET). To determine the maximum rate of fire spread and heat release rate, large-scale simulations were conducted using the level set model in Fire Dynamics Simulator (FDS). The results were coupled with corresponding higher resolution small-scale simulations run with the physics-based model in FDS, where a static fire was simulated at varying distances from the village and the conditions within the village were checked to determine a proper limit-perimeter. The findings of this study show that the minimum limiting distance at which the trigger boundary should be is 200 meters from the village as the temperature can reach over 60 degrees Celsius at a smaller distance. The results provide a more robust approach to determine the fire front arrival distance in WUI areas and inform fire management and public safety strategies. However, the results have certain limitations, including the fact that the simulations were conducted on a single village, and further research is needed to determine the optimal limit-perimeter for other WUI areas. Overall, this study provides a valuable contribution to the field of WUI fire management, and its methodology can serve as an example for future research in this area.

Fire Safety Engineering
Lund University
P.O. Box 118
SE-221 00 Lund
Sweden

http://www.brand.lth.se

Telephone: +46 46 222 73 60

Exploring the Feasibility of Using Fire Dynamics Simulator to Improve the Calculation of the Wildfire Available Safe Egress Time

Alfred El Haddad[1*],
Supervisor: Prof. Eulalia Planas[2],
Secondary Supervisor: Prof. Enrico Ronchi[3]

[1]Study Program: International Master of Science in Fire Safety Engineering (IMFSE)
[2]Centre d'Estudis del Risc Tecnològic (CERTEC), Universitat Politècnica de Catalunya, Campus Diagonal-Besòs, Av. Eduard Maristany, 16, Catalonia, 08019 Barcelona, Spain
[3]Lund University, Division of Fire Safety Engineering, Lund, Sweden

[*]**Alfred El Haddad.** *E-mail address:* haddadalfred7@hotmail.com

Disclamer

This thesis is submitted in partial fulfillment of the requirements for the degree of The International Master of Science in Fire Safety Engineering (IMFSE). This thesis has never been submitted for any degree or examination to any other University/program. The author(s) declare(s) that this thesis is original work except where stated. This declaration constitutes an assertion that full and accurate references and citations have been included for all material, directly included and indirectly contributing to the thesis. The author(s) gives (give) permission to make this master thesis available for consultation and to copy parts of this master thesis for personal use. In the case of any other use, the limitations of the copyright have to be respected, in particular with regard to the obligation to state expressly the source when quoting results from this master thesis. The thesis supervisor must be informed when data or results are used.

Read and approved,
Alfred El Haddad
May 29, 2023

Abstract

Wildland-Urban Interface (WUI) fires pose a significant threat to public safety and property in areas where urban development encroaches upon natural landscapes. This thesis aims to investigate the effect of smoke from a WUI fire on the tenability conditions of a small village and to establish a worst-case-scenario trigger boundary around it as an improved basis for the WUI available safe egress time (WASET). To determine the maximum rate of fire spread and heat release rate, large-scale simulations were conducted using the level set model in Fire Dynamics Simulator (FDS). The results were coupled with corresponding higher resolution small-scale simulations run with the physics-based model in FDS, where a static fire was simulated at varying distances from the village and the conditions within the village were checked to determine a proper limit-perimeter. The findings of this study show that the minimum limiting distance at which the trigger boundary should be is 200 meters from the village as the temperature can reach over 60 degrees Celsius at a smaller distance. The results provide a more robust approach to determine the fire front arrival distance in WUI areas and inform fire management and public safety strategies. However, the results have certain limitations, including the fact that the simulations were conducted on a single village, and further research is needed to determine the optimal limit-perimeter for other WUI areas. Overall, this study provides a valuable contribution to the field of WUI fire management, and its methodology can serve as an example for future research in this area.

Keywords: *Wildfire; Trigger buffer; WUI; WASET; FDS; QGIS; Level set; WUI evacuation*

نبذة مختصرة

تشكل حرائق Wildland-Urban Interface (WUI) تهديدًا كبيرًا للسلامة العامة والممتلكات في المناطق التي تتعدى فيها التنمية الحضرية على المناظر الطبيعية. تهدف هذه الأطروحة إلى التحقيق في تأثير الدخان الناتج عن حريق WUI على شروط الاستمرارية لقرية صغيرة وإنشاء حدود إطلاق سيناريو أسوأ حالة حولها كأساس محسّن لوقت الخروج الآمن المتاح لـ WUI (WASET) . لتحديد الحد الأقصى لمعدل انتشار النار ومعدل إطلاق الحرارة ، أجريت عمليات محاكاة على نطاق واسع باستخدام نموذج مجموعة المستوى في Fire Dynamics Simulator (FDS) . اقترن النتائج بمحاكاة صغيرة الحجم ذات دقة أعلى تم تشغيلها مع النموذج القائم على الفيزياء في FDS ، حيث تمت محاكاة حريق ثابت على مسافات متفاوتة من القرية وتم فحص الظروف داخل القرية لتحديد محيط حد مناسب. تظهر نتائج هذه الدراسة أن الحد الأدنى للمسافة المحددة التي يجب أن تكون عندها حدود الزناد هي ٢٠٠ متر من القرية حيث يمكن أن تصل درجة الحرارة إلى أكثر من ٦٠ درجة مئوية على مسافة أصغر. توفر النتائج نهجًا أكثر قوة لتحديد مسافة الوصول الأمامية للحريق في مناطق WUI وإبلاغ إدارة الحرائق واستراتيجيات السلامة العامة. ومع ذلك ، فإن النتائج لها قيود معينة ، بما في ذلك حقيقة أن عمليات المحاكاة أجريت على قرية واحدة ، وهناك حاجة إلى مزيد من البحث لتحديد محيط الحد الأمثل لمناطق WUI الأخرى. بشكل عام ، تقدم هذه الدراسة مساهمة قيمة في مجال إدارة حرائق WUI ، ويمكن أن تكون منهجيتها بمثابة مثال للبحث المستقبلي في هذا المجال.

Resumen

Los incendios de la interfaz urbano-forestal (WUI, por sus siglas en inglés) representan una amenaza significativa para la seguridad pública y la propiedad en áreas donde el desarrollo urbano invade los paisajes naturales. Esta tesis tiene como objetivo investigar el efecto del humo de un incendio de WUI en las condiciones de sustentabilidad de una pequeña aldea y establecer un límite de activación del peor de los casos a su alrededor como una base mejorada para el tiempo de salida seguro disponible de WUI (WASET). Para determinar la tasa máxima de propagación del fuego y la tasa de liberación de calor, se realizaron simulaciones a gran escala utilizando el modelo de nivel establecido en Fire Dynamics Simulator (FDS). Los resultados se combinaron con las correspondientes simulaciones a pequeña escala de mayor resolución ejecutadas con el modelo basado en la física en FDS, donde se simuló un incendio estático a diferentes distancias de la aldea y se verificaron las condiciones dentro de la aldea para determinar un perímetro límite adecuado. Los hallazgos de este estudio muestran que la distancia límite mínima a la que debe estar el límite de activación es de 200 metros desde la aldea, ya que la temperatura puede alcanzar más de 60 grados centígrados a una distancia más pequeña. Los resultados proporcionan un enfoque más sólido para determinar la distancia de llegada del frente de incendios en las áreas de WUI e informar las estrategias de gestión de incendios y seguridad pública. Sin embargo, los resultados tienen ciertas limitaciones, incluido el hecho de que las simulaciones se realizaron en un solo pueblo, y se necesita más investigación para determinar el perímetro límite óptimo para otras áreas de WUI. En general, este estudio brinda una valiosa contribución al campo de la gestión de incendios de WUI, y su metodología puede servir como ejemplo para futuras investigaciones en esta área.

Resum

Els incendis Wildland-Urban Interface (WUI) representen una amenaça important per a la seguretat pública i la propietat a les zones on el desenvolupament urbà envaeix els paisatges naturals. Aquesta tesi té com a objectiu investigar l'efecte del fum d'un incendi de WUI en les condicions de sostenibilitat d'un petit poble i establir un límit d'activació del pitjor escenari al seu voltant com a base millorada per al temps de sortida segur disponible de WUI (WASET). Per determinar la velocitat màxima de propagació del foc i la velocitat d'alliberament de calor, es van realitzar simulacions a gran escala utilitzant el model de nivell del Fire Dynamics Simulator (FDS). Els resultats es van combinar amb les corresponents simulacions a petita escala de resolució més alta amb el model basat en la física a FDS, on es va simular un foc estàtic a diferents distàncies del poble i es van comprovar les condicions dins del poble per determinar un perímetre límit adequat. Els resultats d'aquest estudi mostren que la distància límit mínima a la qual hauria d'estar el límit del disparador és de 200 metres del poble, ja que la temperatura pot arribar als 60 graus centígrads a una distància més petita. Els resultats proporcionen un enfocament més sòlid per determinar la distància d'arribada del front del foc a les zones WUI i informar sobre estratègies de gestió d'incendis i seguretat pública. Tanmateix, els resultats tenen certes limitacions, inclòs el fet que les simulacions es van dur a terme en un sol poble, i es necessiten més investigacions per determinar el perímetre límit òptim per a altres àrees WUI. En general, aquest estudi proporciona una valuosa contribució al camp de la gestió d'incendis WUI, i la seva metodologia pot servir d'exemple per a futures investigacions en aquesta àrea.

Contents

List of Figures

List of Tables

1. Introduction & Objectives

1.1. Preface

Wildfires are a major source of danger and carry a considerable risk on wild-land areas and residential communities [1]. In recent times, there has been an increase in awareness about the hazards [2] linked to wildfires, due to climate change [3] and accelerated by the modern construction of large residential communities in proximity to vegetation, creating what is called the Wildland Urban Interface (WUI). It is the interface where buildings and vegetation meet [4]. Sometimes, wildfires spread into a WUI community and threaten the displacement of a large number of people [5]. For example, just between 2017 and 2019, around 1.1 million people were forced to evacuate by 11 of the most impactful wildfires recorded in California [6].

In general, wildfires are witnessed on a global scale and present a challenge to the entire world [1]. There have been several research projects that aim to develop a better understanding of the WUI. For example, it is worth mentioning the Europe-Australia project: GEO SAFE which is meant to increase data sharing and expertise exchange between the two areas, thus promoting better decision-making and research guidance for both the EU and Australia [7]. Another example to mention is the National Institute for Standards and Technology (NIST) in the United States (US) that, according to its website, is conducting four projects as of the time of writing and has completed one on this topic area [8]. These projects cover the topic of WUI fires by researching how to avoid ignitions, mitigate the effects of wildfires on WUI communities, diving into ember exposure, and how to collect data from WUI fires [8].

This thesis builds on the Wildland-Urban Interface Virtual Essays Workbench (WUIVIEW) project funded by the Directorate General for European Civil Protection and Humanitarian Aid Operations and coordinated by the Universitat Politècnica de Catalunya (Spain). The WUIVIEW project delivered assessment tools for vulnerability and sheltering, to be implemented in the Mediterranean region and to be adapted for the Scandinavian region [9], especially that recently, Scandinavian countries such as Sweden and Norway [10] are getting aware of the increasing WUI fire risk on their coastal areas.

In the next section, some related literature will be presented.

1.2. Related literature

The literature reviewed presents models developed to help simulate one or multiple parts of the WUI wildfire event, split into three types: wildfire models, evacuation models [11] and coupled models [1] [12] [13]. The models are subject to a level of refinement that determines the accuracy of predicted results [11]. Models that include community evacuation are usually set in one of the three scales: microscopic, mesoscopic, and macroscopic scales; the macroscopic models encompass the largest scale of representation of a WUI community, needing data at the general level about traffic flows, capacity, household density; the microscopic models simulate the individual evacuating entities and their behavior, acting on a relatively high resolution; the mesoscopic models offer a trade-off between the two, including the larger scale but with more details on the microscopic level [14]. These models have been an inspiring factor in the development of a comprehensive multiphysics framework for WUI evacuations based on the concept of a WASET/WRSET (Wildfire available/required safe egress time) timeline [11] which is used to supplement model results and place them on a temporal dimension in other research projects [9] [1] [15].

1.2.1. Fire models

Previously, a review of fire simulation models has been compiled [11], the models reviewed are: Spark [11] [16], Prometheus [11] [17], Phoenix Rapidfire [11] [18], FDS [11] [19], FIRE TEC [11] [20], WRF-FIRE [11] [21], CAWFE [11] [22] and FARSITE [11] [23]. All of them require

some training for users, to some extent. These models were reviewed again as updates could have happened in 4 years:

Spark [11] [16] is a wildfire modelling software developed by the Commonwealth Scientific and Industrial Research Organisation (CSIRO), an Australian government body. It is the only model reviewed that allows user input flexibility and real-time updates to the input parameters during simulations. It is built in Python and offers a low computational cost.

Prometheus [11] [17] on the other hand, offers limited flexibility. It is developed by SCION, a research team from New Zealand, as a Canadian wildland fire simulation model that can be used in New Zealand too. It is of low computational cost and is available for free online.

Phoenix Rapidfire [11] [18] is a commercial tool developed since 2003 by Flare Wildfire Research, a large wildfire research group operating in Australia. The tool is meant for use in emergency contexts and is thus deemed to be of low computational cost.

FDS [11] [19] is Fire Dynamics Simulator, a model that uses computational fluid dynamics to simulate fire plumes in enclosures. FDS is normally used for fires inside compartments but it has an extension to include large scale and small scale wildfire scenarios. Currently, FDS is validated for a very limited scope of application in wildfire modeling. This simulator is normally more computationally expensive as it uses Large Eddy Simulation to solve fluid dynamics and heat transfer equations on small grid cells of typically from 0 to 100cm (depending on the size of the domain and the fire and the resolution needed).

FIRE TEC [11] [20] is a wildfire model developed with the collaboration between Los Alamos National Laboratory (LANL) and the USDA Forest Service Rocky Mountain Research Station (RMRS). Notably, this model simulates the dynamic physical processes happening in a fire and their effect on each other. The model has very large computational costs and is reserved for research purposes by the developers.

WRF-FIRE [11] [21] is developed by the National Center for Atmospheric Research (NCAR) in the United States. It is a wildfire growth model, dynamically sensitive to atmospheric conditions and weather changes. This model is also computationally expensive and is available online.

CAWFE [11] [22], developed by the NCAR too, is similarly sensitive to weather changes as it includes a weather prediction model coupled with a fire growth module. However, CAWFE is not available for access.

FARSITE [11] [23] is the fire area simulator model FARSITE, developed by the United States department of agriculture. Briefly, the software is used to represent fire modeling mainly as an elliptical approaching line and outputs the fire spread on the macro scale [23]. FARSITE has been chosen in a recent paper (2021) to provide fire condition outputs, used as inputs into a wildfire evacuation model WUI-NITY [1], built on the Unity3D engine. It is important to mention that although topography is considered in FARSITE, it does not take spotting or roads into account [1]. FARSITE at the moment of writing is not available as a standalone software anymore, but now is included in FlamMap software [24] which increased FlamMap's capabilities by adding the feature to have variable weather conditions.

SWUIFT [11] [25], the late streamlined WUI fire tracing model developed by Masoudvaziri et al., accounts for fire embers. It was validated with two WUI wildfires. Although the SWUIFT model is sensitive to the community layout, it does not include topography [25].

It is important to note, that WUI research is in the early stages, and apparently, there seems to be a common compromise consisting of models under-predicting the fire spread rate [25]. This is likely due to neglecting the role of the 'spotting' phenomenon which can cause ignition away

from the fire line by wind-transported embers [25]. Table 1 summarizes the models reviewed.

Table 1. Fire spread models summarized

Model	Computational cost	Access status
Spark	Low	Commercial
Prometheus	Low	Open access
Phoenix Rapidfire	Low	Commercial
FDS	High	Open access & Open source
FIRE TEC	High	Research tool
WRF-FIRE	High	Open access
CAWFE	Low	Not accessible
FARSITE	Low	Open access
SWUIFT	Low	Unknown

1.2.2. Evacuation models

In addition, as previously mentioned, WUI fires require considerable evacuation efforts. Local authorities often struggle to predict the progress path of wildfire fire lines, and the required decision-making at each stage which is causing delays in evacuation orders [14]. It is particularly important to consider evacuation routes and capacities when dealing with a WUI evacuation and the research in the literature about it is limited [14]. Normally evacuations take place on foot or using vehicles (cars or buses for example) [14] [26]. In some specific cases, evacuation may need to be performed using alternative means of transportation such as naval or aerial means [26]. There are simulation models that attempt to predict evacuation flows from communities, using hurricane evacuation data due to the lack of data for WUI fires [14], but it is necessary to carefully study the transferability of hurricane evacuation studies to WUI evacuation studies [27]. The data from hurricanes in the US suggests that the vast majority of people evacuate using their own vehicle [28], which made developers neglect pedestrian evacuation in their models [14]. It is important to mention that to the knowledge of the author, none of the existing traffic modeling softwares/frameworks were developed specifically for WUI fires. A recent systematic review paper gathered state-of-the-art knowledge about WUI fire evacuation traffic modeling, for the first time [27]. It concludes that, when using existing traffic models for WUI fire evacuations, dynamic models are preferred because they can include human behavioral variations and road availability real-time variations [27]. In addition, it was suggested that mesoscopic and macroscopic models could be more of use to decision-makers during an emergency [27]. It should be noted that, in WUI evacuation, smoke is known to slow down the movement of evacuees by lowering the visibility [5]. Moreover, as part of evacuation modelling, toxicity determination is normally conducted to assess the smoke's impact on evacuation and if the conditions are tenable [5]. Toxicity can be measured in a number of different ways. Yields of certain effluent products can be examined, or also some overall metrics exist such as the fractional effective dose (FED) or the fractional irritant concentration (FIC) [19]. This was detailed further in later chapters as it relates to the goal of this thesis.

1.2.3. Coupled models

There are some tools that operate on multiple scales and integrate different layers of modelling. In 2016, Beloglazov et al. worked on a multilayered model that uses dynamically determined evacuation triggers based on the evolving wildfire, introducing different departure times for each evacuee based on their proximity to the threat [12]. In a similar effort to combine the modelling layers into one tool, urbanEXODUS, a pedestrian evacuation model was integrated with wildfire propagation data and a traffic model [13]. Moreover, the WUI-NITY model previously mentioned is one of the recent examples, designed to couple models for wildfire

spread, pedestrian evacuation, and traffic (vehicle evacuation) [1]. In contrast to the model by Beloglazov et al., the WUI-NITY platform uses the same evacuation triggers (or trigger buffers) for the entire community [12] [1]. The trigger buffers are used in WUI-NITY in a WRSET/WASET framework [1]. The concepts of WRSET/WASET and trigger buffers are elaborated further in the next section.

1.2.4. WRSET/WASET and trigger buffers

The concept of WRSET and WASET comes from the RSET/ASET (required/available safe egress time) concept normally applied to building fire safety [11]. They were first introduced as timelines for WUI fires in the open multi-physics framework (WUI-NITY) developed for modelling WUI fire evacuation in 2019 [11].

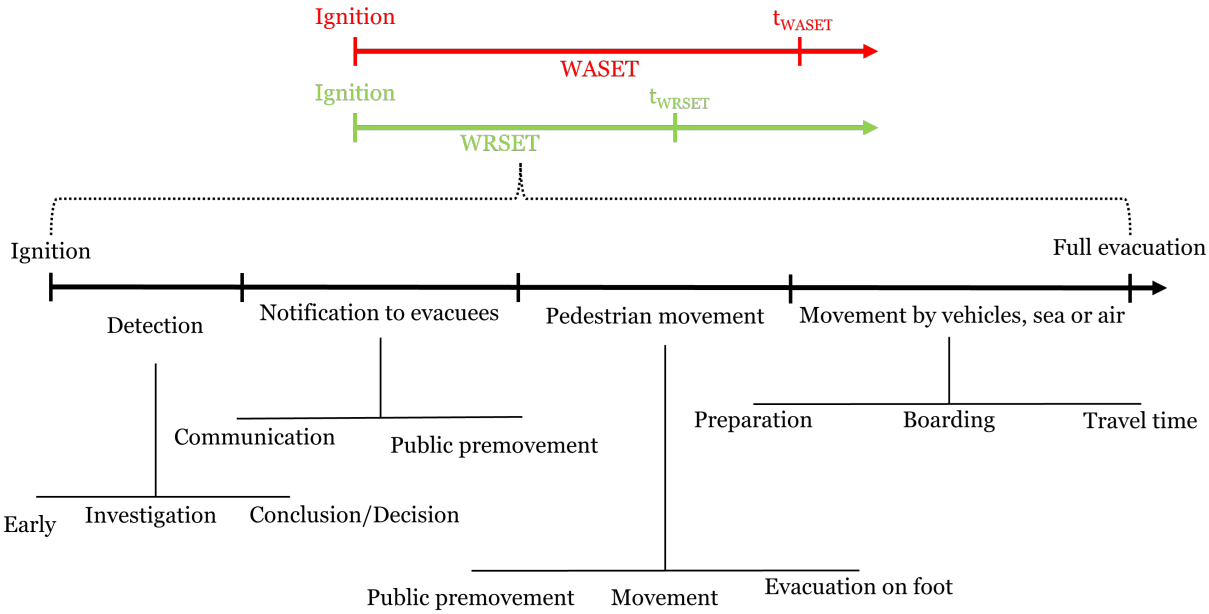

Figure 1. An example of a WRSET timeline

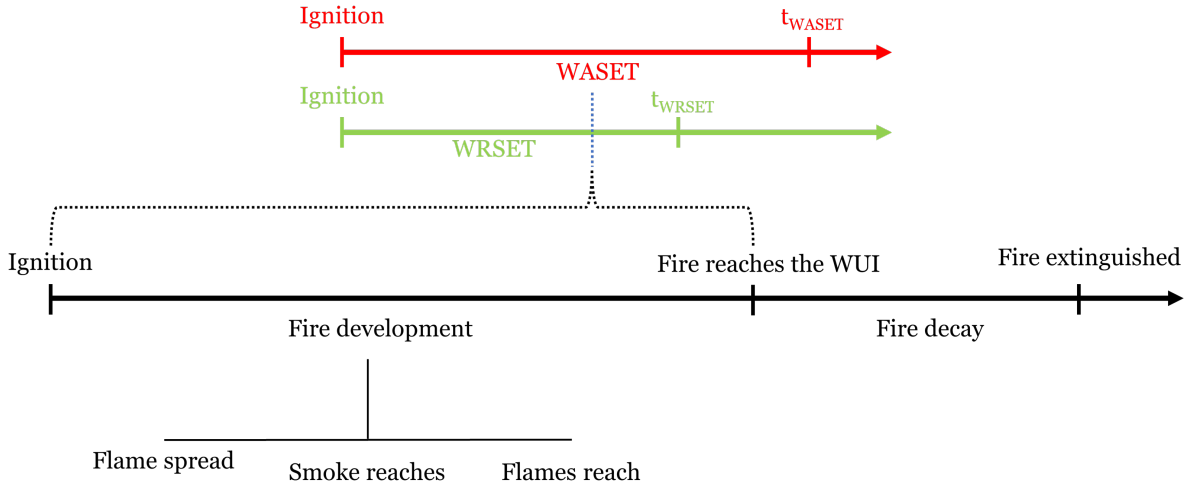

Figure 2. An example of a WASET timeline

The timelines are used along with different 'triggers' or trigger buffers [11] that serve as a trigger to start evacuating. The approach of using trigger buffers for evacuation is first introduced in 2005 by Cova et al. The WUI-NITY uses the PERIL (population evacuation trigger algorithm)

[29] [15] model to incorporate them [11]. Practically, the trigger buffers are normally determined at a time when the fire reaches a certain geographical point of interest, when the authority concerned would then need to provide guidance to evacuees [30]. Examples of WRSET and WASET timelines are shown in Figures 1 and 2 respectively, following the examples shown in [11]. The timelines are just an example and the events might happen in a different order, or there might be more relevant events depending on the specific case studied. Moreover, the trigger buffer can as well be a trigger boundary around the community of interest, where if the fire reaches any point of that boundary, evacuation is ordered [31]. Another study showed that it would be feasible to even have trigger buffers for each household [30].

1.3. Motivation

In the reviewed literature, the WASET is sometimes based on the moment the fire line reaches the community [9] [15] [11]. This could be an overestimation of the WASET considering that the wildfire produces smoke and the smoke could be affecting the evacuation earlier, or even making the conditions untenable. Thus it is a dynamic threat, and the WASET could have been reached at an earlier time than estimated.

Therefore, it would be valuable to introduce community-specific trigger locations where if the fire reaches these locations, the available time to escape would have elapsed. In other words, trigger buffers for the WASET. In this thesis, for simplicity and time limit purposes, efforts are made to establish a WASET trigger boundary instead of specific geographical triggers, thus basing the threat on its proximity to the community.

1.4. Problem statement

This thesis aims to investigate the effect of smoke from a WUI fire on the tenability conditions of a small village and to establish a worst-case-scenario trigger boundary around it as an improved basis for the WASET.

1.5. Research questions

The thesis ideally tackles the problem statement by supplying answers to the following research questions:

1. What is the effect of wind velocity on the WUI fire front development and total heat release rate, considering a WUI fire modelling approach?
2. What are the proper criteria for tenability conditions in a village exposed to a WUI fire, and can modelling be used to find out which criteria would be the most critical?
3. Can WUI fire modelling be employed to find out, in villages exposed to WUI fires, how distant would the fire front need to be for smoke to cause untenable conditions?

1.6. Outline

The study first presents in section 2 the methodology followed, then the results are examined in section 3 before discussing them in section 4 and concluding (section 5).

2. Methodology

As wildfires are highly unpredictable and very case-specific, the main objectives of this thesis have to be reached through a case study in order to demonstrate the proposed methodology and show the results.

The related literature was found mainly by searching on Google Scholar (https://scholar.google.com/) and the local library search engines at Universitat Politècnica de Catalunya and Lund University, using the following keywords: WUI fire, WUI flames, WUI spread, Wildfire spread, Wildfire evacuation, WUI evacuation, WUI model, WUI simulations. Other sources were specifically target-searched when an assumption needed to be made. An estimated 20 papers were reviewed in order to write the 'Related literature' section (section 1.2).

Previously in the WUIVIEW project, the Moninhos Cimeiros village in Portugal was deemed vulnerable to wildfires and efforts were made to assign an existing building as community shelter since most of the other ones are in poor condition [9]. The village was chosen for this thesis as, during the WUIVIEW project, its WASET was determined based on when the fire line reached the community and the authors mention that it could be better to base the WASET on performance criteria instead [9]. In addition, vegetation and weather data for this location was relatively more accessible due to the link between the WUIVIEW project [9] and Universitat Politècnica de Catalunya where this thesis was conducted.

2.1. Community location

The Moninhos Cimeiros village in Portugal is a small community with around 70 structures [9].

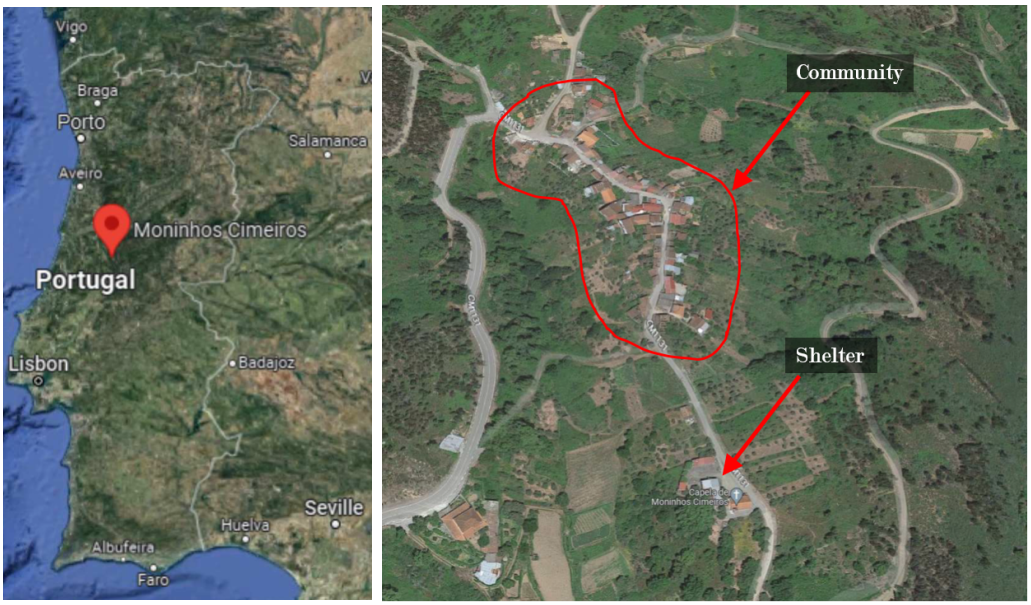

Figure 3. Location of the case study terrain from Google Earth

As can be seen in Figure 3, the shelter is located about 450 meters from the farthest building in the community of the village. This study assumes that evacuation transportation can happen on foot or by car, except for the sensible population like children or older people, they are assumed to travel by car only.

2.2. Choice of FDS and the level set method

FDS can model wildfires using either the physics based model (PB) or a level set based model (LS), a recent new capability of FDS. The PB model is CFD-based and models the physical

phenomena present when gas-phase combustion is explicitly included; the LS model is intended for fire spread on a terrain's surface and it incorporates the Rothermel-Albini empirical model into its engine while including the freedom to add a wind profile, thus combining the empirical calculations of fire spread with the interaction of the wind with the topography and including the effect of the fire on the ambient conditions (the mesh dependency needs to be examined) [19].

In FDS the level set approach is utilized by discretizing the spatial domain into a 3D grid and representing the fire front as a zero-level set of a scalar field. The scalar field is updated over time via a partial differential equation that describes the evolution of the fire front [19].

To update the scalar field, FDS must be using the level set equation normally used in fire front propagation level set methods [32] [33], which is expressed as:

$$\frac{\delta\phi}{\delta \mathrm{t}} + \mathrm{S}|\delta\phi| = 0 \tag{1}$$

Here, ϕ refers to the level set function, t represents time, $\delta\phi$ is the gradient of the level set function, and S denotes the speed of the fire front. FDS solves the level set equation numerically using finite difference methods, and the resulting scalar field is used to estimate the fire behavior, such as flame height, temperature, and heat flux.

For S, FDS incorporates several sub-models that estimate the input variables, such as fuel properties, weather conditions, and topography. These sub-models are leveraged to calculate S, which is then used in the level set equation to track the fire's movement over time. The sub-models include combustion, radiation, turbulence, wall heat transfer, atmospheric boundary layer, and pyrolysis [19]. The combustion sub-model estimates the fuel consumption rate and heat release rate, while the radiation sub-model calculates radiative heat transfer to the surrounding environment [19]. The turbulence sub-model estimates turbulence in the flow field, while the wall heat transfer sub-model calculates heat transfer from the fire to surrounding surfaces [19]. The atmospheric boundary layer sub-model estimates the effects of weather conditions on fire behavior, and the pyrolysis sub-model estimates fuel decomposition and volatile gas release [19]. By using all of these sub-models in the level set simulations, FDS can provide a more accurate prediction of fire behavior in complex environments.

In addition, instead of manually modeling the terrain and approximating from pictures and satellite imaging, QGIS could be used. QGIS is a software that can import 3D topography and vegetation data from a real world vegetation database [35], and qgis2fds is a plug-in developed to export this data as geometry (obstacles) into FDS's level set vegetation based classification [34]. There is also the option to add a fire front polygon and the wind profile right from QGIS. QGIS determines the obstacle size according to the mesh resolution specified by the user. Figure 4 [34] sums up the features provided by the qgis2fds plug-in for QGIS. Note that at the time of writing, the "FDS terrain extent" uses the OBST family in FDS not the GEOM as shown in Figure [34], meaning that the terrain is built using `&OBST` input lines instead of `&GEOM`.

In fact, a CFD approach like FDS is computationally expensive specifically because it solves the governing flow equations with heat transfer and combustion in a fluid dynamics gridded framework, thus it is more precise [36]. Between the fire models discussed (refer to table 1), FDS has been chosen for this study as it is open source, and widely used in the fire engineering and fire science community. Moreover, by using FDS, the thesis can build on the results from the WUIVIEW project for the same case study [9]. The most recent version at the time of writing, FDS6.7.9 is used.

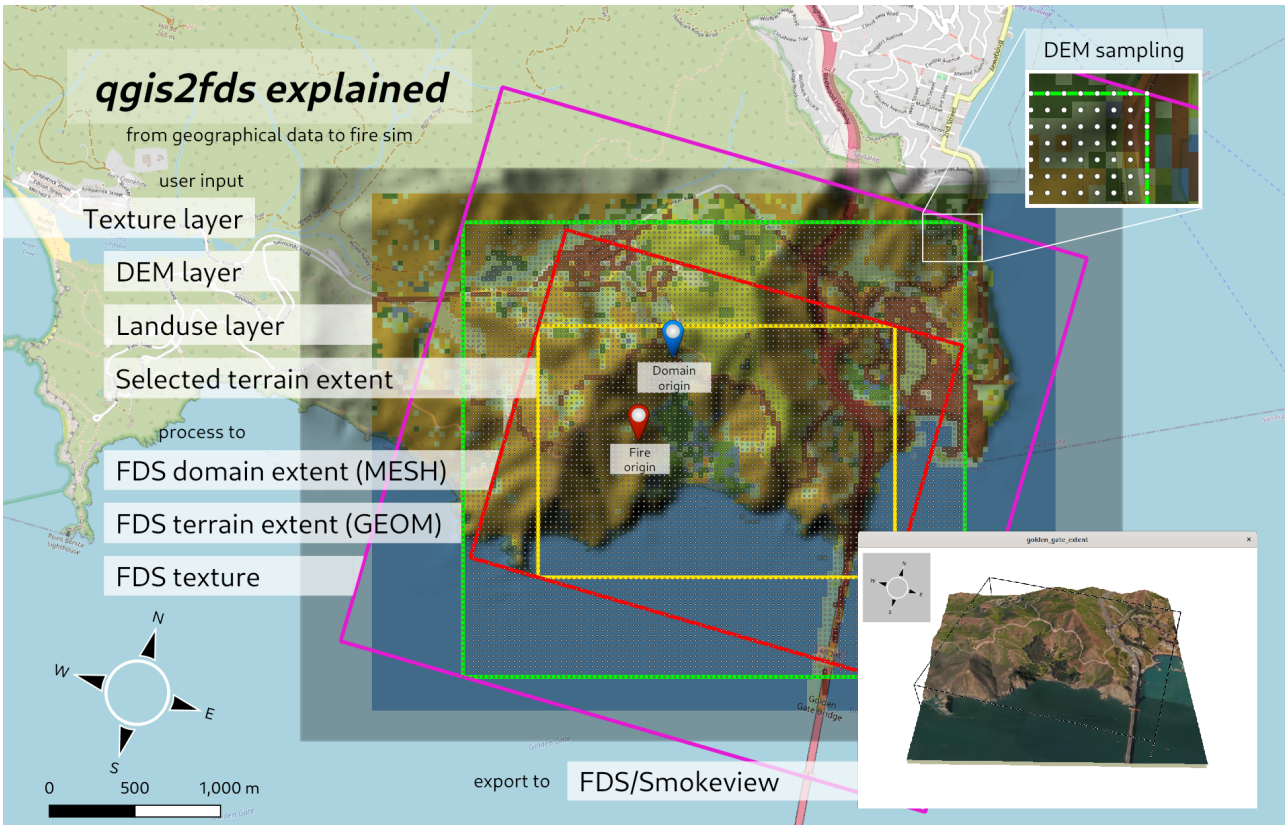

Figure 4. Summary figure for qgis2fds from source [34]

2.3. Level set model in FDS

The level set model in FDS has four different mode options ranging from 1 to 4 inclusive [19].'`LEVEL_SET_MODE=1`' does not simulate a fire, only employs the empirical correlations, and the wind is not affected by the topography. '`LEVEL_SET_MODE=2`' allows for the setup of wind but then it freezes when the fire starts. '`LEVEL_SET_MODE=3`' still produces no fire but the wind is guided by the terrain. '`LEVEL_SET_MODE=4`' has wind and fire coupling and allows surface cells to burn when the fire reaches them. In this thesis, '`LEVEL_SET_MODE=4`' is used. Each surface cell must have a certain fuel index, provided in FDS documentation as fuel types from 1 to 13, corresponding to the 13 fuel types from the Rothermel-Albini fuel models [19]. The type specifies fuel characteristics as shown in Table 2 [19].

Table 2. Parameters of the 13 fuel models from Rothermel-Albini

	Fuel Type	Dead Fuels						Live Fuels				Fuel Depth (m)	$M_{x,dead}$	No-Wind, No-Slope RoS (m/s)
		Fine		Medium		Large		Woody		Herbaceous				
		σ (m^{-1})	m (kg/m^2)	σ (m^{-1})	m (kg/m^2)	σ (m^{-1})	m (kg/m^2)	σ (m^{-1})	m (kg/m^2)	σ (m^{-1})	m (kg/m^2)			
1	Short Grass	11500	0.17	-	-	-	-	-	-	-	-	0.30	0.12	0.030
2	Timbergrass	9840	0.45	358	0.22	98	0.11	4920	0.70	4920	0.70	0.30	0.15	0.017
3	Tall Grass	4920	0.68	-	-	-	-	-	-	-	-	0.76	0.25	0.034
4	Chaparral	6560	1.12	358	0.90	98	0.45	-	-	4920	1.12	1.83	0.20	0.035
5	Brush	6560	0.22	358	0.11	-	-	4920	0.45	-	-	0.61	0.20	0.010
6	Dormant Brush	5740	0.34	358	0.56	98	0.45	-	-	-	-	0.76	0.25	0.013
7	Southern Rough	5740	0.26	358	0.42	98	0.34	4920	0.08	-	-	0.76	0.40	0.010
8	Closed Timber Litter	6560	0.34	358	0.22	98	0.56	-	-	-	-	0.06	0.30	0.002
9	Hardwood Litter	8200	0.66	358	0.09	98	0.03	-	-	-	-	0.06	0.25	0.006
10	Timber	6560	0.68	358	0.45	98	1.12	4920	0.45	-	-	0.30	0.25	0.007
11	Light Slash	4920	0.34	358	1.01	98	1.24	-	-	-	-	0.30	0.15	0.004
12	Medium Slash	4920	0.90	358	3.15	98	3.71	-	-	-	-	0.70	0.20	0.010
13	Heavy Slash	4920	1.57	358	5.17	98	6.29	-	-	-	-	0.91	0.25	0.014

With m being the mass per unit area of the fuel. σ being the surface area to volume ratio of the fuel which affects the rate at which an obstacle ignites. $M_{x,dead}$ is the dead fuel extinction

moisture content as a ratio.

For all of the fuels:

- The total mineral content: $S_t = 0.056$
- The effective mineral content: $S_e = 0.01$
- The heat of combustion: $\Delta H = 18600$ kW/kg
- The density: $\rho_p = 510$ kg/m^3
- The moisture content of fine, medium, large vegetation respectively: $M_{d,1} = 0.03$, $M_{d,2} = 0.04$, $M_{d,3} = 0.05$. And the moisture content of live woody and herbaceous vegetation is $M_{l,w} = M_{l,h} = 0.70$.

Note that this method is not well documented in the most recent FDS user guide [19] as of the time of writing. To get more information, the author resorted to the Github forums and sometimes posted about his concerns, to which the developers of FDS replied. Github is the name of a popular social website among code developers where the community collaborates on projects sometimes. The expected outputs from this method are, the time variable total heat release rate of the spreading fire, the fire front spread, and the soot measurements that were possible to make with devices.

The fire spread is represented by the level set value slice: AGL slice, showing the value of the level set of the obstacles as follows: -1 means the surface hasn't ignited yet, 0 means ignition and from 0 to 1, the surface is burning with its prescribed heat release rate per unit area. 1 means that the surface has already burned.

The lack of documentation could be due to the fact that the method is still in development and the capabilities of FDS in wildfire modeling are still in their early stages, in accordance with the entire wildfire modeling field.

2.4. Strategy proposed

To model fire spread on a large scale, terrain elevation data and real weather conditions such as temperature and wind are used, and the level set model is simulated on FDS with an appropriate mesh resolution. It's important to conduct a mesh analysis to understand the mesh dependency of the method as there are no guidelines available in the literature. Outputs from the simulation include the time-based location of the fire front and the time-based total heat release rate.

In the WUIVIEW project [9], the time at which the WASET is determined was estimated to be when the fire front reaches the community. However, this may not be the most accurate determination, as tenability conditions around the houses and on the road serving as an escape route from the houses to the community shelter could already be life-threatening before the fire reaches the community. The real WASET could be smaller in a real event.

This thesis proposes an improvement in the estimation used to address the challenge of determining the appropriate time for WASET. The proposed approach involves creating a smaller model from the worst performing large scale simulation model, with a static burner to represent the fire front at given distances D_i from the community and at corresponding moments in time T_i. The heat release rate for the model is obtained from the large-scale simulation. The smaller domain of the model allows for a higher resolution mesh that can more accurately capture temperature measurements and other life safety criteria. If the tenability conditions are suitable at distance D_{n-1} but unsuitable at distance D_n, D_{n-1} is used to establish a perimeter at which the WASET would be determined in future WRSER/WASET studies. The reason for reducing the domain size is to make it computationally feasible to use a suitable mesh resolution for CFD gas-phase calculations and to more accurately represent the flame plume. The approach is summarized in the Figure 5.

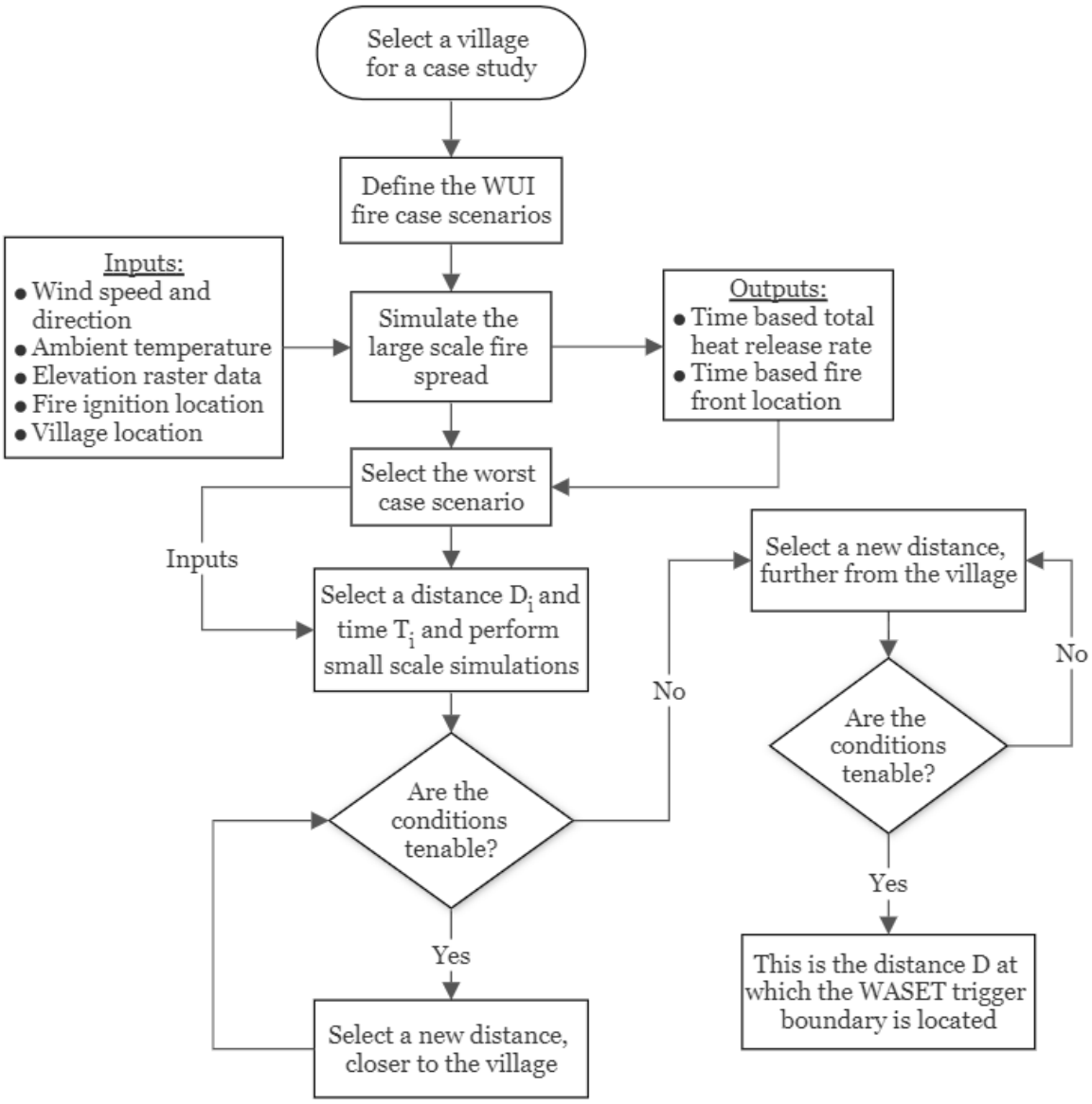

Figure 5. This thesis' proposed approach to determining the WASET trigger boundary

2.5. Large terrain draft model creation

The first step is using QGIS to export an initial FDS file, using the 'qgis2fds' plug-in. In order to do that, the digital elevation model layer (DEM file) needs to be imported, along with a land-use layer. The DEM layer specifies the height of each cell of the land area, indicating the height of the obstacles in FDS which will replicate a topography. The land-use layer data specifies the vegetation distribution on the cells, which is later converted to one of the level set vegetation types to be used in FDS.

The DEM and land-use layers were provided by the research group that conducted the WUIV-IEW project [9]. The resolution of the GIS data is made by squares with a 5 meters dimension, meaning that the land is made of areas of 5 by 5 meters, with a height and vegetation setting for each. The domain of the data spans 2 by 2 kilometers as a square around the Moninhos Cimeiros community.

As shown in Figure 6, the three layers are overlapping, the third one being the Google Maps terrain layer. This layer is purely aesthetic and could be loaded in Smokeview (visualizing software for FDS results) as a picture over the terrain.

The qgis2fds plug-in shown in Figure 7 exports the desired domain to an FDS level set simula-

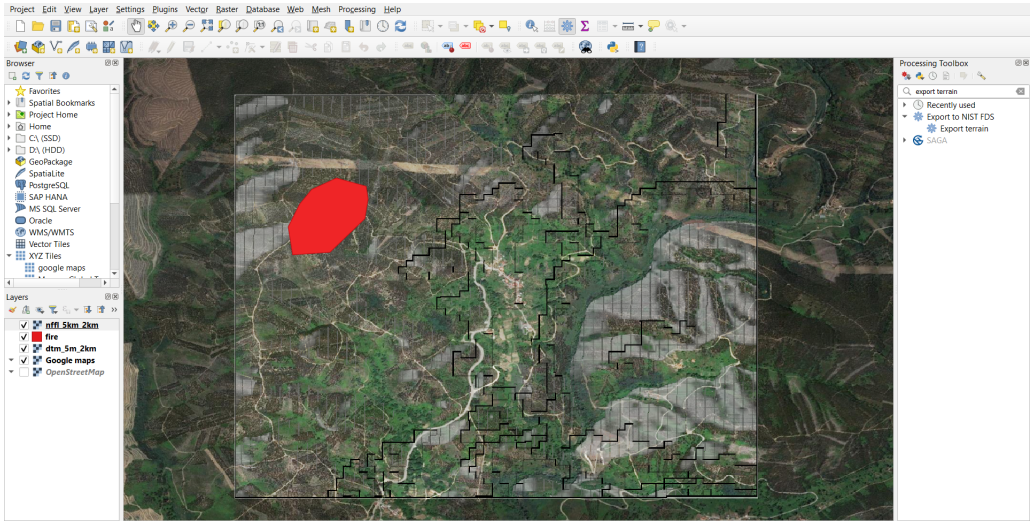

Figure 6. GIS domain as shown in QGIS software before exporting

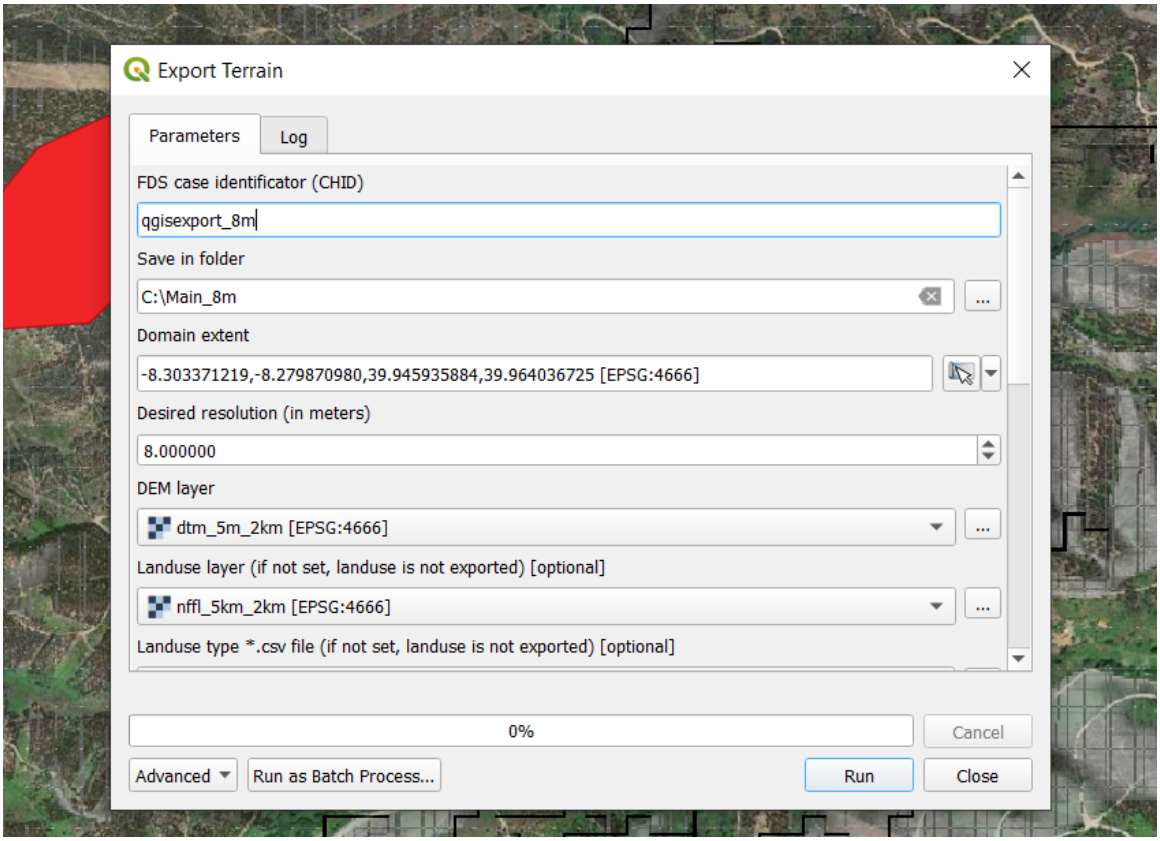

Figure 7. qgis2fds plug-in parameters shown before exporting

tion, with customizable wind conditions and desired mesh resolution. The draft model created for mesh analysis is made with a fire front similar to the developed fire in the WUIVIEW study [9], as the first case is for testing purposes. The wind is also input with equal characteristics as the case ran in the WUIVIEW project [9]: a constant velocity of 10 m/s and coming from the north-west towards the south-east. In FDS, the north is in direction of +y and the east is in direction of +x [19].

As the mesh size is enormous compared to the building, it was added as a 15 x 15 x 10-meter obstacle in Pyrosim (a Thunderhead Engineering company commercial software, accessed with a student license), only to represent its location and determine its distance to the fire front.

The shelter is shown in Figure 8 as the black dot near the center of the terrain. The black area represents the area already burned by the simulation and its red contour represents the fire front at time 0.

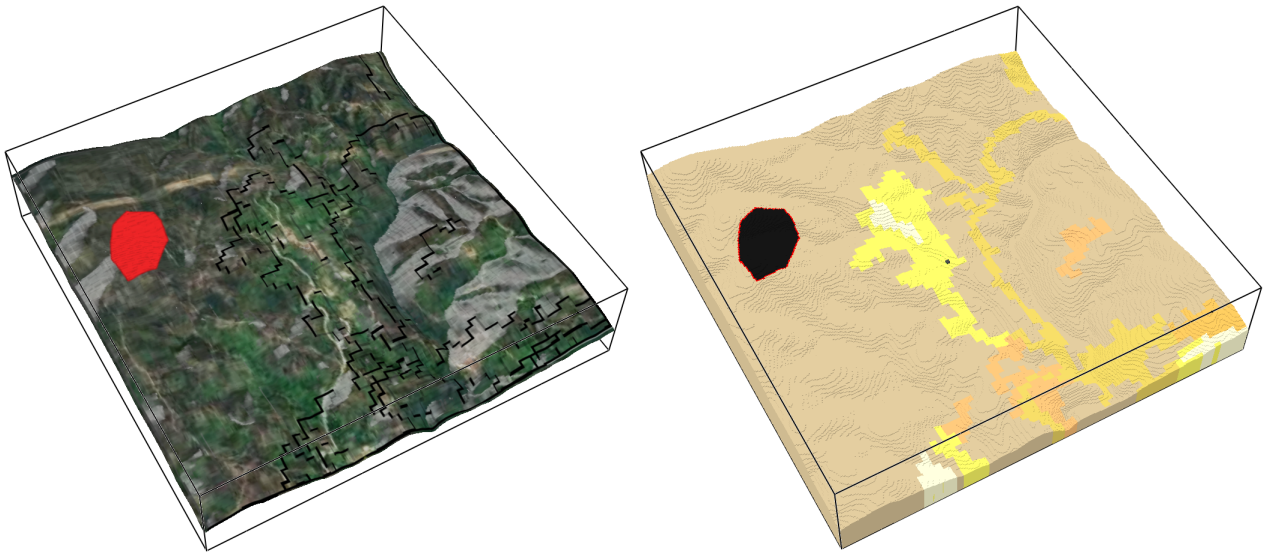

Figure 8. Terrain model shown as realistic terrain (left) and as obstacles (right)

The next step was to try and determine a suitable mesh size that can be feasible given the time constraints of the study.

2.6. Large terrain mesh sensitivity

The size of cubic cells making up the mesh has a lower limit since the domain is 2 kilometers in x and y, and needs a good amount of z height to accurately simulate the wind conditions. Thus, using the same resolution as the DEM and land-use layers (5 meters), the total number of cells to simulate would already reach over 14 million. The largest computer available for parallel computing has 44 cores available, with parallel computing, the simulation takes around an estimated 6 days to run 3000 seconds. In conclusion, the smallest grid cell size is not feasible for the time constraints of this study, in case multiple cases with different parameters need to be run, the results would need more than a month.

The approach taken will be to simulate the same base case already elaborated, with grid cell sizes of 15, 10, 9, 8, 7 and 6 meters. The outputs of these cases are compared in section 3.1 for a better understanding of the accuracy. Devices were put on different heights over the shelter, to measure the soot mass fraction and volume fraction. The suitable mesh size was chosen in section 3.1 to be 9 meters.

2.7. Weather inputs

It is often theorized that climate conditions can have an effect on wildfire spread and size [37]. The weather conditions for the area could not be gathered, but there are weather stations near the Moninhos Cimeiros community shelter (in portuguese: Abrigo Communitario de MC) such as Gramatinha, IPMA 716 and Penela (see Figure 9).

From Gramatinha, the author was able to receive data from June, July, August and September, of 2019. From IPMA 716, data was available from June and July of 2019. As for Penela, there is data from 2018 and 2019 for the months of June, July, August and September.

The average of the maximum wind speeds of all the available months recorded was 9.7 m/s and the average of the average wind speeds of these months was 1.24 m/s; the author takes 10 m/s as maximum wind speed and 1.5 m/s as average for the simulations.

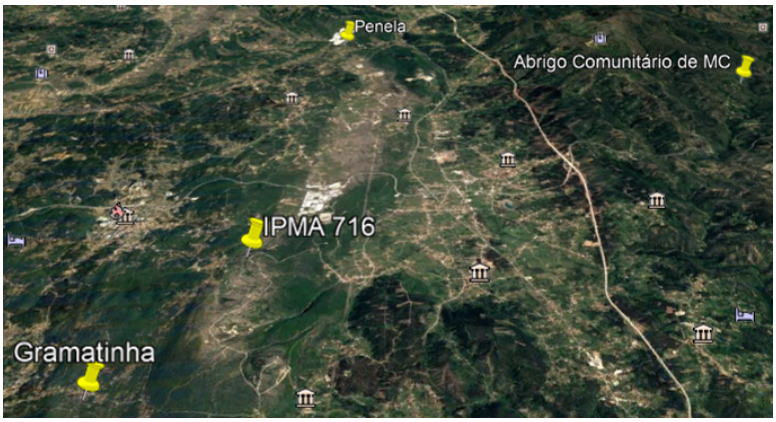

Figure 9. Nearby weather stations

High temperatures are associated with drier vegetation in areas that go through a dry summer [37]. Thus, the average of the maximum temperatures of the recorded months is 37.5 C and so the ambient temperature in the simulations is taken as 37 C.

2.8. Combustion inputs

The '`&REAC`' line in FDS specifies the combustion reaction to be followed for the fire. In wildfires with vegetation, the common assumption [38][39] is to take the characteristics of the closest fuel available in Table A.39 of the SFPE Handbook of Fire Protection Engineering [40] which is wood. The red oak wood is used as it is the only wood fuel with information about its soot yield. Thus from Table A.38 and A.39 [40], the inputs in the simulation for the '`&REAC`' line are shown in the Table 3 below.

Table 3. Inputs for the reaction line in FDS simulations

Chemical formula	$CH_{1.7}O_{0.72}N_{0.001}$
Soot yield (kg/kg)	0.015
CO yield (kg/kg)	0.004
Heat of combustion (kJ/kg)	17100
Radiative fraction	0.371

2.9. Large scale cases set-up

Overall, the fire could be coming from either side of the community. The sides taken in the scope of this thesis are north, south, east and west. Wildfire spread is normally estimated as an elliptical shape [41]. As the elevation data available to the author is limited to a domain of 2 x 2 km where the community is in the center, the wildfire is assumed to have started at a point much farther away and the fire front is modeled at the edge of the model as part of a large ellipse. The obstacles are set to be 9 x 9 meters in area as the mesh cells will be cubic of 9m.

In future studies, one can obtain a larger elevation data domain and input the ignition point to get a more accurate fire front arriving to the area of study.

The community could be modeled over the large scale model in Pyrosim as walls and roofs, along with the main road. Figure 10a is a 2 x 2 km full view of the large scale model with the initial fire front located at the south in black. Figure 10b is a 500 x 300 meter (east to west x north to south) zoomed-in view of the community, with the shelter being located to the south. The height of all the buildings is taken as 5 m as an estimated average, as most of the

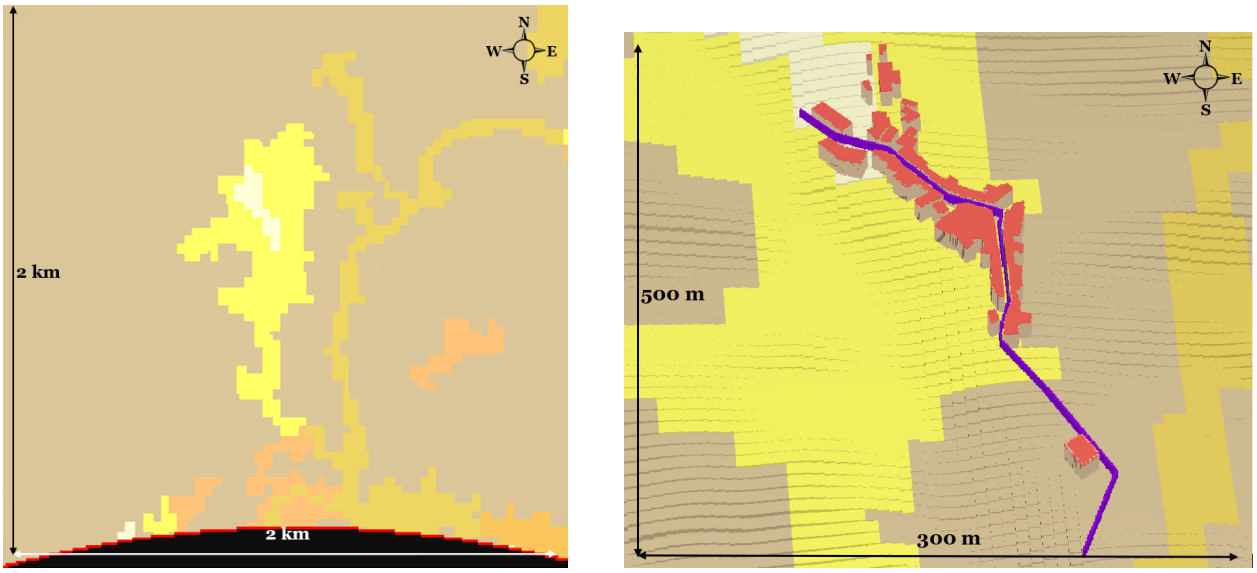

(a) Large scale model exported from QGIS **(b)** A zoomed-in view of the modeled community

Figure 10. Figures showing the basic model and the added community obstacles

buildings are village buildings and their heights as seen in Google Maps street view correspond to that average.

There are 8 large scale cases in total, varying between a southern, northern, eastern and western fire front and wind, and between a highly fast wind (maximum wind speed of 10 m/s) and an average wind (average wind speed of 1.5 m/s). The following Table 4 summarizes the simulations and code-names them.

Table 4. Table summarizing large scale simulations

Simulation	Fire front source	Wind direction (source)	Wind speed (m/s)
S-MWS	South	South	Maximum: 10
N-MWS	North	North	Maximum: 10
E-MWS	East	East	Maximum: 10
W-MWS	West	West	Maximum: 10
S-AWS	South	South	Average: 1.5
N-AWS	North	North	Average: 1.5
E-AWS	East	East	Average: 1.5
W-AWS	West	West	Average: 1.5

The height of the mesh domain is set to be 240 meters higher than the highest point in the model, in order to make sure the wind profile is included as much as it is possible with a mesh resolution of 9 meters. The large scale simulations are ran for 10 000 seconds and force-stopped a little after it is seen in Smokeview (an FDS results viewer) that the fire front had reached any part of the community (structure or road).

As for outputs, the devices mentioned in section 2.11 are included in the large scale simulations, at a height around 9 meters over the buildings' roofs. More is explained in section 2.11 as these measurements are more proper for a higher resolution simulation. The level set method in FDS also has the AGL slice outputting the level set value from -1 to 1 as previously elaborated in section 2.3.

2.10. Small scale mesh resolution

The small scale case needs to be run with a sufficiently fine mesh resolution to capture the physical processes and the fire plume produced. The proper way to examine the mesh sensitivity

is to start with a coarse mesh and refine it as needed until there are no differences in the outputs anymore [19]. To situate what's a relatively coarse or fine mesh, the FDS user guide proposes a method based on Heskestad's flame height correlation, setting $\frac{D^*}{\delta x}$ as a constant where D^* is the characteristic fire diameter in meters and δx is the mesh cubic cell size in meters [19]. The validation guide proposes that to model the fire plume accurately, let's say that $\chi = \frac{D^*}{\delta x}$, χ can range from $\chi = 5$ to $\chi = 20$ [19]. Thus solving for δx in the following equation:

$$\delta x = \frac{D^*}{\chi} \tag{2}$$

And replacing D^* by the expression in the following equation [19]:

$$D^* = \left(\frac{\dot{Q}}{\rho_\infty c_p T_\infty \sqrt{g}} \right)^{\frac{2}{5}} \tag{3}$$

Having:

- $\dot{Q}$ as the total heat release rate (variable) in kW;
- $\rho_\infty = 1.2$ kg/m^2 as the density of ambient air;
- $c_p = 1$ J·kg^{-1}·K^{-1} as the specific heat capacity of ambient air;
- $T_\infty = 298$ K as the temperature of ambient air;
- $g = 9.81$ N/kg as the gravitational acceleration constant.

Looking at the large scale mesh analysis HRR results (section 3.1.2), the relevant part of the plot is before the fire reaches the shelter. The average total HRR value before the fire reaches the shelter, as seen in Figures 14a to 14f is $\dot{Q} = 2000$ MW. Assuming in the small scale model that $\dot{Q} = 2000$ MW, and inputting it in Equation 2 and 3, the range of δx results to be from $\delta x = 1$ meters to $\delta x = 4$ meters. Thus, The mesh analysis case have been run at a mesh with cubic grid cells of 1.5 meters size and 1 meters size as a smaller size is not computationally feasible. The outputs of these simulations are examined in section 3.2.

2.11. Small scale cases set-up

The model is needed to fit a village that spans on more than 300 meters of distance with a large wildfire too. It also has to contain enough cells in the vertical direction to capture enough of the interaction between the wind and the fire plume. When using a mesh resolution of 1 meter, the number of mesh cells quickly becomes too high to be computationally feasible. Thus, the model has to be as limited as possible, due to the computational challenges. It is crucial that the entire village is represented, with the fire it's exposed to. In addition, the fire front should not be trimmed excessively as by trimming it, some of the secondary effects could be lost. For example, the smoke passing next to the village could possibly be affecting the temperatures of the smoke in the village. In this section, efforts were made to ensure the model is cropped as little as possible, while keeping the number of cells for the mesh in an acceptable range.

The small scale cases were made according to the worst case of the previous 8 large scale cases. It is trivially only important to consider a deeper WASET study based on the worst WASET received from the large scale cases. The model is trimmed, to include the community buildings and roads on one side, and the fire front on the other. The fire front is modeled as a 3D static burner with the same '`&REAC`' properties and with a heat release rate sourced from the large scale simulation at the exact time studied. Since the southern fire case (S-MWS) was deemed to be the worst case (section 3.3), its results were used to make the small scale simulations.

As the fire front is trimmed, the total HRR from the large scale results cannot be used as it would be a large over prediction, since the entire fire front contributes towards that HRR value.

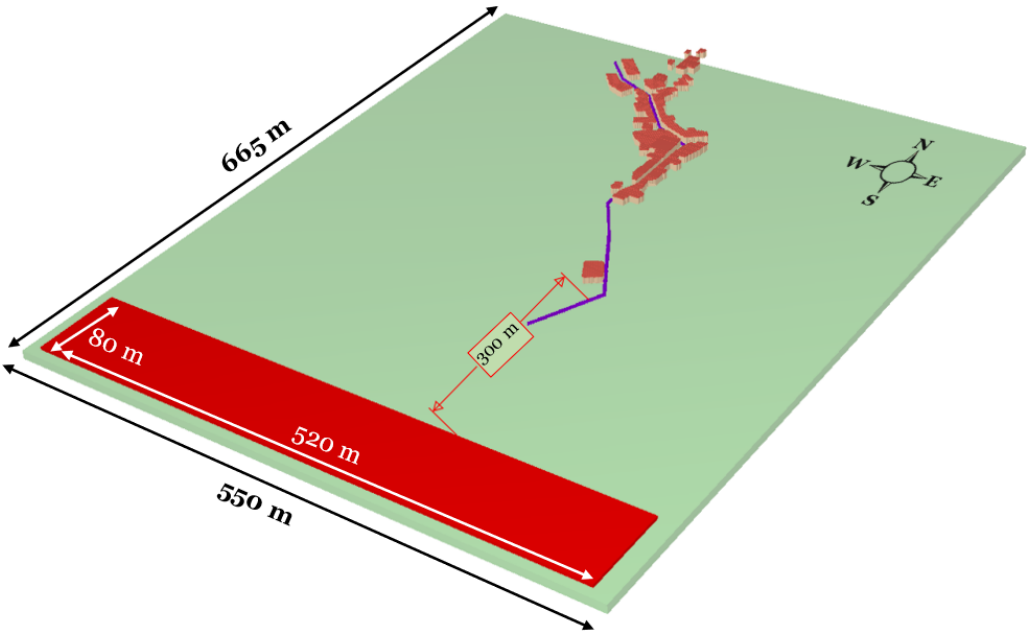

Figure 11. Small scale model example

Figure 12. Horizontal location of devices used

The example in Figure 11 shows a southern fire distant 200 meters from the first building of the village (being the shelter in this case). Here the width is the dimension parallel to the

fire front (dimension in x) and the length is the one parallel to the 200 meter measurement (dimension in y).

The domain width was taken as 550 meters which was the maximum feasible width and the fire front width as 520 meters (ratio of around 1/4 with the large domain), leaving room of 15 meters on each side to avoid any possible implications that a fire spanning the whole width of the mesh might bring. The domain length was 665 meters and the height was 35 meters. For simplicity, it was assumed that the HRRPUA is constant across the fire front. The prescribed HRR then should be reduced by the same ratio used to reduce the fire front width: 1/4. But as this method is an estimation that could be inaccurate, scientific judgement was used and a factor of safety of 2 was taken, the heat release rate would then be reduced with a ratio of 1/2 only. Although the fire front length could be estimated on average from the large scale simulations, generally the front in these simulations, is not a rectangular shape, and might affect a larger area because of the sinusoidal shape seen in some of the results. The fire front length was set as 80 meters. As there are no available methods of determining a proper length for the burner, 80 meters was a suggestion, as a rectangular shape would not be too thin nor would its length be greatly increasing the domain length. In order to better represent 3D burning vegetation, the burner was given a depth of 2.75 meters too, making it a cube. The fire front estimation simplification to a cubic burner, and the assumption for its HRR is a large source of uncertainty in this study. Future studies could look into the sensitivity of the results depending on the burner shape and HRR estimation.

FDS devices are used at multiple locations along the road to measure gas-phase conditions. The locations are shown in Figure 12. The devices are intended to cover the length of the main road used for evacuation, they are spaced on average around 13-20 meters from each other. Lower spacing distances are used where there are many buildings around the road. The idea was to collect enough data to get a better understanding of the conditions next to the houses and on the road while analysing the results.

The devices were added in sets at heights 1 m, 2 m, 3 m, 4 m and 5 m for temperature, soot mass fraction, soot volume fraction, carbon monoxide (CO) mass fraction, CO volume fraction, carbon dioxide (CO_2) mass fraction, CO_2 volume fraction, radiant heat flux and visibility.

2.12. WASET life safety criteria

The tenability conditions checked at each moment or distance in the small scale models, need performance criteria to decide whether the conditions are acceptable or not anymore. In structural fire protection engineering, there is considerable guidance [40] for determining life safety criteria for designing buildings. The novelty of the WUI wildfire research means that there are no specific general guides for tenability criteria for evacuation or life safety, or for firefighters in WUI fires [42]. For that reason, the criteria in this study are suggested on a common sense basis, inspired by criteria from building design, awaiting more research and standardisation.

It is important that the considered criteria for untenable conditions include temperature. According to the SFPE guide to performance based design [40], at a temperature of 60 C, if the air was fully saturated with water, it wouldn't be breathable. However, in a fire scenario, unless a large amount of water was thrown on the fire without succeeding to extinguish it, the air will not be saturated with water, it would reach a maximum of 50% relative humidity [40]. 60 C would be questionable for some portion of the population, particularly older people. But as this study assumes they would be travelling by car, and as the travel distance is < 450 meters (see section 2.1), it is assumed that they wouldn't be exposed to that temperature for a long time anyways. Thus a temperature of 60 C is chosen as the comfort limit or tenability limit in this study.

Another thermal phenomena that affects evacuating people is radiation, measured with the heat flux received at a certain point. Thus the critical heat flux considered in this study as the limit for comfort is 1.7 kW/m^2 because it is the critical heat flux below which no pain is felt for any duration of time [40].

An important hazard in fire scenarios is smoke inhalation, leading to CO, carbon dioxide CO_2 and soot inhalation. CO, CO_2 and soot are included in the fractional effective dose (FED) calculation in FDS. The total FED is calculated in FDS according to the following equation [19]:

$$FED_{tot} = (FED_{CO} + FED_{CN} + FED_{NO_x} + FLD_{irr}) \times HV_{CO_2} + FED_{O_2} \tag{4}$$

FED in the nomenclature of the parameters means the fractional effective dose, the subscript is the chemical whose FED is calculated. FLD_{irr} is the fractional lethal dose of irritants. HV_{CO_2} is the hyperventilation factor induced by carbon dioxide.

The fractional effective dose of CO intake FED_{CO} is calculated as [19]:

$$FED_{CO} = \int_0^t 2.764 \times 10^{-5} \left(C_{CO}(t)\right)^{1.036} \, dt \tag{5}$$

With t as time in minutes, and C_{CO} as the CO concentration in ppm.

The FED_{CN} and FED_{NO_x} are zero in this study because the input does not specify an HCN or NO_x yield. FLD_{irr} is also zero, as it is calculated from concentrations of HCl, HBr, HF, SO_2, NO_2, C_3H_4O, CH_2O which are not specified explicitly in the input either.

HV_{CO_2} and FED_{O_2} are calculated with the equations [19]:

$$HV_{CO_2} = \frac{\exp\left(0.1903 C_{CO_2}(t) + 2.0004\right)}{7.1} \tag{6}$$

$$FED_{O_2} = \int_0^t \frac{dt}{\exp\left[8.13 - 0.54\left(20.9 - C_{O_2}(t)\right)\right]} \tag{7}$$

With C_{CO_2} as the CO_2 concentration in volume percentage and C_{O_2} as the O_2 concentration in volume percentage.

There are FED thresholds for incapacitation and for lethality [43]. FED threshold of 1 means that 50% of people would have been incapacitated. For lethality, the threshold is taken at 2 or 3 [43]. The tenability limit in this study is taken as 0.3 as a conservative limit [40] [44]. In buildings, if the occupancy would comprise a sensitive population (e.g: older people, people with disabilities), a limit of 0.1 would need to be applied. However, in this study, it is assumed that the sensitive population will reach the shelter by vehicle transportation and thus would not be exposed to a high dose, especially if the windows of the vehicle are closed.

The criteria of the study for unacceptable conditions are summarized in Table 5.

Table 5. Performance criteria for finding the ASET

Criteria	Location(s) of measurement	Limit
Temperature	z <3 meters	<60 C
Heat flux	z <3 meters	<1.7 kW/m^2
FED	z = 2 meters (head level)	<0.3

3. Results

3.1. Large scale mesh sensitivity analysis

In this section, the results from the mesh analysis of the large scale draft case are examined and a conclusion is reached. This is particularly important as there are no mesh dependency studies in FDS documentation for the level set method.

The mesh cubic cell sizes used are 15, 10, 9, 8, 7 and 6 meters. All other inputs are kept the same. The mesh sensitivity of the results is to be determined according to qualitative judgement of the fire spread shape and rate of spread, the HRR and the soot mass fraction. Thus, the mesh sizes will be compared, going from the coarsest to the finest, and the resolution that is deemed both feasible and accurate enough is to be chosen. The general results as of run times are shown below in table 6, with details about the number of meshes and cores used, and the number of cells. The 'Computing time' column is an indicator of how long the simulation runs compared to its simulation time needed.

Table 6. Summary of mesh analysis simulations, 'ST' represents 'Simulation Time'

Cubic size	Total cells	Meshes/Cores used	Simulation time	Run time	Computing Time
15 meters	655360	4	3060 seconds (51 minutes)	2 hours	2 × ST
10 meters	2091320	16		19 hours	22 × ST
9 meters	2839252	16		15 hours	18 × ST
8 meters	4082400	16		24 hours	28 × ST
7 meters	6072000	16		22 hours	26 × ST
6 meters	8190720	32		14 hours	16 × ST

It was expected that the run time increases positively with the total number of cells. However, it is possible that the allocated computer cores (same as the number of meshes shown) were not appropriate for the 10 meters, 8 meters and 7 meters sizes. The author allocated the maximum number of cores on a computer (16) to all the cases between 10 and 7 (inclusive) meters size as it was assumed that using more cores allows a faster execution. This hypothesis was proved wrong, likely because there might be an optimal range of number of cells per mesh. The run time does not surpass 24 hours, whatever the mesh resolution. Thus, from a computational cost perspective, any resolution is feasible.

3.1.1. Fire spread

The simulations in general result in similar fire spread behavior in terms of the shape of the fire spread profile and the qualitatively judged average rate of fire spread. In the level set value slice, red means burned, blue means unburned, and the colors in between represent burning areas.

Figures 13a to 13f show that the fire front is very similar looking for most simulations after the 15 meter size. It can be seen that the fire spread follows the prescribed northwestern wind direction. The fire sizes, especially at 46 minutes, differ from one simulation to another. There is no clear trend on how this varies with the mesh resolution. However, the differences in results can be explained as they are likely due to the different unit obstacle sizes, affecting the wind profile at the terrain level differently. As with finer meshes than 6 meters, there might still be slight differences in the fire shape, these differences are not then very critical and can be accepted. Then since the fire shape in the 9 meters case looks the most like the shape in the 6 meters case, a resolution of at least 9 meters would be acceptable from the fire spread perspective.

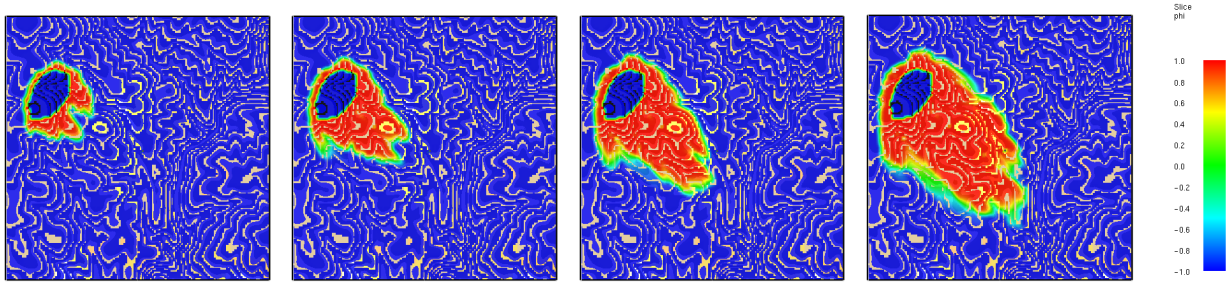

(a) 15 meters case

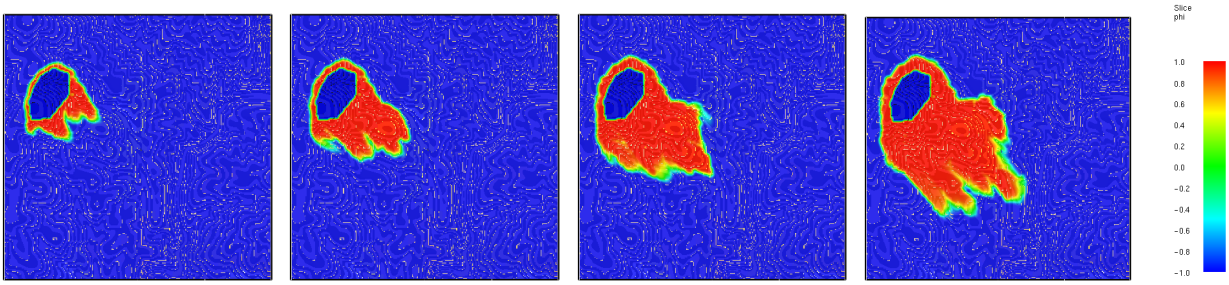

(b) 10 meters case

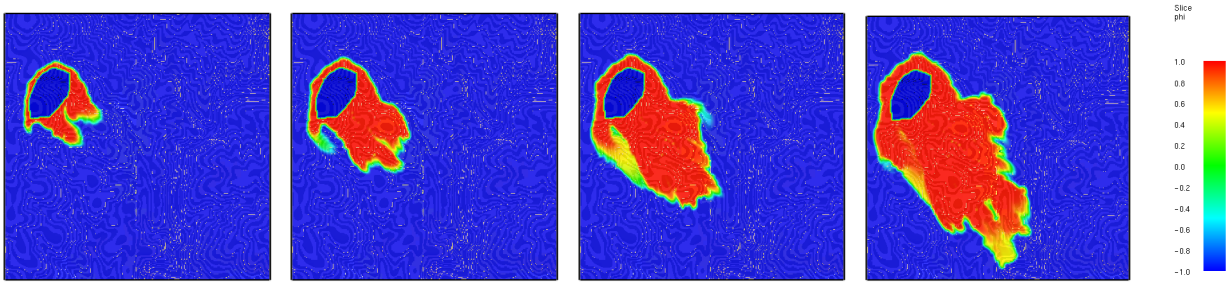

(c) 9 meters case

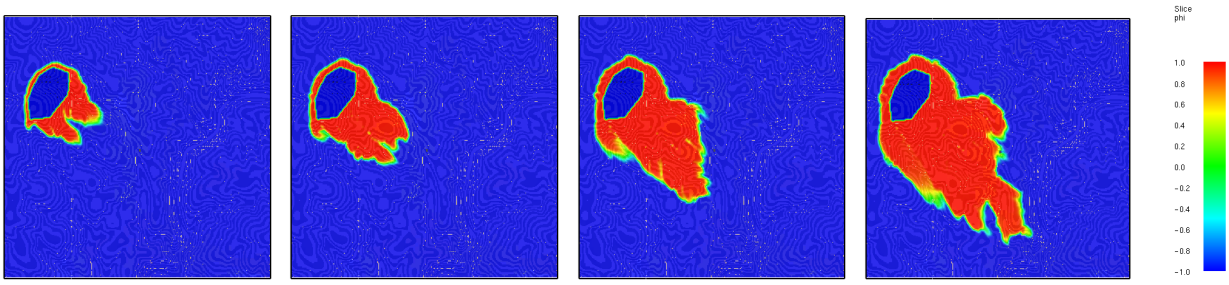

(d) 8 meters case

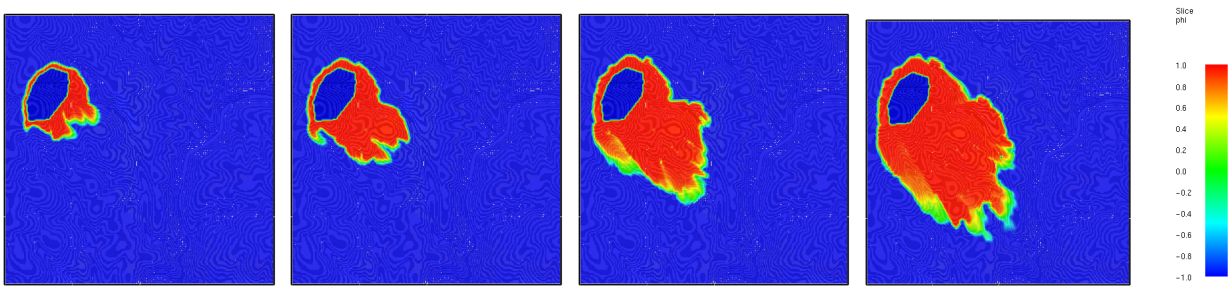

(e) 7 meters case

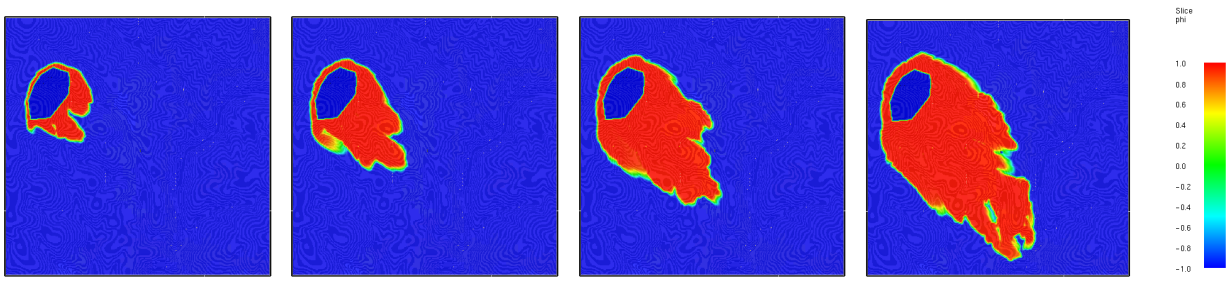

(f) 6 meters case

Figure 13. Fire spread at 11, 23, 35 and 46 minutes (left to right)

3.1.2. Heat release rate

In general, it is shown in Figures 14a to 14f that the total heat release rate seems to be relatively similar on average for all the simulations. For cases other than the 9 meter size, the time for the fire front to reach the shelter was between 39 and 44 minutes with no clear trend for the variation. It could be linked to the difference in obstacles sizes as well and its interaction with the wind direction.

For all the simulations and especially for the 9 meters case (fire reaches the shelter late compared to other cases), the path that the fire spread takes is also affected by the topography. Figures 15a and 15a are from the 9 meters case AGL slide results and show the shelter (in black) with the fire front (green and yellow) next to it, as well as the downward slopes (coloured in porcelain) between the obstacles with different heights. As the shelter is located in a relative valley or lower height than the areas around it, the fire front passes by it first, then slowly spreads towards the shelter.

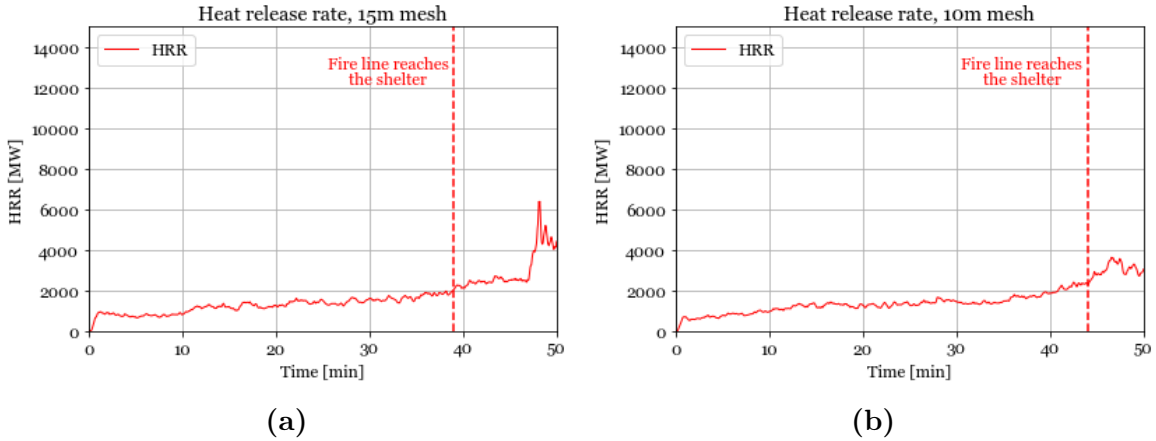

(a)

(b)

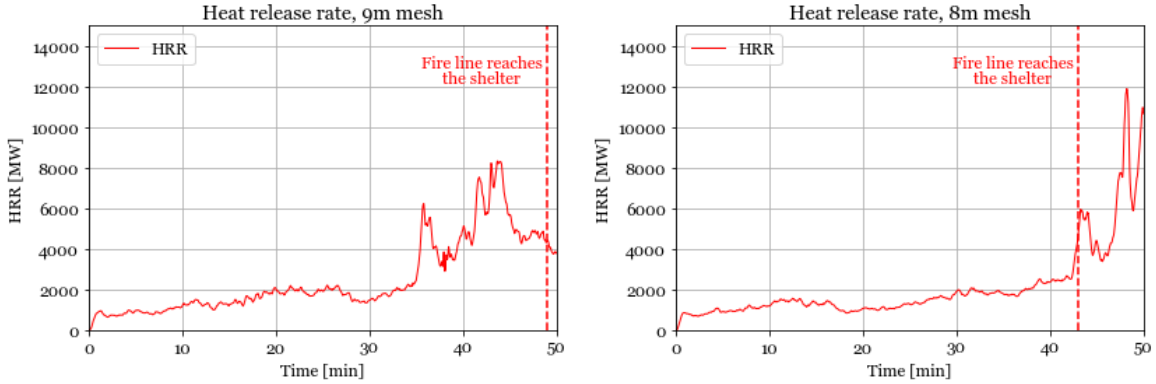

(c)

(d)

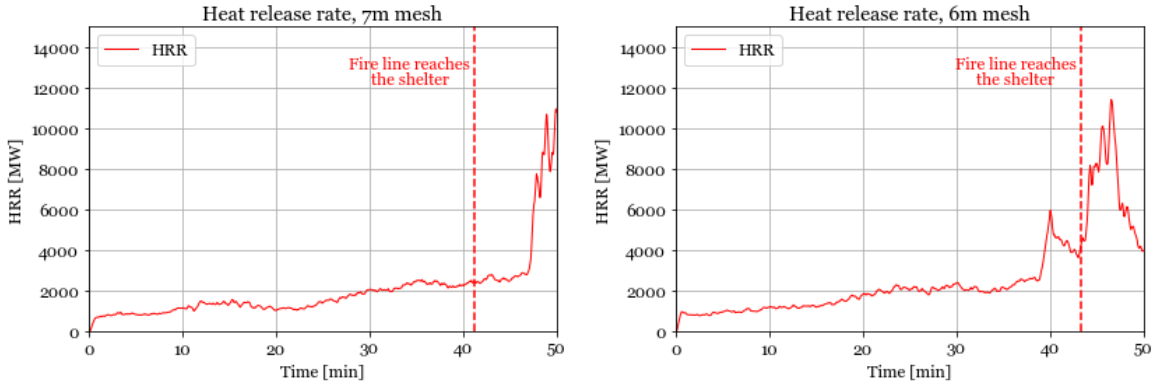

(e) **(f)**

Figure 14. Heat release rate plots for the large scale mesh analysis

When fire spread and heat release rate figures are jointly studied, it can be seen that when the fire reaches the southern part of the domain, the heat release rate and the fire spread rate significantly increase.

This is due to the presence of tall grass and chaparral vegetation only located in the south eastern part of the terrain. As shown in table 2 the tall grass and chaparral vegetation has a much larger mass per unit area than the dormant brush located in most of the terrain ($m_{tallgrass} = 2 \times m_{dormantbrush}$). In addition, the tall grass vegetation has around 260% the rate of spread of the dormant brush (table 2). As it was observed that the HRR depends on the areas reached by the fire, and since it was seen that at the moments when the same areas were burning, the resultant total HRR was the same on average for any mesh resolution, the HRR was deemed to not depend on the mesh resolution directly, but indirectly through the fire spread.

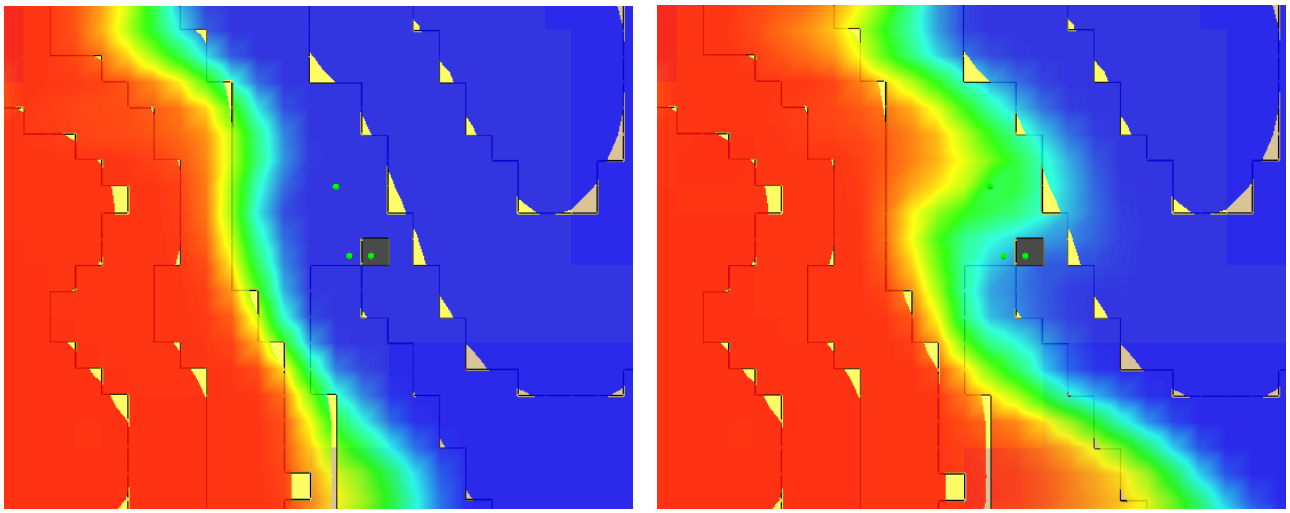

(a) 9m run at 45 minutes zoomed **(b)** 9m run at 50 minutes zoomed

Figure 15. 9m case fire spread analysed

3.1.3. Soot mass fraction

As for the soot mass fraction, the results look very similar for all the cases except the 15m mesh size. Figures 16a to 16f show that all the cases have a local maximum of the soot mass fraction at the height of 15 meters, at the moment when the fire line reaches the shelter. For the 15m mesh size, this maximum is at $5e^{-6}$ while for the other cases, it is between $6e^{-6}$ and

$8e^{-6}$ with no clear trend on the variation. It is best if the 15 meter mesh is avoided in this case. From the soot mass fraction perspective, any size smaller than 15m for the mesh cells would be acceptable.

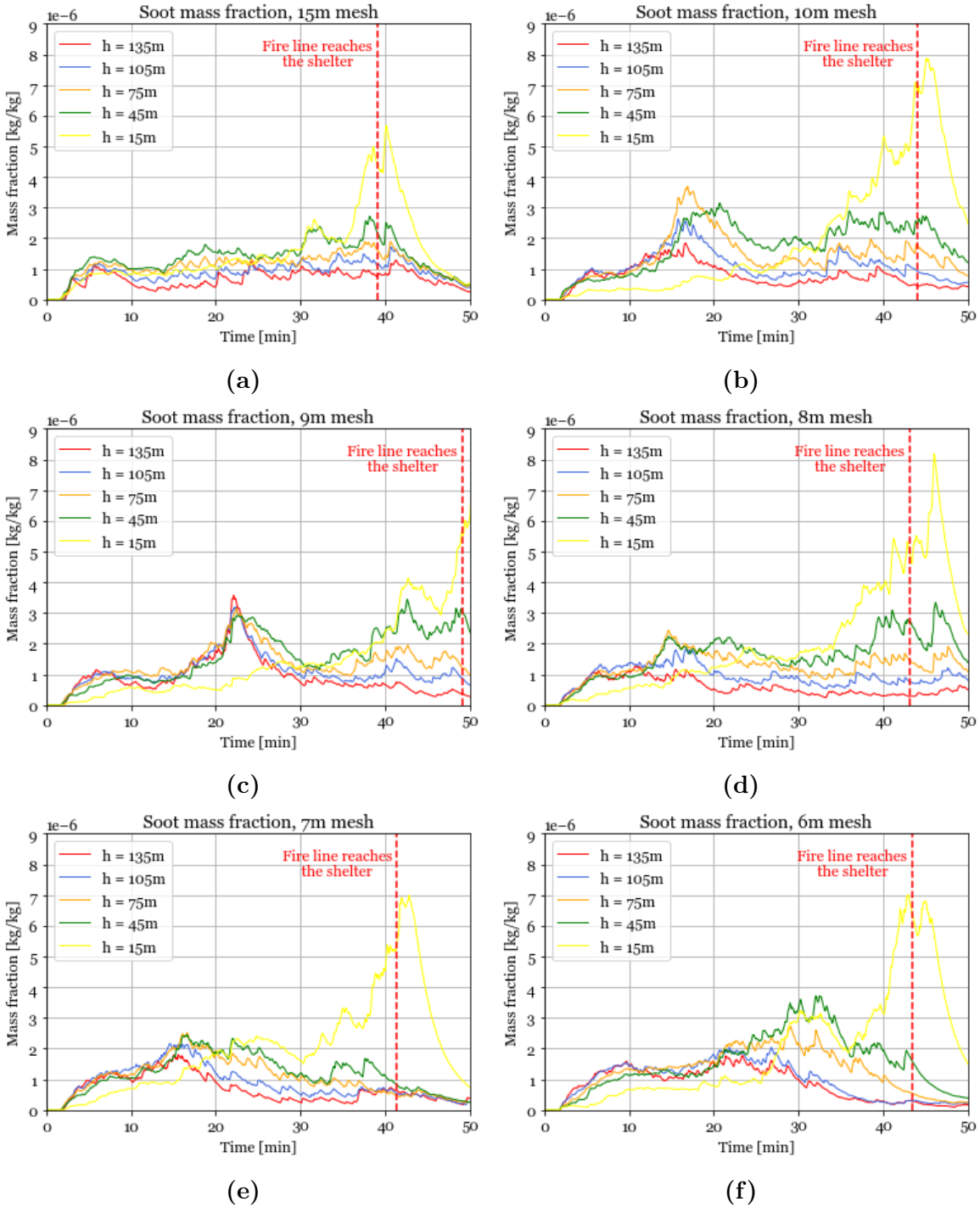

Figure 16. Soot mass fraction plots for the large scale mesh analysis

3.2. Small scale mesh sensitivity analysis

In this part, the small scale model mesh dependency is examined with a modified model according to the small scale model set-up in section 2.11. The case was set up strictly for mesh analysis purposes and was not intended to have the details included in the final small scale cases. In this part, the village is on the east (+x) and the shelter is not simulated. The model (see Figure 17) was according to a western fire, with a western wind of 10 m/s. The burner

was 326 x 18 meters and the domain spanned 476 meters in x, 382 meters in y and 75 meters vertically in z. The HRR was prescribed as 2000 MW as an example number inspired by the HRR results for the large scale mesh analysis. According to equation 2, the cell size with this HRR can range from 1 to 4 meters.

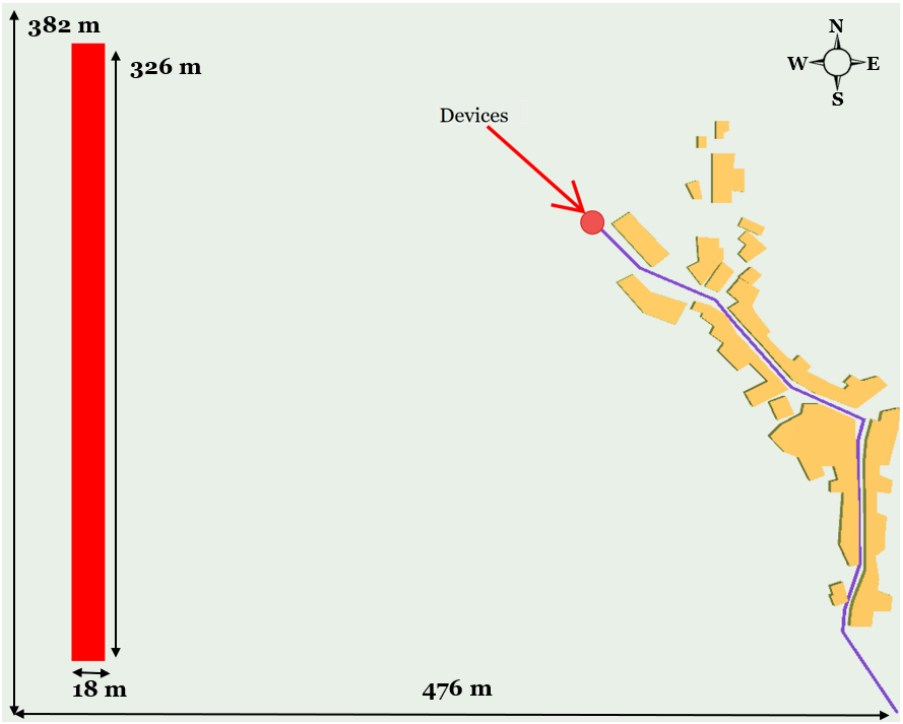

Figure 17. Small scale mesh sensitivity model

Since the model is large, a cubic cell size lower than 1 meter could not be run. For example, if the size was 50 cm, the number of cells would be in the hundreds of millions. It was not computationally feasible to use less than 1m cell size. It was run with a 1.5 and 1 meter cell sizes.

Upon looking at the heat release rate (HRR) graph of both simulations, it shown in 18a that the HRR line for the 1 meter mesh is very consistently constant and reproduces the prescribed HRR much more accurately than the 1.5 meters mesh line.

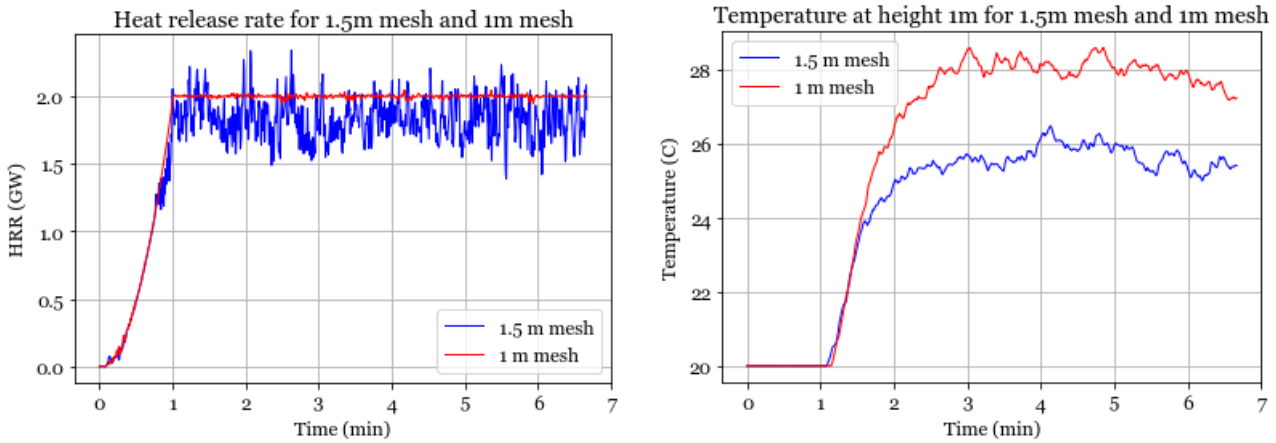

(a) (b)

Figure 18. Results plotted from 1.5m and 1m mesh simulations

Moreover, looking at the temperature graphs of each simulation, at the device location shown

in Figure 18b, at 1 meter height, the difference is already significant and the author decides to use a mesh cell cubic size of 1 m.

3.3. Large scale simulations

The results of the 8 large scale simulations run with a 9 meter resolution are shown in this section. The cases will be compared on the basis of the average rate of spread (RoS_{avg}) in section 3.3.1, calculated from the distance traveled by the fire divided by the duration it took to reach the community's closest point, and the heat release rate in section 3.3.2. The worst case is to be chosen as the case with the largest RoS_{avg} that is hypothesised to correspond to the case with the largest HRR, as it was previously elaborated in section 3.1.2 that the difference in RoS between the vegetation types in the model is accompanied by a similar difference in fuel mass per unit area which proportionally affects the heat release rate.

3.3.1. Average rate of spread

The average rate of spread is determined according to the following equation:

$$RoS_{avg} = \frac{D_{fire}}{t_{reach}} \tag{8}$$

Where:

- RoS_{avg} is the average rate of spread of the fire in meters per seconds (km/h);
- D_{fire} is the linear (non-topographic) distance traveled by the fire front from the fire at $t = 0$ s to $t = t_{reach}$, in meters (m);
- t_{reach} is the time at which the fire front collides with a structure or road in the modeled village, in seconds (s).

The distance of the fire to the community (including the shelter) in each of the cases is shown in the table 7 below:

Table 7. Distances between the initial fire line & community

Case	D_{fire} (m)
Southern fire	686
Northern fire	563
Eastern fire	813
Western fire	850

For the average wind speed, the four cases (S-AWS, N-AWS, E-AWS and W-AWS from nomenclature in table 4) are shown at the time of reach in the snapshots illustrated in Figures 19a-19d.

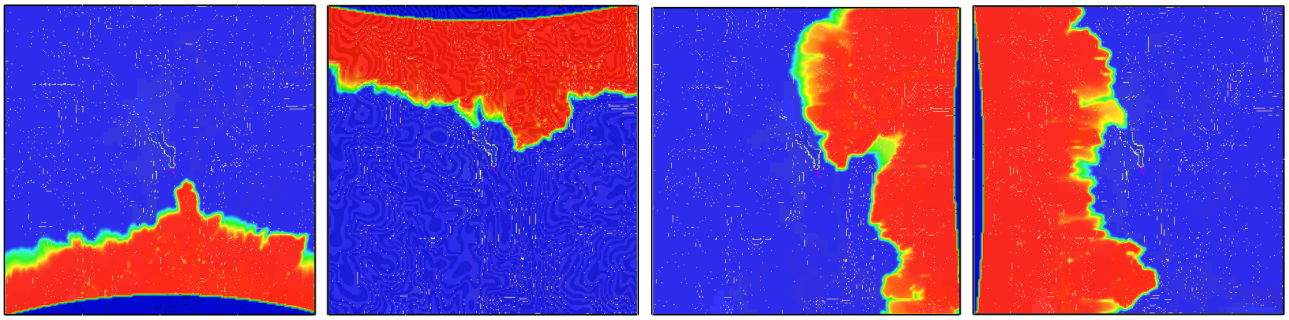

(a) $t_{S-AWS} = 41$ min **(b)** $t_{N-AWS} = 80$ min **(c)** $t_{E-AWS} = 78$ min **(d)** $t_{W-AWS} = 137$ min

Figure 19. Average wind speed cases with their respective t_{reach}

The results show that in case S-AWS, the fire reaches the community in 50% of the time of cases N-AWS and E-AWS. In addition, the fire from W-AWS takes the longest, around 328% the time it took for S-AWS fire.

Note that the fire line does not particularly look like an ellipse, and grows in some areas more than others. One of the reasons can be due to the topography, especially knowing that the fire evidently grows faster uphill than downhill due to buoyancy increase the heat transfer from convection, and the radiation increasing due to the smaller angle between the flame and the receiving surface. Another reason could be: the incident wind upon contact with an uphill topography can produce re-circulation which increases the turbulence and results in a larger RoS. It is also highly likely that this difference is linked to the difference in the vegetation contents of each mini-area, with different vegetation having different RoS as previously discussed in section 3.1.2.

The uneven fire line shape causes the fire to reach the community in an irregular way. Thus, to avoid confusion, and since this method will not be used to determine the ASET, the time at which the fire line reaches the community was defined as the time at which any part of the fire reaches any point of the community. It will be explained in further sections how a radius-based method, to determine the moment of fire contact with the community, would be more appropriate.

For the high speed wind cases (S-MWS, N-MWS, E-MWS and W-MWS from nomenclature in table 4), the results are shown in Figures 20a-20d.

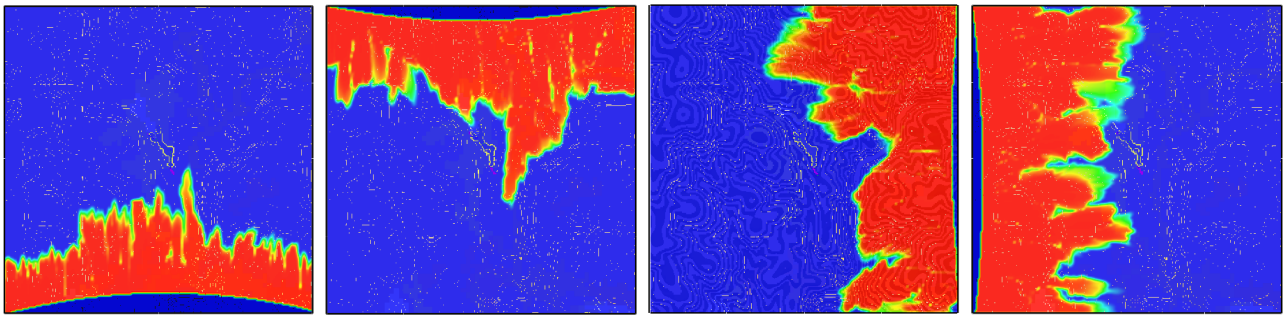

(a) $t_{S-MWS} = 7$ min **(b)** $t_{N-MWS} = 20$ min **(c)** $t_{E-MWS} = 22$ min **(d)** $t_{W-MWS} = 30$ min

Figure 20. Maximum wind speed cases with their respective t_{reach}

It is clear that the maximum wind cases produce a fire front line looking like an irregular asymmetric sinusoidal wave. Similarly in these cases, the fire in S-MWS reaches the community with the least elapsed time.

The calculated RoS_{avg} shown in table 8 show that the S-MWS case is the worst case scenario, in terms of the RoS_{avg} of the fire.

Table 8. Resulting RoS_{avg} of all the large scale cases in km/h

RoS of each case (km/h)							
Average wind speed				Maximum wind speed			
Southern fire (S-AWS)	Northern fire (N-AWS)	Eastern fire (E-AWS)	Western fire (W-AWS)	Southern fire (S-MWS)	Northern fire (N-MWS)	Eastern fire (E-MWS)	Western fire (W-MWS)
0.99	0.42	0.62	0.37	**5.64**	1.69	2.22	1.70

Based on the RoS_{avg}, the S-MWS (southern fire with maximum wind conditions) is the worst case scenario as it produces a RoS_{avg} equal to 5.64 km/h, around 254% of the second largest RoS_{avg} (E-MWS).

3.3.2. Heat release rate

The total heat release rate curves of the cases for average wind speed (AWS) and maximum wind speed (MWS) are plotted in Figures 21a and 21b respectively.

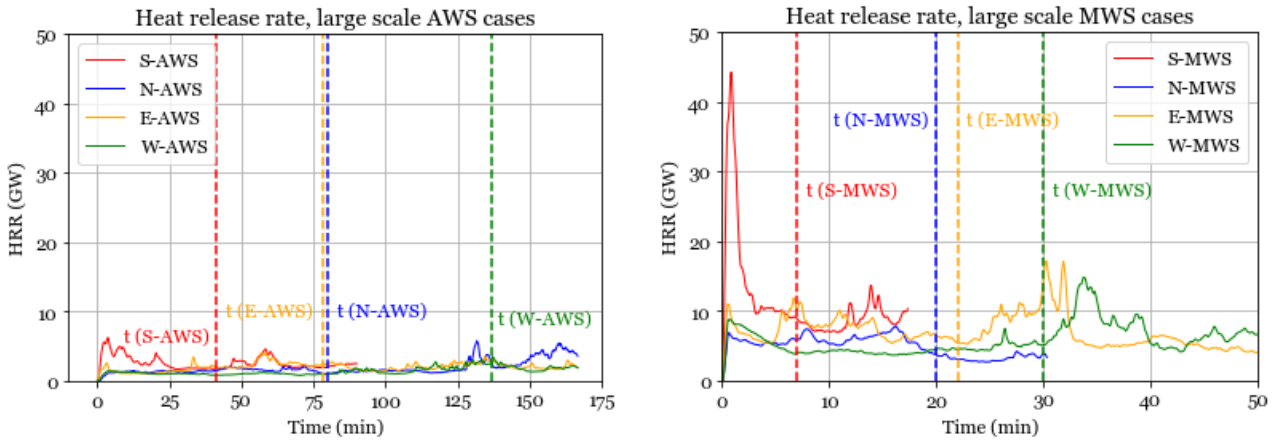

(a) AWS **(b)** MWS

Figure 21. AWS and MWS cases HRR comparisons, the vertical dotted lines represent $t = t_{reach}$ of each case

As can be seen in Figure 21a, for the AWS cases, the heat release rates do not differ drastically on average, to make the study consider a slower RoS of the fire as a potentially worse case. In the Figure 21b, it is seen that the HRR of the S-MWS case is considerably larger than the general average (10 GW), during the first quarter of the fire spread time t(S-AWS).

The results for the HRR confirm the previous statement that the S-MWS is the worst case scenario.

3.4. Small scale simulations

The results of all the small scale simulations are shown in this section. As it was determined in section 3.3 that S-MWS is the worst case scenario, its output was used to determine the prescribed HRR in the static burner. The same wind speed is also used (10 m/s) and the fire is situated south of the community. As shown in Figure 21b in section 3.3.2, in the duration leading up to the fire front reaching the community, for S-AWS, the HRR was 10 GW on average. Thus since the domain taken has a burner with a width of around 54% of the width of the original fire front or domain, the resulting prescribed HRR would need to be 5.4 GW.

As detailed in section 2.11, the burner has been put as a 3D object with dimensions of 520 x 80 x 2.75 meters and loaded with a surface type prescribing burning with a constant HRR per unit area (HRRPUA) of 120 kW/m^2 with its initial growth being exponential over 60 seconds. As the surface was applied to all the sides of the object, the total resulting HRR is:

$$\mathrm{HRR}_{\mathrm{total}} = 120 \times (520 \times 80 + 2 \times 520 \times 2.75 + 2 \times 80 \times 2.75) = 5.4\mathrm{GW}$$

The HRR plot for all the small scale cases is shown in Figure 22

The first distance checked is at 300 meters from the shelter, as a first guess of the critical distance. The next sections will emulate the journey of locating the first distance with untenable conditions.

The axis shown in Figure 23 will be filled with information from next cases and serves as a graphical guide to understand the logic followed during this study. This part basically follows a trial and error methodology to find the last safe distance. The performance criteria specified

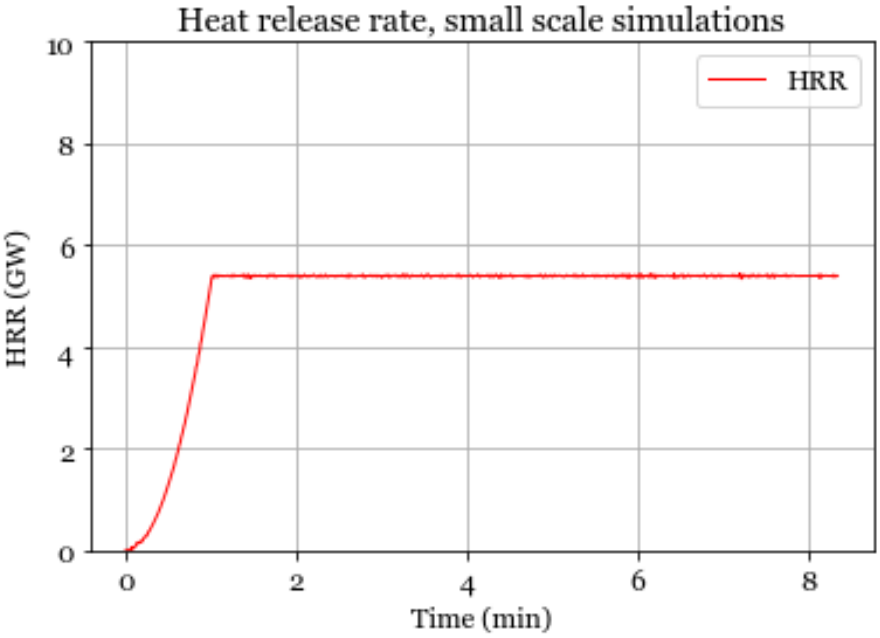

Figure 22. HRR of small scale simulations

Figure 23. Axis 0 to illustrate the case scenarios

in section 2.12 will be evaluated. For the temperature and radiative heat flux, as the limit must not be reached at heights < 3 meters, the values at 3 meters will be checked, for 6 road locations between location 1 and 26 (locations shown in section 2.11 Figure 12) as plotting 26 curves would be unclear.

As for the FED, the output from FDS is the integral of the instantaneous FED as shown in section 2.12 equation 4. As the instantaneous FED depends directly on the concentrations of the different toxic gases and soot, and as these concentrations are higher when the fire is closer to the community, the instantaneous FED in these small scale cases is evidently larger than earlier during the fire spread. Thus, if it is assumed that this slope (instantaneous FED) has been equal for the duration of the fire spread before reaching the shelter for the S-MWS large scale case examined (7 minutes for S-MWS), the total FED would be over-predicted making the checked value, a conservative one. Thus, from the total FED output of the following simulations, the slope is extracted (in min^{-1}) and multiplied by 7 minutes (see Equation 9), and the resulting value is checked with a tenability limit of 0.3 maximum.

$$\text{FED}_{\text{total,inhaled}} = 7 \times \frac{\delta}{\delta \text{t}} \text{FED}_{\text{graph}} \tag{9}$$

3.4.1. Case: 300 meters distance

The results from this simulation are shown in Figures 24a to 24f. As can be seen, the temperature is very similar at 2 meters and at 3 meters, suggesting that it was indeed important to look at both heights. It is fluctuating between $\approx$ 40 C and $\approx$ 56 C which is lower than 60 C. From the temperature perspective, the conditions are tenable.

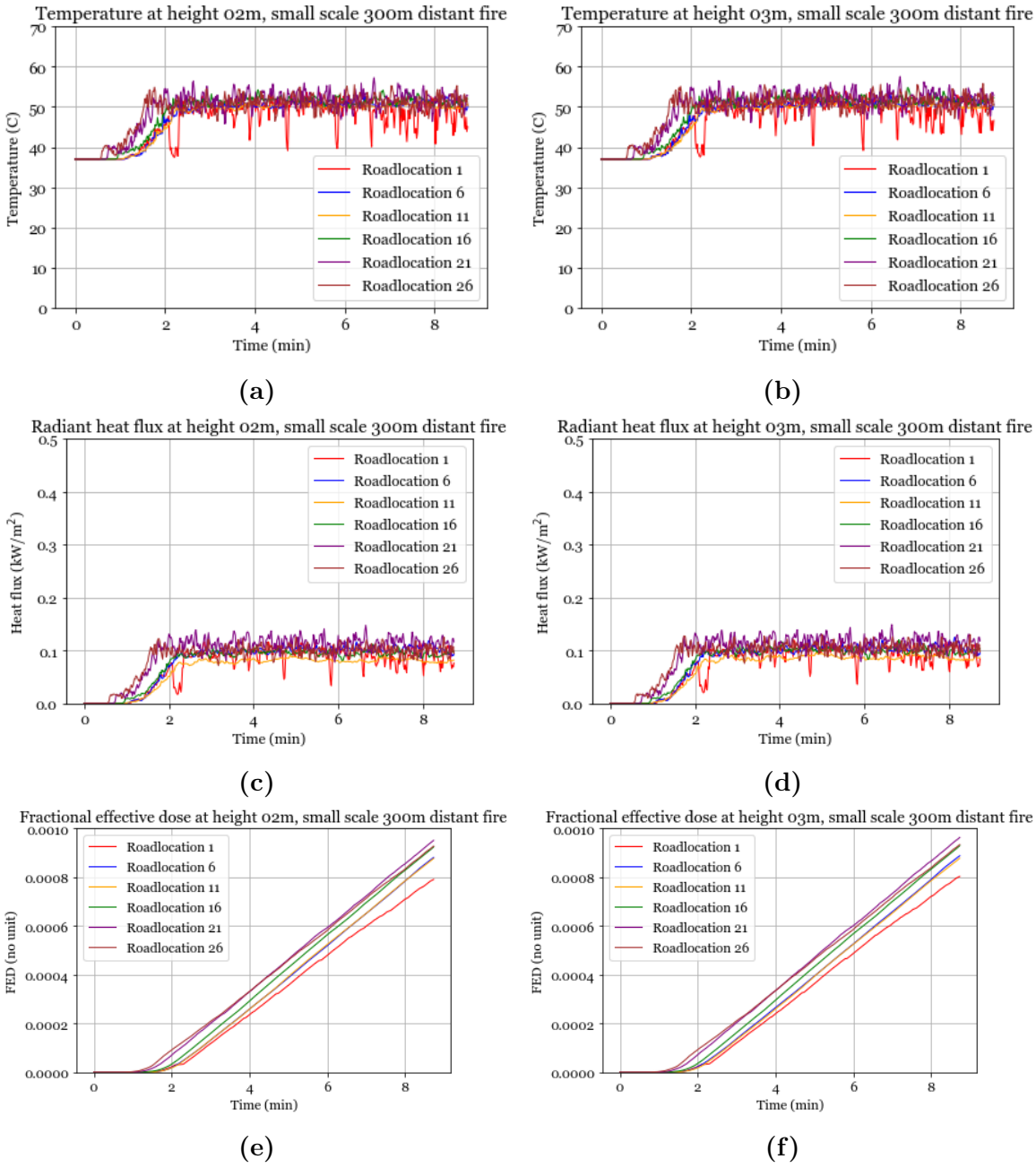

Figure 24. Plotted results for the 300m case

For the heat flux, the values reach a maximum of $\approx$ 0.125 kW/m^2 which is considerably lower than 1.7 kW/m^2. From the radiant heat flux perspective, the conditions are tenable.

The FED slope from Figure 24f is extracted: 0.00013; the total FED is calculated according to equation 9 to be 0.00091 which is negligible compared to 0.3. From the FED perspective, the conditions are tenable.

Thus the distance 300 m is associated with tenable conditions, the next distance to be examined is the 200 m (Figure 25).

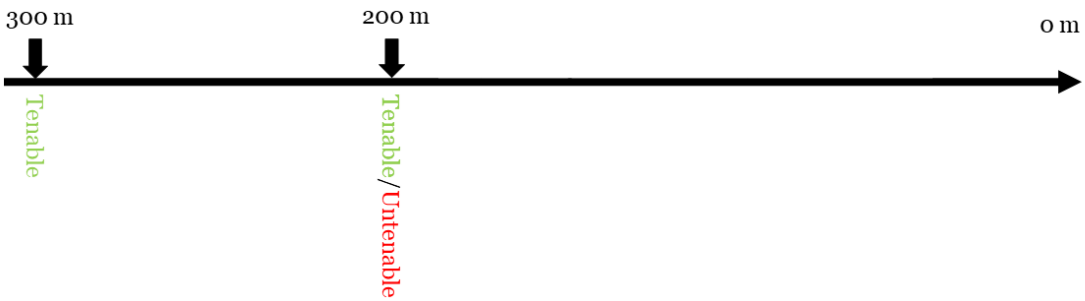

Figure 25. Axis 1 to illustrate the case scenarios

3.4.2. Case: 200 meters distance

The results from this simulation are shown in Figures 26a to 26f.

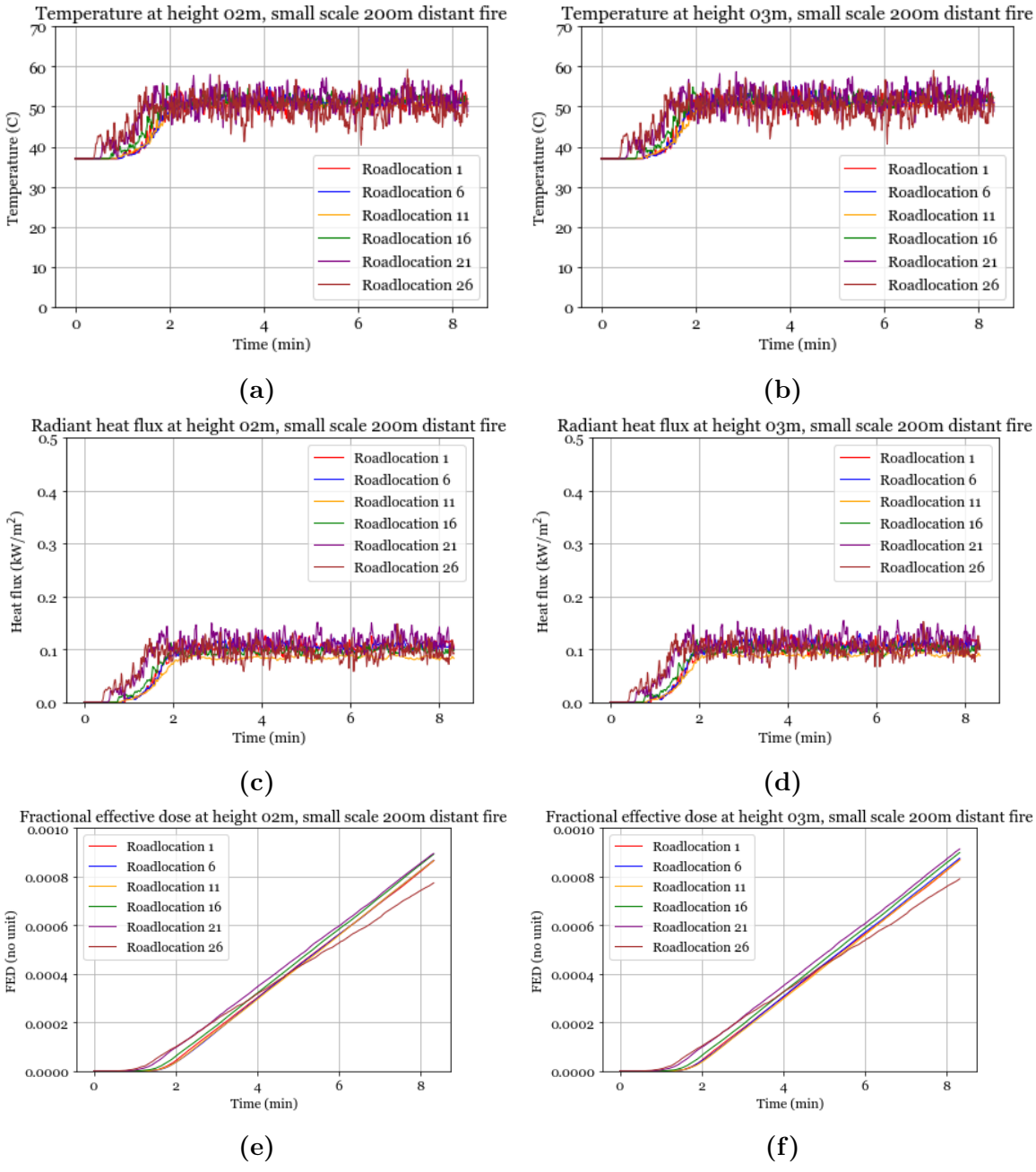

Figure 26. Plotted results for the 200m case

The temperature is seen to be fluctuating between ≈ 41 C and ≈ 56 C which is lower than 59 C. From the temperature perspective, the conditions are tenable.

For the heat flux, the values reach a maximum of ≈ 0.15 kW/m^2 which is considerably lower than 1.7 kW/m^2. From the radiant heat flux perspective, the conditions are tenable.

The FED slope from Figure 26f is extracted: 0.00013 again; the total FED is calculated according to equation 9 to be 0.00091 again which is negligible compared to 0.3. From the FED perspective, the conditions are tenable.

Thus the distance 200 m is associated with tenable conditions, the next distance to be examined is the 100 m (Figure 27).

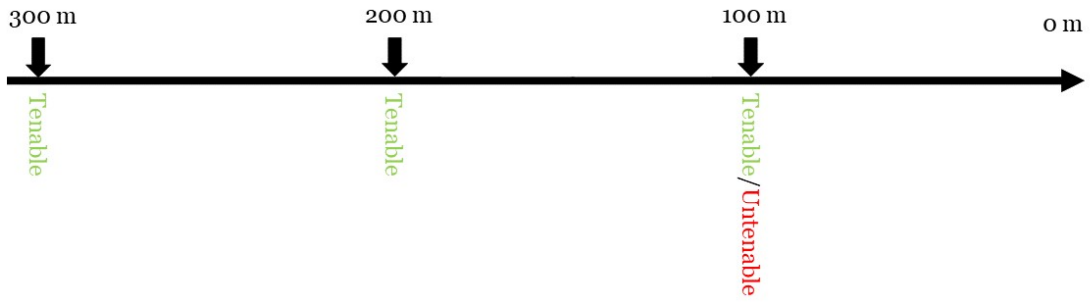

Figure 27. Axis 2 to illustrate the case scenarios

3.4.3. Case: 100 meters distance

The results from this simulation are shown in Figures 28a to 28f. As can be seen, the temperature is fluctuating between ≈ 40 C and ≈ 69 C which is 15% higher than 60 C.

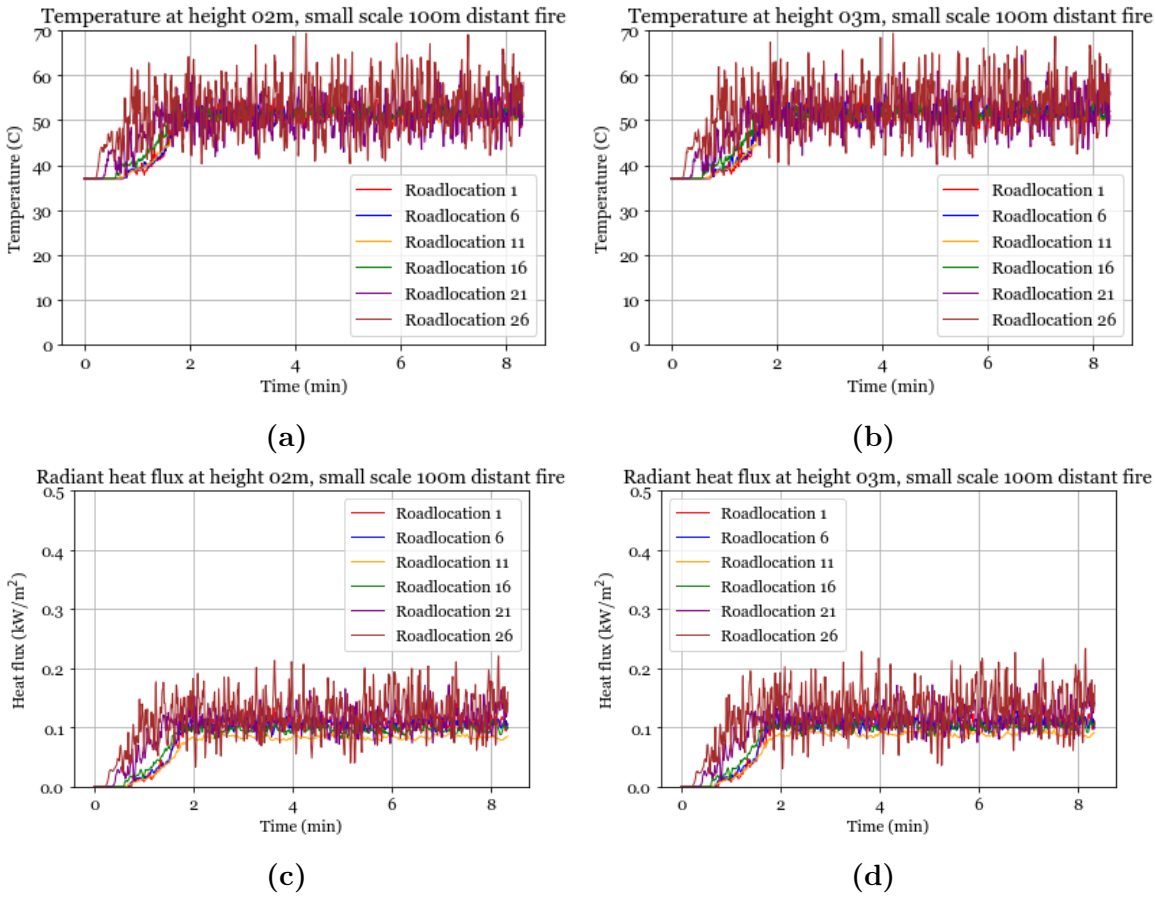

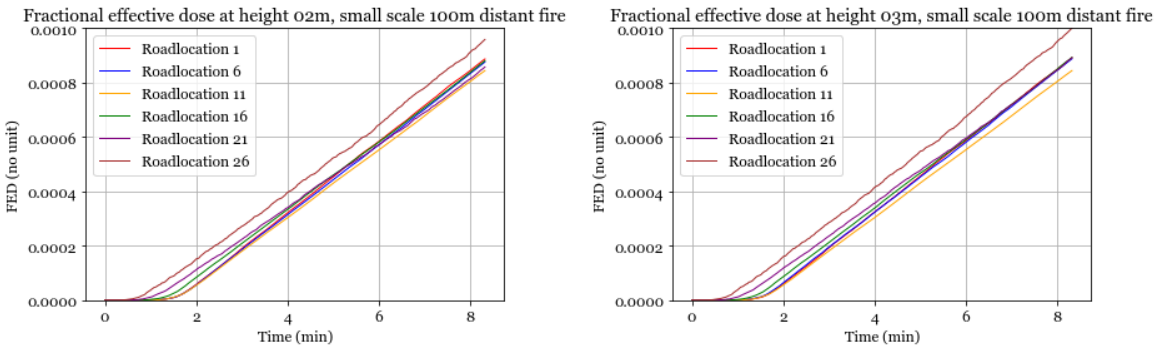

(e) **(f)**

Figure 28. Plotted results for the 100m case

Thus, from the temperature perspective, the conditions are untenable.

For the heat flux, the values reach a maximum of ≈ 0.235 kW/m^2 which is considerably lower than 1.7 kW/m^2. From the radiant heat flux perspective, the conditions are tenable.

The FED slope from Figure 28f is extracted: 0.00013 again; the total FED is calculated according to equation 9 to be 0.00091 again which is negligible compared to 0.3. From the FED perspective, the conditions are tenable.

Thus the distance 100 m is associated with untenable conditions because of the temperature reaching 15% over the acceptable 60 C, the next distance to be examined is the middle between 100 and 200 m: 150 m (Figure 29).

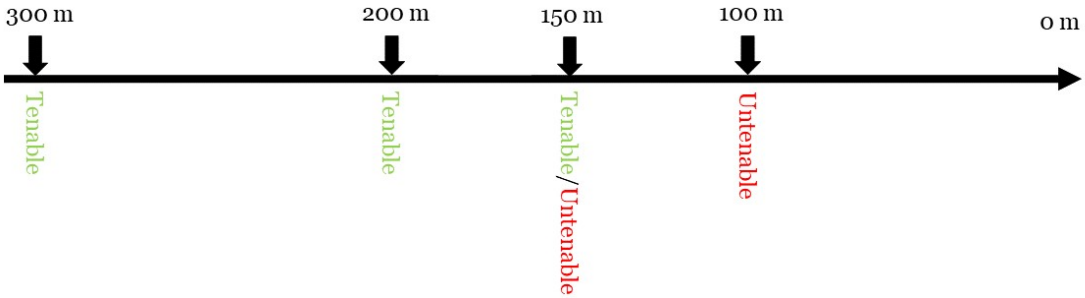

Figure 29. Axis 3 to illustrate the case scenarios

3.4.4. Case: 150 meters distance

The results from this simulation are shown in Figures 30a to 30f.

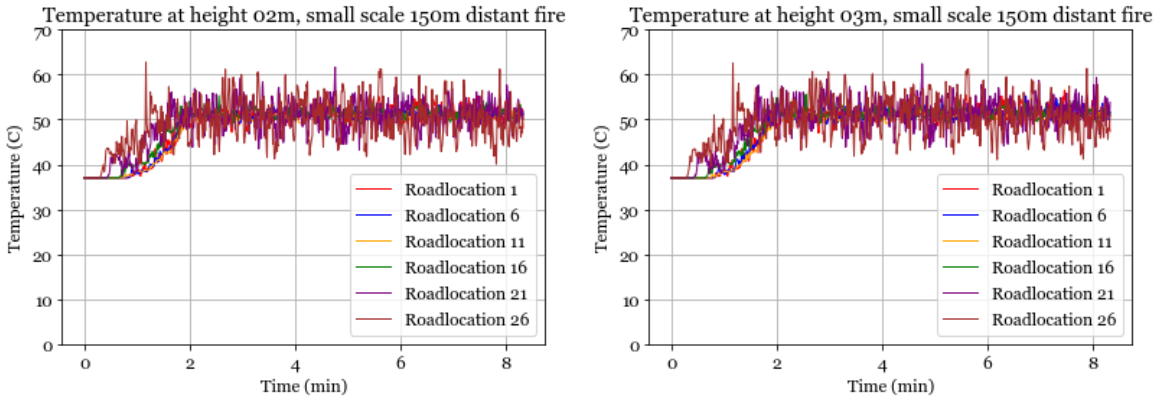

(a) **(b)**

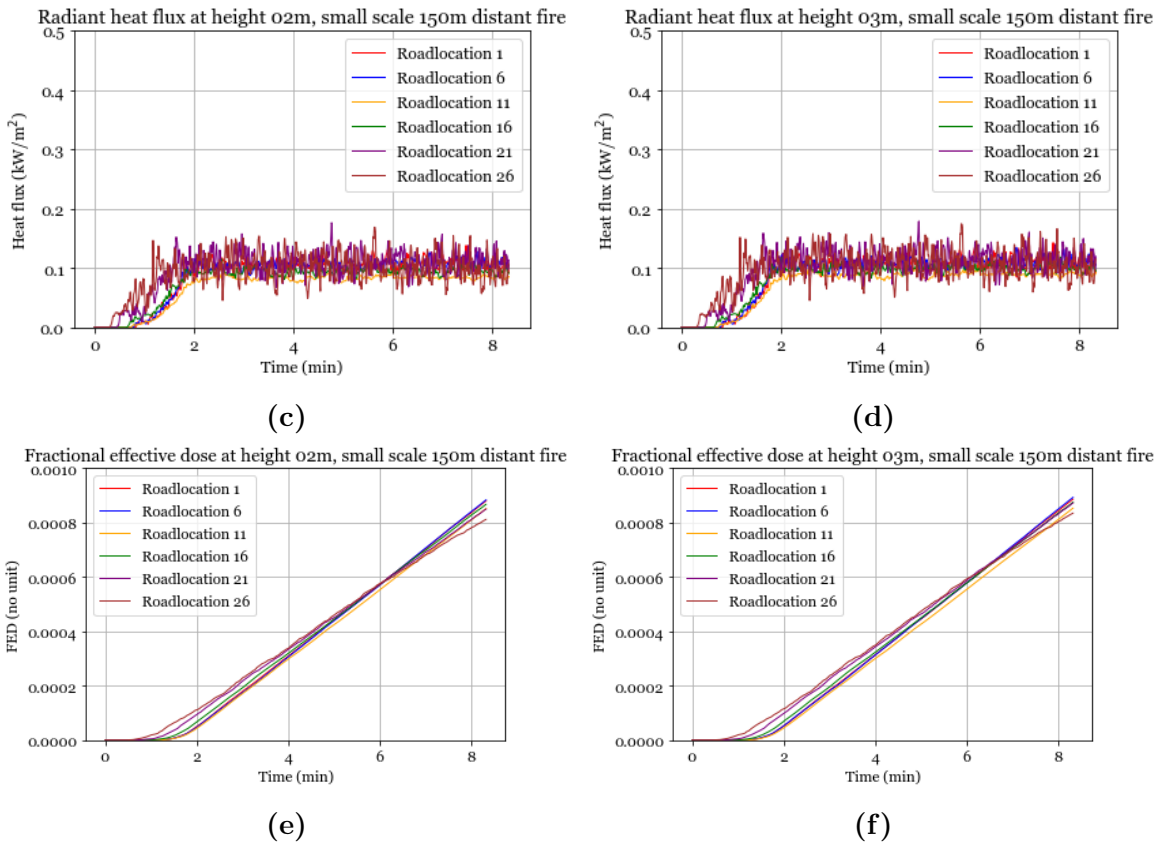

Figure 30. Plotted results for the 150m case

As can be seen, the temperature is fluctuating between ≈ 40 C and ≈ 63 C which is 5% higher than 60 C. From the temperature perspective, the conditions are untenable.

For the heat flux, the values reach a maximum of ≈ 0.18 kW/m^2 which is considerably lower than 1.7 kW/m^2. From the radiant heat flux perspective, the conditions are tenable.

The FED slope from Figure 30f is extracted: 0.00013 again; the total FED is calculated according to equation 9 to be 0.00091 again which is negligible compared to 0.3. From the FED perspective, the conditions are tenable.

Thus the distance 150 m is associated with untenable conditions because of the temperature reaching 5% over the acceptable 60 C, the next distance to be examined is the middle between 150 and 200 m: 175 m (Figure 31).

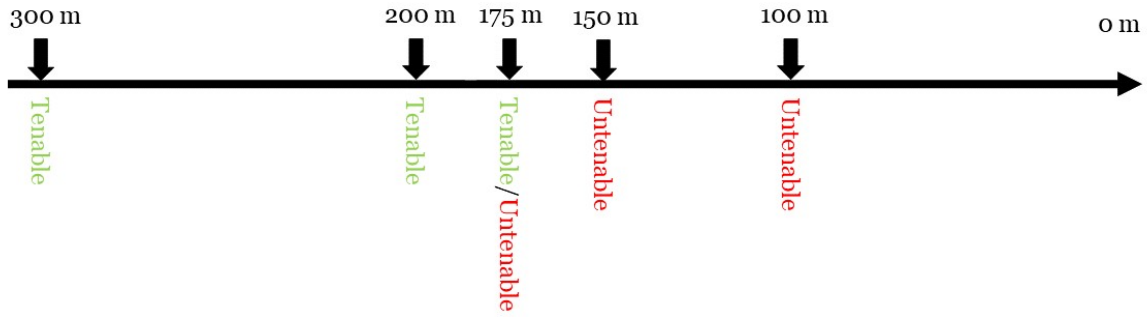

Figure 31. Axis 4 to illustrate the case scenarios

3.4.5. Case: 175 meters distance

The results from this simulation are shown in Figures 32a to 32f. As can be seen, the temperature is fluctuating between ≈ 40 C and ≈ 61.5 C which is 2.5% higher than 60 C. From the

temperature perspective, the conditions are untenable.

For the heat flux, the values reach a maximum of ≈ 0.16 kW/m^2 which is considerably lower than 1.7 kW/m^2. From the radiant heat flux perspective, the conditions are tenable.

The FED slope from Figure 32f is extracted: 0.00013 again; the total FED is calculated according to equation 9 to be 0.00091 again which is negligible compared to 0.3. From the FED perspective, the conditions are tenable.

Thus the distance 175 m is associated with untenable conditions because of the temperature reaching 2.5% over the acceptable 60 C.

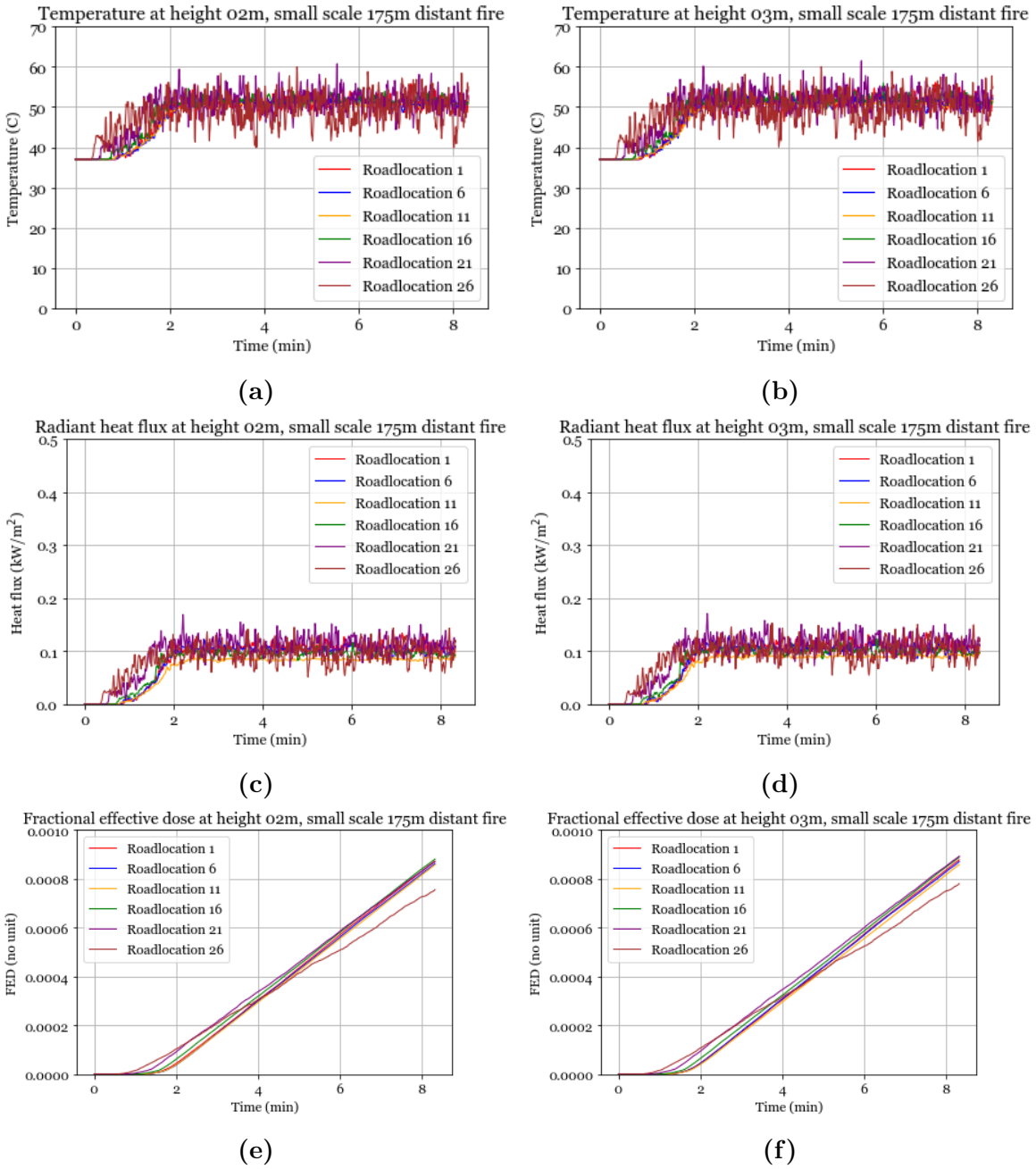

Figure 32. Plotted results for the 175m case

3.4.6. Small scale results

The simulation distances and their tenability is summarised in the Figure 33 showing that a distance of 200 meters is proper for the performance criteria that were specified. The tem-

perature reached was the critical criterion as the other criteria weren't close to reaching the limits.

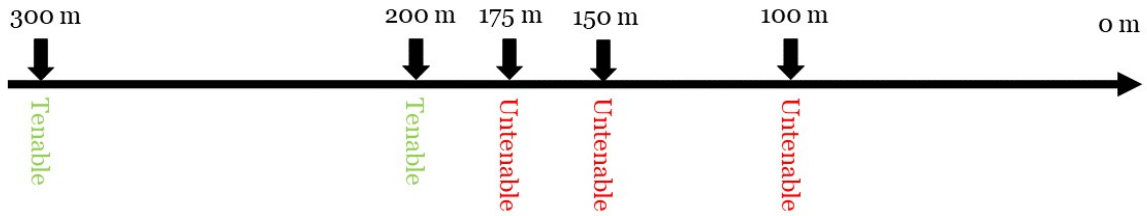

Figure 33. Summarising axis to illustrate the case scenarios

3.5. Establishing a perimeter

The results suggest that it is better to implement a safe distance of 200 meters from any point in the village as a perimeter at which ASET is determined. It is more conservative to form an encasing rectangle, with sides 200 meters away from the most southern, most northern, most eastern and most western points (forming the yellow rectangle as seen in Figure 34). The resulting perimeter would be the rectangle in blue.

Figure 34. Monhinos Cimeiros village delimited in yellow with its new ASET perimeter shown in blue

The new times of the fire front reaching the village (according to the new basis) are shown in figures 35a to 35d. As seen in table 9 there is a difference of 3.6 minutes for the worst case scenario in the Southern case when using the 200 meter perimeter. As for the Northern, Eastern and Western scenarios, there is a difference of 11.6, 13.1 and 15.3 minutes respectively. This shows the direct effect of the followed methodology on the ASET, overall reducing the time available for habitants to reach the shelter, by up to 15.3 minutes in strong wind cases.

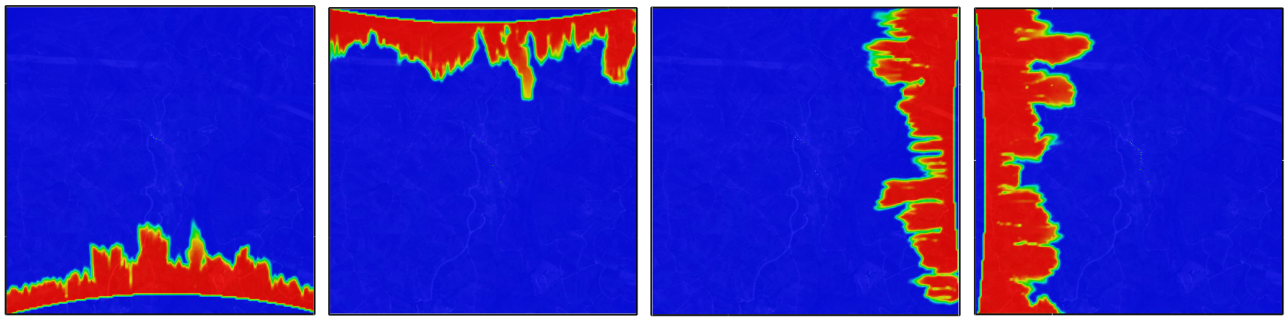

(a) $t_{S-MWS} = 3.4$ min **(b)** $t_{N-MWS} = 8.4$ min **(c)** $t_{E-MWS} = 8.9$ min **(d)** $t_{W-MWS} = 14.7$ min

Figure 35. Maximum wind speed cases with their respective t_{reach} for the new perimeter

Table 9. The effect of the new perimeter in terms of minutes lost from the WASET

Time until the fire reaches the community (minutes)				
Fire	Southern	Northern	Eastern	Western
Taken from first contact with village	7	20	22	30
Taken from first contact with WASET perimeter	3.4	8.4	8.9	14.7
WASET resulting difference	-3.6	-11.6	-13.1	-15.3

4. Discussion

4.1. Observations

In this section, the author will discuss his observations in four parts, about the four main parts of the results: the large scale mesh analysis, the small scale mesh analysis, the large scale simulations and the small scale simulations.

In the case of life safety, the results show that the untenable conditions are first reached due to the air temperature reaching 60 C which is a reasonable limit for comfort, especially noting that the village habitants might largely be composed of older people. This could mean that convection is the main threat from a WUI fire before it reaches the area (at distances >200 meters). Note that this could be due to the strong wind implemented in the simulation, as it could be greatly influencing the air temperature at 2 and 3 meters height by horizontally transporting the hot air from the fire to the village, before it can vertically be transported with buoyancy. This makes the approach more conservative as the maximum wind speed would not usually be maintained constant.

4.1.1. Observations in large scale mesh analysis

The simulation run time was different for each cell size. Normally, there would be a lower run time for a coarser grid, but it appears that the optimal number of cells per computer core was not used. This resulted in large run times overall. Another factor that could be affecting the run time results is the computer used for simulations, as two different computers with different processors were used, comparing the run times is not beneficial.

The fire spread has been shown to depend on the wind direction as the fire spread overall direction is the same as the prescribed wind direction. Although these findings are expected as the level set method takes the wind direction as input to calculate the fire front next location, the results still show that the model is working as intended and that the wind is coupled with the empirical model in FDS.

The total heat release rate, just like the fire spread profile, has been shown to be relatively similar for mesh sizes from 15 meters to 6 meters. It is dependent on the fuel burned, if the fire reaches an area with a higher fuel load, the heat release rate increases. The differences in the HRR results between the different mesh sizes, are due to the fire reaching areas with a different fuel type at different times, as these areas lie on the sides of the main fire spread cone. It can thus be concluded that the mesh resolution or the obstacle sizes, did not affect the relationship between the fuel beds and the resulting HRR. In other words, the HRR plot differences are attributed to small secondary fire spread differences that come from differences in obstacle size (figure 15).

The soot mass fraction results were only used to compare mesh sizes, as with coarse meshes, it is not possible to look at measurements at 2 and 3 meters heights where they matter. The results suggest again that there is little difference between a coarser mesh (15 meters) and a finer one (6 meters).

The capability of FDS of implementing the level set method, with a high speed wind, has been shown to be possible even at cubic mesh sizes of 15 meters, with very small differences in the results compared to finer meshes. This allows larger domains to be run with reasonable computing time and power, while implementing a safety factor on the results to make up for the coarse grid. A lower number of mesh cells also allows for many case scenarios to be run. For example, this thesis studies a fire that supposedly already started far away from the village, but simulates it when it's at around 900 meters distant. The findings suggest that it is possible, having a larger elevation data domain, to simulate the fire from its ignition, and see how the ignition location affects the fire spread. Moreover, future research can also examine whether or not certain ignition locations lead to the wildfire reaching the village.

In addition, with more simulations of more cases, with different mesh sizes, the validity of using a 15 meter mesh or coarse will be confirmed or denied. Also, simulations representing a real life case of a WUI fire, could theoretically be used to validate the model and its inputs.

4.1.2. Observations in small scale mesh analysis

As for the small scale mesh analysis, the mesh size has been shown to accurately represent the flame, judging qualitatively from the HRR plot: a constant HRR is prescribed and the plot is very close to a straight line with the 1 meter cubic cell size. Finer meshes could not be examined as the computing power does not allow getting results in a timely manner that fits the current study's duration. In future studies, the mesh dependency can be further examined, while also looking at quantitative methods such as the measure of turbulent resolution, the wavelet error measure, the local cell Reynold's number and the near-wall grid resolution [19].

4.1.3. Observations in large scale cases

Overall, the results agree with the initial expectation that a larger wind velocity would increase the fire spread rate. The source of the fire also plays a role as the terrain contains different types of vegetation, some with a higher fuel content and a larger fire rate of spread. For the Moninhos Cimeiros and according to the available data for vegetation and elevation, a fire coming from the south likely to have a much larger average rate of spread than other directions, on average. It's important to take this result noting the assumption that the fires would have an equally developed and equally distant fire front, at time 0. Simulations with larger domains, taking into the scope, the initial point ignition, could lead to different results. Thus, the results in this study serve more as an example of the methodology proposed.

The results also show that the HRR, is on average around five times larger when the wind speed is maximum (10 m/s) compared to when it is the average (1.5 m/s). Upon looking at the fire spread profiles, one explanation could be that the fast wind cases have uneven spread progress across the fire front, while the average wind cases look like the fire spread progress is even on all the fire front. In other words, the area of the fire front with fast wind is larger than the one with average, so more area is being burned at a given moment compared to the average wind case. The reason for this behaviour is unclear. One observation could be that the fast fire reaches some areas of the fire front more than others, accelerating the spread at these areas only. Uphill areas can be more affected by incident wind and thus spreading fire more rapidly. The average wind could be too weak to affect uphill and flat areas differently. A study done in 2016 [41] comments that the fire spread results in level set simulations as well as the merging behaviour of the fire front are not well studied, especially for complex terrain as in this thesis. Perhaps more large scale simulations should be conducted, after determining the proper mesh to use, to be able to explore the role of the terrain on the behaviour of the fire spread.

In general, not many comments can be made about the values of the RoS for the simulations as this is a specific case. It is best to not focus on the results of this thesis from a fire spread perspective, but from a safe perimeter definition method. Although the thesis used the Monhinos Cimeiros village as a case example and FDS level set model for fire spread, any other fire spread model discussed in 1 can be used with its outputs, replacing the level set method. The takeaway is to use the small scale simulations in FDS to determine the tenability conditions, in order to understand the severity level when the fire is still at a distance from the village and define a safe perimeter acting as a safety barrier for the WASET.

4.1.4. Observations in small scale cases

The small scale fire simulations made according to the large southern fire case, are an oversimplification in many aspects. The simulations assume that the fire stopped at a certain distance

and maintained a constant rate of heat release. Although this assumption is considered safe, it is a worse-case scenario compared to the actual behavior of the fire. In reality, the fire travels and is much farther away before it reaches the 300-meter mark, for example. At greater distances, the fire has less of an impact on the tenability conditions in the village. Therefore, assuming a static fire at 300 meters over-predicts the impact because it approximates the traveling fire to a closer static fire.

In this part, the fine mesh used allowed the production of a resolved flame examining the temperature, radiative heat flux and the FED. The results were used to determine if the conditions would be tenable in the village at a certain distance of the fire front.

The radiative heat flux results are in large disagreement with the values empirically calculated according to [45] using the correlations from [40] (see appendix A). The results from FDS are considerably lower than the calculated ones. This is likely be due to the fact that FDS accounts for radiation losses to particles in the air, including the highly absorbing soot [19]. However, even when looking at the empirical results, the 200 meter perimeter would still be satisfying the radiant heat flux criteria.

The temperatures in the result are measured in the air along the main and only road of the village. As the temperature limit is reached first, before the FED or heat flux get any close to their limits, it is learned that the main hazard from a distant wildfire could be the ambient temperature.

The FED results carry a very high uncertainty. The slope being constant in the graphs is expected. As the FED in FDS ultimately depends on the concentrations of CO, CO_2 and O_2 (see section 2.12 equation 9) [19], the yields are constant as the HRR is constant, meaning the concentrations will be constant as the prescribed wind is also constant. The method employed in this thesis did not incorporate HCN, NO_x, HCl, HBr, HF, SO_2, NO_2, C_3H_4O, CH_2O yields. Thus the FED could be misrepresenting the reality of the toxicity conditions. Depending on which of the latter is emitted in wildfires, the yields should be included in future analysis to measure more accurately the FED.

4.2. Main findings

The current thesis contributes to the WUI wildfire research through the following main findings:

- In FDS, using the level set model, the mesh resolution had little effect on the results of the fire spread. Moreover, it was shown that the mesh resolution had little effect on the heat release rate output from identical fuel types.
- The level set model in FDS is not yet ready for operational uses for real-time prediction of the fire spread because its simulation time is larger than the time simulated.
- There is a significant need for a developed guide on WASET criteria in WUI fires derived from state of the art research, or at least a preliminary recommendation on which life safety criteria to consider. It would be valuable to investigate how smoke visibility can be studied in the context of WUI fires, and how it can be modelled properly.
- A preliminary performance-based approach was proposed to establish a perimeter around a WUI community as a safety buffer at which the WASET is determined (when the fire spread reaches the perimeter).
- For the Moninhos Cimeiros village, it was determined that a rectangular perimeter whose sides are 200 meters away from the community's encasing rectangle is needed. It was found that when the fire is at this perimeter, the air temperature in the community at 2 and 3 meter heights might reach over 60 degrees Celsius.
- There is a need for more combustion data for vegetation that would also be compatible with the FDS combustion input methods.

- The methods used in this thesis entail considerable uncertainties and assumptions necessary to its development, but detrimental to the accuracy of the results. It is thus important to carefully proceed and improve the sources of uncertainties first before utilizing the results for real life applications.

4.3. Relation to research questions

The research questions posed in section 1.5 were explored and after the study conducted, the corresponding answers would be as follows:

1. What is the effect of wind velocity on the WUI fire front development and total heat release rate, considering a WUI fire modelling approach?

As hypothesized, a high wind velocity was shown to increase the average rate of spread of the wildfire by up to more than 5 times in the worst case scenario, compared to an average velocity. Thus, it is important to consider the worst case climate and highest wind speeds recorded in a case study location. Moreover, high speed wind was shown to cause a more heterogeneous fire front line, and uneven fire growth. It also resulted in a much larger heat release rate (5 times larger on average). It is unclear whether the larger heat release rate was caused by the uneven fire line causing more areas to be burning at a time.

2. What are the proper criteria for tenability conditions in a village exposed to a WUI fire, and can modelling be used to find out which criteria would be the most critical?

The literature is limited to non-existent when it comes to any guidance for performance criteria in villages exposed to WUI fires. The field of research is still in its early stages, but it is studies like this thesis that help future research determine proper criteria. This thesis found that air temperature in the village was the first criteria to reach failure, but this is largely affected by the FED limitations. It is unsure whether the FED, in improved modelling efforts, would be the most critical.

3. Can WUI fire modelling be employed to find out, in villages exposed to WUI fires, how distant would the fire front need to be for smoke to cause untenable conditions?

The methodology followed successfully established a trigger perimeter around the Monhinos Cimeiros community at a distance of 200 meters. This was based on the temperature in the village reaching 60 degrees Celsius, if the fire line in the worst case scenario (largest total heat release rate and average rate of spread) would reach the trigger perimeter. Although the results are largely affected by the discussed limitations in section 4.4, this new trigger for the WASET is an improvement over considering that the WASET is reached when the fire line reaches the community.

4.4. Limitations

Several limitations affect the usefulness of wildfire models and of this thesis' results.

When it comes to the WRSET and WASET, they cannot be calculated independently as the conditions in the studied community could be affected by the fire or smoke [5] and thus the evacuation could be slowed down. As previously discussed, the problem is highly dynamic and models should include a dynamic WRSET/WASET analysis that would be based on the modelled wildfire spread and evacuation.

A large part of the uncertainties lie in the use of the FDS level set method. The original vegetation and topography data-set used in this study and received from the supervisors after being taken from the WUIVIEW project [9], could be misrepresenting the vegetation around the village by approximating to the nearest fuel type from the 13 Rothermel Albini fuel types discussed in section 2.3. As for the combustion prescribed in FDS, assuming that all the vegetation is made from red oak wood is a large limitation. In addition, the results are greatly

affected by the assumed corresponding soot yield value as the soot concentration is included in FED calculations and affects the radiation from the fire, which is one of the drivers of fire spread. These inputs should be examined further in future studies that want to use the level set model in FDS. On another note, FDS does not differentiate between smoke coming from smouldering and from flaming fires, the smoke in the simulations are a direct result of the heat release rate with the soot yield prescribed [19]. For that reason, in this thesis, it wasn't possible to include smouldering fire smoke, a very important factor in wildfire spread.

Another consequence of using FDS, is that the FED is calculated at static locations while in reality, a person would be moving and would consume different doses depending on their behaviour. In engineering approaches for evacuation modelling, human behaviour is mostly accounted for by using a probabilistic approach [46], which means evacuation simulations would need to be run multiple times before reaching a realistically reasonable range of possible FED values.

On another note, using wind data from nearby weather stations could be inaccurate. As they all are situated on the west side of the community, the wind on the east side could have different properties, possibly a larger maximal wind speed. This limitation could be hard to fix as there are limited weather stations where the weather conditions could be consistently recorded. Moreover, the wind is assumed to have a constant speed, which under-represents the wind gusts that happen in real life, which could influence the fire spread.

The mesh analysis of the level set model simulations was conducted qualitatively and could not show a clear trend describing the dependency of the fire spread on the mesh resolution. It is proposed that future mesh analysis studies include terrains built with the same obstacle sizes as different obstacle sizes contributed to changing the terrain complexity. As FDS requires the obstacles to snap to its mesh grid, perhaps the largest grid size could be used for all the simulations. It is also important that these studies examine the results quantitatively too.

In both the large scale and small scale simulations, the height of the domain contributed to increasing the domain size and subsequently the simulation run time. Future studies should try to choose the minimum acceptable domain height that can still capture the wind/terrain interactions.

The small scale simulations are formed by reducing the entirety of the fire front with its complexity to a smaller static burner. It is not known if, in this thesis, the burner size or the HRR reduction ratio taken are suitable or accurate. This part is responsible for a share of the limitations as well.

The temperature criterion of 60 degrees Celsius taken in this thesis for comfort could be high for some. It would be interesting to explore the sensibility of the results to lower temperature limits. It is suggested by the results that the temperature causes conditions to be untenable but there is a possibility that the toxicity could be the first. Previous studies [40] suggest that the presence of hydrogen cyanide (HCN) in the analysis would greatly increase the FED. In order to find out, future research should look to somehow include yields for species that would exist in specific WUI fire cases, that weren't considered in this study, such as HCN.

5. Conclusion

This thesis examined the effect of smoke on the tenability conditions in the Monhinos Cimeiros community when exposed to a wildfire, in an effort to establish a worst-case-scenario trigger boundary around it.

Fire spread scenarios were simulated with FDS' level set method on realistic complex terrain, from 4 directions of the fire and wind, and 2 wind speeds. According to the rate of spread and heat release rate results, the worst case was determined to be the case where the fire and wind come from south of the village and the wind speed is maximum (10 m/s). Then, a high resolution small scale model was built according to these results, and simulated with different distances of the fire from the village. It was found that for the Moninhos Cimeiros village, it is safer to use a 200-meter buffer distance around the village when looking at the fire spread and determining the WASET. The reason is that when the fire gets closer than that, the air temperature in the village and specifically on the evacuation road (main and only road) might reach more than 60 degrees Celsius on a day with high temperatures (37 degrees Celsius) and with very windy conditions (10 m/s). Thus it is recommended that any evacuation, away from the village or to the designated shelter, happens before the trigger perimeter is reached by the fire line.

It is important to note that while the findings of this study provide a more robust approach for determining the fire front arrival distance and a proper limit-perimeter for WUI areas, they also have certain limitations. These limitations include the fact that the simulations were conducted on a single village, and the results may not be directly generalized to other WUI areas. Therefore, it is crucial for researchers in WUI fire spread and evacuation modeling to conduct similar studies in other villages and take into account the specific characteristics of each location to obtain more accurate and comprehensive results.

Furthermore, while the results of this study did provide an improvement to the results of the WUIVIEW project, it showed to have far too many limitations to be considered a robust and reliable method for wildfire risk assessment, and thus remains as a research tool until the limitations are reduced or mitigated. Researchers can use the methodology developed in this study to investigate other aspects of WUI fires, such as the impact of different vegetation types, terrain features, and building materials on fire spread and evacuation. These findings can help improve our understanding of WUI fires and inform the development of more effective strategies for managing them.

In conclusion, while this study has provided valuable insights into the determination of a proper limit-perimeter for WUI areas, there is still much more work to be done in this field. It is important for researchers to build upon the findings of this study and continue to explore new ways of improving fire management and public safety in WUI areas.

Acknowledgement

This thesis could not have been conducted without the immense sacrifice my parents went through to make sure I get quality education. I dedicate any success I get to my parents and my family.

Many thanks to my supervisor Dr. Eulalia Planas, PhD, for the guidance, the resources and the hospitable welcome in Barcelona. In addition, I thank the CERTEC research team and especially Dr. Alba Àgueda, PhD, for her crucial guidance and her time. Not to forget, my secondary supervisor Dr. Enrico Ronchi, PhD, gave me great insight into improving this thesis.

Finally, on a personal level I thank my partner for cheering me up and encouraging me to wake up every morning to a productive day.

References

[1] Jonathan Wahlqvist et al. "The simulation of wildland-urban interface fire evacuation: The WUI-NITY platform". en. In: *Safety Science* 136 (Apr. 2021), p. 105145. ISSN: 09257535. DOI: 10.1016/j.ssci.2020.105145. URL: https://linkinghub.elsevier.com/retrieve/pii/S0925753520305415 (visited on 01/19/2023).

[2] James M. Jeffers. "Particularizing adaptation to non-predominant hazards: A history of wildfires in County Donegal, Ireland from 1903 to 2019". en. In: *International Journal of Disaster Risk Reduction* 58 (May 2021), p. 102211. ISSN: 22124209. DOI: 10.1016/j.ijdrr.2021.102211. URL: https://linkinghub.elsevier.com/retrieve/pii/S2212420921001771 (visited on 02/07/2023).

[3] Yongqiang Liu, John Stanturf, and Scott Goodrick. "Trends in global wildfire potential in a changing climate". en. In: *Forest Ecology and Management* 259.4 (Feb. 2010), pp. 685–697. ISSN: 03781127. DOI: 10.1016/j.foreco.2009.09.002. URL: https://linkinghub.elsevier.com/retrieve/pii/S0378112709006148 (visited on 02/07/2023).

[4] William E. Mell et al. "The wildland - urban interface fire problem - current approaches and research needs". en. In: *International Journal of Wildland Fire* 19.2 (2010), p. 238. ISSN: 1049-8001. DOI: 10.1071/WF07131. URL: http://www.publish.csiro.au/?paper=WF07131 (visited on 01/19/2023).

[5] Paolo Intini et al. "Modelling the impact of wildfire smoke on driving speed". en. In: *International Journal of Disaster Risk Reduction* 80 (Oct. 2022), p. 103211. ISSN: 22124209. DOI: 10.1016/j.ijdrr.2022.103211. URL: https://linkinghub.elsevier.com/retrieve/pii/S2212420922004307 (visited on 01/19/2023).

[6] Jacquelyn C. Broader Stephen D. Wong. "Review of California Wildfire Evacuations from 2017 to 2019". In: (2020). DOI: 10.7922/G29G5K2R. URL: https://escholarship.org/uc/item/5w85z07g (visited on 01/19/2023).

[7] European Commission. *Geospatial based Environment for Optimisation Systems Addressing Fire Emergencies*. Tech. rep. 691161. Apr. 2020. URL: https://cordis.europa.eu/project/id/691161.

[8] NIST. *WILDLAND-URBAN INTERFACE FIRE GROUP: Projects/Programs*. URL: https://www.nist.gov/laboratories/projects-programs/org/6736.

[9] Pascale Vacca et al. *Wildland-Urban Interface Virtual Essays Workbench: Deliverable D7.2 Report on case studies*. English. Jan. 2021. URL: https://mydisk.cs.upc.edu/s/kZDyRtnSM7qr45E?dir=undefined&openfile=76015130.

[10] Anna Marie Gjedrem and Maria Monika Metallinou. "Wildland-urban interface fires in Norwegian coastal heathlands – Identifying risk reducing measures". en. In: *Safety Science* 159 (Mar. 2023), p. 106032. ISSN: 09257535. DOI: 10.1016/j.ssci.2022.106032. URL: https://linkinghub.elsevier.com/retrieve/pii/S092575352200371X (visited on 01/23/2023).

[11] Enrico Ronchi et al. "An open multi-physics framework for modelling wildland-urban interface fire evacuations". en. In: *Safety Science* 118 (Oct. 2019), pp. 868–880. ISSN: 09257535. DOI: 10.1016/j.ssci.2019.06.009. URL: https://linkinghub.elsevier.com/retrieve/pii/S0925753518312281 (visited on 01/19/2023).

[12] Anton Beloglazov et al. "Simulation of wildfire evacuation with dynamic factors and model composition". en. In: *Simulation Modelling Practice and Theory* 60 (Jan. 2016), pp. 144–159. ISSN: 1569190X. DOI: 10.1016/j.simpat.2015.10.002. URL: https://linkinghub.elsevier.com/retrieve/pii/S1569190X15001483 (visited on 05/04/2023).

[13] L Filippidis et al. "Multimodal wildfire evacuation at the microscopic level". In: *SafeGreece 2020 On-Line Proceedings* (2020), pp. 193–196.

[14] Erica Kuligowski. "Evacuation decision-making and behavior in wildfires: Past research, current challenges and a future research agenda". en. In: *Fire Safety Journal* 120 (Mar.

2021), p. 103129. ISSN: 03797112. DOI: 10.1016/j.firesaf.2020.103129. URL: https://linkinghub.elsevier.com/retrieve/pii/S0379711220302204 (visited on 01/20/2023).

[15] Harry Mitchell et al. "Integrating wildfire spread and evacuation times to design safe triggers: Application to two rural communities using PERIL model". en. In: *Safety Science* 157 (Jan. 2023), p. 105914. ISSN: 09257535. DOI: 10.1016/j.ssci.2022.105914. URL: https://linkinghub.elsevier.com/retrieve/pii/S0925753522002533 (visited on 01/19/2023).

[16] Claire Miller et al. "SPARK – A Bushfire Spread Prediction Tool". en. In: *Environmental Software Systems. Infrastructures, Services and Applications*. Ed. by Ralf Denzer et al. Vol. 448. Series Title: IFIP Advances in Information and Communication Technology. Cham: Springer International Publishing, 2015, pp. 262–271. ISBN: 978-3-319-15993-5 978-3-319-15994-2. DOI: 10.1007/978-3-319-15994-2_26. URL: http://link.springer.com/10.1007/978-3-319-15994-2_26 (visited on 04/20/2023).

[17] Cordy Tymstra et al. "Development and structure of Prometheus: the Canadian wildland fire growth simulation model". In: *Natural Resources Canada, Canadian Forest Service, Northern Forestry Centre, Information Report NOR-X-417.(Edmonton, AB)* (2010).

[18] Kevin Tolhurst, Brett Shields, and Derek Chong. "Phoenix: development and application of a bushfire risk management tool." In: *Australian journal of emergency management* 23.4 (2008), pp. 47–54.

[19] Kevin B McGrattan and Glenn P Forney. *Fire dynamics simulator (version 4) :: user's guide*. en. Tech. rep. NIST SP 1019. Gaithersburg, MD: National Institute of Standards and Technology, 2004, NIST SP 1019. DOI: 10.6028/NIST.SP.1019. URL: https://nvlpubs.nist.gov/nistpubs/Legacy/SP/nistspecialpublication1019.pdf (visited on 02/14/2023).

[20] Rodman R. Linn et al. "Modeling wind fields and fire propagation following bark beetle outbreaks in spatially-heterogeneous pinyon-juniper woodland fuel complexes". en. In: *Agricultural and Forest Meteorology* 173 (May 2013), pp. 139–153. ISSN: 01681923. DOI: 10.1016/j.agrformet.2012.11.007. URL: https://linkinghub.elsevier.com/retrieve/pii/S0168192312003449 (visited on 04/20/2023).

[21] Janice L Coen et al. "WRF-Fire: coupled weather–wildland fire modeling with the weather research and forecasting model". In: *Journal of Applied Meteorology and Climatology* 52.1 (2013). Publisher: American Meteorological Society, pp. 16–38.

[22] Terry L. Clark, Janice Coen, and Don Latham. "Description of a coupled atmosphere - fire model". en. In: *International Journal of Wildland Fire* 13.1 (2004), p. 49. ISSN: 1049-8001. DOI: 10.1071/WF03043. URL: http://www.publish.csiro.au/?paper=WF03043 (visited on 04/20/2023).

[23] M.A. Finney and Rocky Mountain Research Station–Ogden. *FARSITE, Fire Area Simulator–model Development and Evaluation*. FARSITE, Fire Area Simulator–model Development and Evaluation no. 4. U.S. Department of Agriculture, Forest Service, Rocky Mountain Research Station, 1998. URL: https://books.google.com.lb/books?id=nfcTAAAAYAAJ.

[24] Mark A Finney et al. "An overview of FlamMap fire modeling capabilities". In: *Fuels management—how to measure success: conference proceedings*. Vol. 28. USDA Forest Service, Rocky Mountain Research Station, Fort Collins, CO. 2006, p. 30.

[25] Nima Masoudvaziri et al. "Streamlined wildland-urban interface fire tracing (SWUIFT): Modeling wildfire spread in communities". en. In: *Environmental Modelling & Software* 143 (Sept. 2021), p. 105097. ISSN: 13648152. DOI: 10.1016/j.envsoft.2021.105097. URL: https://linkinghub.elsevier.com/retrieve/pii/S1364815221001407 (visited on 01/20/2023).

[26] Tyler, Rona. *Requirements for Modelling WUI Fire Evacuation by Unconventional Means*. eng. Series: LUTVDG/TVBB. 2021.

[27] Paolo Intini et al. "Traffic Modeling for Wildland–Urban Interface Fire Evacuation". en. In: *Journal of Transportation Engineering, Part A: Systems* 145.3 (Mar. 2019), p. 04019002. ISSN: 2473-2907, 2473-2893. DOI: 10.1061/JTEPBS.0000221. URL: https://ascelibrary.org/doi/10.1061/JTEPBS.0000221 (visited on 02/11/2023).

[28] Pamela Murray-Tuite and Brian Wolshon. "Evacuation transportation modeling: An overview of research, development, and practice". en. In: *Transportation Research Part C: Emerging Technologies* 27 (Feb. 2013), pp. 25–45. ISSN: 0968090X. DOI: 10.1016/j.trc.2012.11.005. URL: https://linkinghub.elsevier.com/retrieve/pii/S0968090X12001386 (visited on 01/20/2023).

[29] Harry Mitchell and Guillermo Rein. *Matlab Code for PERIL (Population Evacuation tRigger aLgorithm)*. Oct. 2020. DOI: 10.5281/ZENODO.4106654. URL: https://zenodo.org/record/4106654 (visited on 05/09/2023).

[30] Dapeng Li, Thomas J. Cova, and Philip E. Dennison. "A household-level approach to staging wildfire evacuation warnings using trigger modeling". en. In: *Computers, Environment and Urban Systems* 54 (Nov. 2015), pp. 56–67. ISSN: 01989715. DOI: 10.1016/j.compenvurbsys.2015.05.008. URL: https://linkinghub.elsevier.com/retrieve/pii/S0198971515000629 (visited on 05/05/2023).

[31] Philip E. Dennison, Thomas J. Cova, and Max A. Mortiz. "WUIVAC: a wildland-urban interface evacuation trigger model applied in strategic wildfire scenarios". en. In: *Natural Hazards* 41.1 (Apr. 2007), pp. 181–199. ISSN: 0921-030X, 1573-0840. DOI: 10.1007/s11069-006-9032-y. URL: http://link.springer.com/10.1007/s11069-006-9032-y (visited on 05/05/2023).

[32] V. Mallet, D.E. Keyes, and F.E. Fendell. "Modeling wildland fire propagation with level set methods". en. In: *Computers & Mathematics with Applications* 57.7 (Apr. 2009), pp. 1089–1101. ISSN: 08981221. DOI: 10.1016/j.camwa.2008.10.089. URL: https://linkinghub.elsevier.com/retrieve/pii/S0898122108006329 (visited on 03/27/2023).

[33] Angelo Alessandri et al. "Parameter estimation of fire propagation models using level set methods". en. In: *Applied Mathematical Modelling* 92 (Apr. 2021), pp. 731–747. ISSN: 0307904X. DOI: 10.1016/j.apm.2020.11.030. URL: https://linkinghub.elsevier.com/retrieve/pii/S0307904X2030682X (visited on 03/27/2023).

[34] Emanuele Gissi. *qgis2fds*. URL: https://github.com/firetools/qgis2fds/wiki/.

[35] QGIS development team. *QGIS*. URL: https://qgis.org/en/site/.

[36] Mocellin Paolo et al. "Interface Fires in Built-up Areas. a Real-case Study on the Risk Assessment of Fires Interacting with Urban Domains." In: *Chemical Engineering Transactions* 82 (Oct. 2020), pp. 259–264. DOI: 10.3303/CET2082044. URL: https://doi.org/10.3303/CET2082044 (visited on 02/14/2023).

[37] Matthew G. Slocum et al. "Effect of Climate on Wildfire Size: A Cross-Scale Analysis". en. In: *Ecosystems* 13.6 (Sept. 2010), pp. 828–840. ISSN: 1432-9840, 1435-0629. DOI: 10.1007/s10021-010-9357-y. URL: http://link.springer.com/10.1007/s10021-010-9357-y (visited on 03/28/2023).

[38] Isaac T. Leventon, Jiuling Yang, and Morgan C. Bruns. "Thermal decomposition of vegetative fuels and the impact of measured variations on simulations of wildfire spread". en. In: *Fire Safety Journal* 137 (May 2023), p. 103762. ISSN: 03797112. DOI: 10.1016/j.firesaf.2023.103762. URL: https://linkinghub.elsevier.com/retrieve/pii/S0379711223000309 (visited on 03/28/2023).

[39] Kevin McGrattan. "Progress in Modeling Wildland Fires using Computational Fluid Dynamics". en. In: 10th U.S. National Combustion Meeting, College Park, MD, June 2017. URL: https://tsapps.nist.gov/publication/get_pdf.cfm?pub_id=922922.

[40] Morgan J. Hurley, ed. *SFPE handbook of fire protection engineering*. Fifth edition. New York: Springer, 2016. ISBN: 978-1-4939-2564-3.

[41] Anthony S. Bova, William E. Mell, and Chad M. Hoffman. "A comparison of level set and marker methods for the simulation of wildland fire front propagation". en. In: *International Journal of Wildland Fire* 25.2 (2016), p. 229. ISSN: 1049-8001. DOI: 10.1071/WF13178. URL: http://www.publish.csiro.au/?paper=WF13178 (visited on 04/14/2023).

[42] Greg Penney et al. "The CAED Framework for the Development of Performance-Based Design at the Wildland–Urban Interface". en. In: *Fire* 5.2 (Apr. 2022), p. 54. ISSN: 2571-6255. DOI: 10.3390/fire5020054. URL: https://www.mdpi.com/2571-6255/5/2/54 (visited on 03/28/2023).

[43] David Purser. "Behavioural impairment in smoke environments". en. In: *Toxicology* 115.1-3 (Dec. 1996), pp. 25–40. ISSN: 0300483X. DOI: 10.1016/S0300-483X(96)03493-2. URL: https://linkinghub.elsevier.com/retrieve/pii/S0300483X96034932 (visited on 05/05/2023).

[44] ISO. *ISO 13571:2012 - Life-threatening components of fire — Guidelines for the estimation of time to compromised tenability in fires*. Standard 13571. ISO, Sept. 2012.

[45] Björn Karlsson and James G. Quintiere. *Enclosure fire dynamics*. Second edition. Boca Raton, FL: CRC Press, 2022. ISBN: 978-1-138-05866-8 978-1-03-228646-4.

[46] Enrico Ronchi, Paul A. Reneke, and Richard D. Peacock. "A Method for the Analysis of Behavioural Uncertainty in Evacuation Modelling". en. In: *Fire Technology* 50.6 (Nov. 2014), pp. 1545–1571. ISSN: 0015-2684, 1572-8099. DOI: 10.1007/s10694-013-0352-7. URL: http://link.springer.com/10.1007/s10694-013-0352-7 (visited on 05/09/2023).

[47] B. Mike Wotton et al. "Flame temperature and residence time of fires in dry eucalypt forest". en. In: *International Journal of Wildland Fire* 21.3 (2012), p. 270. ISSN: 1049-8001. DOI: 10.1071/WF10127. URL: http://www.publish.csiro.au/?paper=WF10127 (visited on 04/16/2023).

Appendix

A. Radiative heat flux empirical calculations

The calculation in this section is followed according to the SFPE handbook of fire protection [45] and its section on heat flux calculation from a flame. As the flame in the source is assumed to be a cylinder, and the burner in this thesis is a long cube, the cube has to be estimated as multiple adjacent cylinder fires as seen in Figure 36. It will be assumed that each fire has an equal HRR.

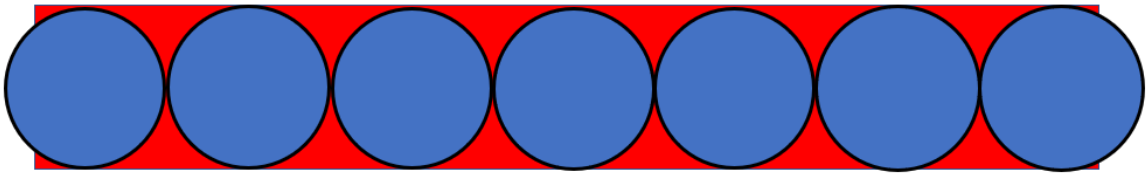

Figure 36. Fire shape estimation

As the burner is 520 meters wide and 80 meters long, cylinders would have a diameter of 80 meters. That would divide the rectangle to 6.5 fitting cylinders. In order to have full cylinders, 7 are used by leaving on the sides 0.25 of the spilling cylinders. The HRR is then divided by 7 and the analysis is conducted from one cylinder. Then, the calculation result is multiplied by 6.5 to represent the initial burner.

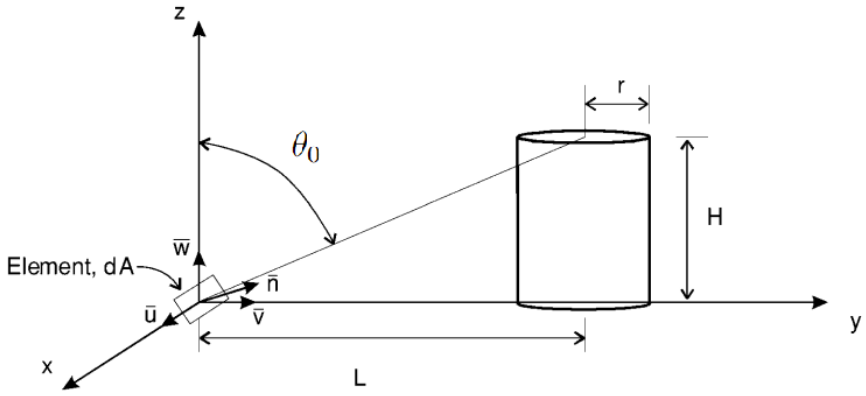

Figure 37. Calculation schematic from [45]

The incident heat flux at the element dA is calculated according to the equation [45]:

$$\ddot{q}'' = \sigma T_f{}^4 \varepsilon (F_1 + F_2 + F_3) \tag{10}$$

With σ being the Stephan-Boltzman constant equal to 5.6704×10^{-8} W/m$^2 \cdot$K. Then T_f is the flame temperature assumed as the maximum flame temperature previously measured in [47] which is 1450 K. Where [45]:

$$\varepsilon = 1 - \exp(-0.7\mu) \tag{11}$$

and [45]

$$\mu = \frac{2r\kappa}{\sin\beta} \tag{12}$$

where [45]

$$\beta = \frac{\theta_0 + \pi/2}{2} \tag{13}$$

r is the radius of the cylinder flame in meters (40 meters in this case). κ is the effective flame absorption coefficient in m^{-1}. θ_0 is the angle shown in Figure 37, the angle that the element makes with the top of the flame.

The view factors F_1, F_2 and F_3 are calculated according to the equations [45]:

$$F_1 = \frac{u}{4\pi}\left(\frac{r}{L}\right)^2 (\pi - 2\theta_0 + \sin 2\theta_0) \tag{14}$$

$$F_2 = \frac{v}{2\pi}\left(\frac{r}{L}\right)^2 (\pi - 2\theta_0 + \sin 2\theta_0) \tag{15}$$

$$F_3 = \frac{w}{\pi}\left(\frac{r}{L}\right)\cos^2\theta_0 \tag{16}$$

u, v and w are coefficients that affect the normal vector $\vec{n}$, in our case, as the cylinder is assumed to be directly in front of the village point of interest, it is only v that is not 0, $v = 1$. Thus, $F_1 = F_3 = 0$. L is the distance of the element dA from the cylinder's center as shown in Figure 37.

θ_0 can be found using the equation [45]:

$$\theta_0 = \tan^{-1}\frac{L}{H} \tag{17}$$

As the distances examined in the thesis are from the border of the burner, L values are equal to these distances plus the radius. H, the height of the flame is unknown. As the model incorporates vegetation of the type: tall grass, chaparral vegetation and dormant brush, there are no trees in the model. Even if the flame height was 10 meters, which is an abnormally large height, the L/H ratio would still be at least 10 using $L = 100$ meters. That would set a minimum $\theta_0 = 84$ degrees. Thus, since the flame height is not known and there is no method to calculate it that applies to wildfires (to the knowledge of the author), H is taken as 10 meters.

In [45], for wood (combustion material assumed in the simulations) and at $T_f = 1350$ K, κ is taken equal to 0.8 m^{-1}. Since all the unknowns were assigned values, the calculations with $L = 150$; $L = 175$; $L = 200$ and $L = 300$ yield the following results (multiplied by 7 to represent all the burner).

Table 10. Incident radiant heat flux calculation results

Case study	L (m)	$q_{calculated}$ (kW/m^2)	q_{max} from results of FDS (kW/m^2)
100m	140	6.01	0.24
150m	190	2.42	0.18
175m	215	1.67	0.16
200m	240	1.20	0.15
300m	340	0.42	0.13

The results are shown in Table 10 and the steps followed are:

- Find β through equation 13
- Find μ through equation 12
- Find ε through equation 11
- Find F_3 through equation 16
- Find $\ddot{q}''$ through equation 10 and multiply it by 6.5

B. FDS code

The following codes are part of an example, corresponding to the southern fire case. The FDS obstacle lines &OBST have been omitted from the large scale cases because otherwise the code would have 130000 lines and would add too many pages to the current document. In the small scale cases code, the houses, road and roofs were omitted too. Also, the mesh was made unique instead of divided. In the small scale cases code, the devices used were included only on height 1 meter, contrary to the full file that includes them on heights 1, 2 and 3 meters. For the full input document, contact the author through the email on the cover page number 6.

B.1. Large scale cases

```
&HEAD CHID='largestudycases_south' TITLE='Description of largestudycases_south
   ↪ ' /


&MISC ORIGIN_LAT=39.9564104
      ORIGIN_LON=-8.2929699
      NORTH_BEARING=0.
      TERRAIN_IMAGE='largestudycases_south_tex.png'
      LEVEL_SET_MODE=4
      THICKEN_OBSTRUCTIONS=T /


&MISC TMPA=37.0/


&TIME T_BEGIN=0, T_END=4000/


&DUMP DT_RESTART=300.0/


&REAC ID='SFPE WOOD_OAK',
        FYI='SFPE Handbook, 5th Ed, Tables A.38 and A.39 "Red oak"',
        FUEL='REAC_FUEL',
        C=1.0,
        H=1.7,
        O=0.72,
        N=1.0E-3,
        CO_YIELD=4.0E-3,
        SOOT_YIELD=0.015,
        HEAT_OF_COMBUSTION=1.71E+4,
        RADIATIVE_FRACTION=0.371 /


Domain and its boundary conditions
&MESH ID='MESH-01', IJK=215, 215, 62, XB=9.0, 1944.0, 9.0, 1944.0, 250.0,
   ↪ 808.0, MPI_PROCESS=0/
```

```
Vents
&VENT ID='Mesh Vent: MESH [XMIN]', SURF_ID='OPEN', XB
   ↪ =9.0,9.0,9.0,1944.0,250.0,808.0/
&VENT ID='Mesh Vent: MESH [XMAX]', SURF_ID='OPEN', XB
   ↪ =1944.0,1944.0,9.0,1944.0,250.0,808.0/
&VENT ID='Mesh Vent: MESH [YMIN]', SURF_ID='OPEN', XB
   ↪ =9.0,1944.0,9.0,9.0,250.0,808.0/
&VENT ID='Mesh Vent: MESH [YMAX]', SURF_ID='OPEN', XB
   ↪ =9.0,1944.0,1944.0,1944.0,250.0,808.0/
&VENT ID='Mesh Vent: MESH [ZMAX]', SURF_ID='OPEN', XB
   ↪ =9.0,1944.0,9.0,1944.0,808.0,808.0/


Devices
&DEVC ID='Temp-A1', QUANTITY='TEMPERATURE', XYZ=1106.46, 825.45, 430.0,
   ↪ ORIENTATION=0.0,0.0,1.0/
&DEVC ID='Temp-A2', QUANTITY='TEMPERATURE', XYZ=1096.983191, 840.914324,
   ↪ 430.0, ORIENTATION=0.0,0.0,1.0/
&DEVC ID='Temp-A3', QUANTITY='TEMPERATURE', XYZ=1086.46, 859.45, 430.0,
   ↪ ORIENTATION=0.0,0.0,1.0/
&DEVC ID='Temp-A4', QUANTITY='TEMPERATURE', XYZ=1076.46, 876.45, 430.0,
   ↪ ORIENTATION=0.0,0.0,1.0/
&DEVC ID='Temp-A5', QUANTITY='TEMPERATURE', XYZ=1062.96, 897.45, 430.0,
   ↪ ORIENTATION=0.0,0.0,1.0/
&DEVC ID='Temp-A6', QUANTITY='TEMPERATURE', XYZ=1047.96, 919.95, 430.0,
   ↪ ORIENTATION=0.0,0.0,1.0/
&DEVC ID='Temp-A7', QUANTITY='TEMPERATURE', XYZ=1046.96, 944.45, 430.0,
   ↪ ORIENTATION=0.0,0.0,1.0/
&DEVC ID='Temp-A8', QUANTITY='TEMPERATURE', XYZ=1052.194368, 969.769196,
   ↪ 430.0, ORIENTATION=0.0,0.0,1.0/
&DEVC ID='Temp-A9', QUANTITY='TEMPERATURE', XYZ=1052.383621, 991.438649,
   ↪ 430.0, ORIENTATION=0.0,0.0,1.0/
&DEVC ID='Temp-A10', QUANTITY='TEMPERATURE', XYZ=1052.0282, 1014.556623,
   ↪ 430.0, ORIENTATION=0.0,0.0,1.0/
&DEVC ID='Temp-A11', QUANTITY='TEMPERATURE', XYZ=1052.0282, 1027.67672, 430.0,
   ↪  ORIENTATION=0.0,0.0,1.0/
&DEVC ID='Temp-A12', QUANTITY='TEMPERATURE', XYZ=1054.46, 1038.45, 430.0,
   ↪ ORIENTATION=0.0,0.0,1.0/
&DEVC ID='Temp-A13', QUANTITY='TEMPERATURE', XYZ=1037.840188, 1046.060112,
   ↪ 430.0, ORIENTATION=0.0,0.0,1.0/
&DEVC ID='Temp-A14', QUANTITY='TEMPERATURE', XYZ=1019.838194, 1053.993194,
   ↪ 430.0, ORIENTATION=0.0,0.0,1.0/
&DEVC ID='Temp-A15', QUANTITY='TEMPERATURE', XYZ=1008.96, 1063.95, 430.0,
   ↪ ORIENTATION=0.0,0.0,1.0/
&DEVC ID='Temp-A16', QUANTITY='TEMPERATURE', XYZ=1000.96, 1073.45, 430.0,
   ↪ ORIENTATION=0.0,0.0,1.0/
&DEVC ID='Temp-A17', QUANTITY='TEMPERATURE', XYZ=991.96, 1082.95, 430.0,
   ↪ ORIENTATION=0.0,0.0,1.0/
&DEVC ID='Temp-A18', QUANTITY='TEMPERATURE', XYZ=983.96, 1091.95, 430.0,
   ↪ ORIENTATION=0.0,0.0,1.0/
```

```
&DEVC ID='Temp-A19', QUANTITY='TEMPERATURE', XYZ=976.46, 1101.45, 430.0,
   ↪ ORIENTATION=0.0,0.0,1.0/
&DEVC ID='Temp-A20', QUANTITY='TEMPERATURE', XYZ=964.96, 1106.45, 430.0,
   ↪ ORIENTATION=0.0,0.0,1.0/
&DEVC ID='Temp-A21', QUANTITY='TEMPERATURE', XYZ=952.96, 1111.45, 430.0,
   ↪ ORIENTATION=0.0,0.0,1.0/
&DEVC ID='Temp-A22', QUANTITY='TEMPERATURE', XYZ=945.96, 1114.45, 430.0,
   ↪ ORIENTATION=0.0,0.0,1.0/
&DEVC ID='Temp-A23', QUANTITY='TEMPERATURE', XYZ=935.96, 1119.45, 430.0,
   ↪ ORIENTATION=0.0,0.0,1.0/
&DEVC ID='Temp-A24', QUANTITY='TEMPERATURE', XYZ=927.96, 1127.45, 430.0,
   ↪ ORIENTATION=0.0,0.0,1.0/
&DEVC ID='Temp-A25', QUANTITY='TEMPERATURE', XYZ=921.96, 1133.45, 430.0,
   ↪ ORIENTATION=0.0,0.0,1.0/
&DEVC ID='Temp-A26', QUANTITY='TEMPERATURE', XYZ=915.96, 1139.45, 430.0,
   ↪ ORIENTATION=0.0,0.0,1.0/
&DEVC ID='Smf-A1', QUANTITY='MASS FRACTION', SPEC_ID='SOOT', XYZ=1106.46,
   ↪ 825.45, 430.0, ORIENTATION=0.0,0.0,1.0/
&DEVC ID='Smf-A2', QUANTITY='MASS FRACTION', SPEC_ID='SOOT', XYZ=1096.983191,
   ↪ 840.914324, 430.0, ORIENTATION=0.0,0.0,1.0/
&DEVC ID='Smf-A3', QUANTITY='MASS FRACTION', SPEC_ID='SOOT', XYZ=1086.46,
   ↪ 859.45, 430.0, ORIENTATION=0.0,0.0,1.0/
&DEVC ID='Smf-A4', QUANTITY='MASS FRACTION', SPEC_ID='SOOT', XYZ=1076.46,
   ↪ 876.45, 430.0, ORIENTATION=0.0,0.0,1.0/
&DEVC ID='Smf-A5', QUANTITY='MASS FRACTION', SPEC_ID='SOOT', XYZ=1062.96,
   ↪ 897.45, 430.0, ORIENTATION=0.0,0.0,1.0/
&DEVC ID='Smf-A6', QUANTITY='MASS FRACTION', SPEC_ID='SOOT', XYZ=1047.96,
   ↪ 919.95, 430.0, ORIENTATION=0.0,0.0,1.0/
&DEVC ID='Smf-A7', QUANTITY='MASS FRACTION', SPEC_ID='SOOT', XYZ=1046.96,
   ↪ 944.45, 430.0, ORIENTATION=0.0,0.0,1.0/
&DEVC ID='Smf-A8', QUANTITY='MASS FRACTION', SPEC_ID='SOOT', XYZ=1052.194368,
   ↪ 969.769196, 430.0, ORIENTATION=0.0,0.0,1.0/
&DEVC ID='Smf-A9', QUANTITY='MASS FRACTION', SPEC_ID='SOOT', XYZ=1052.383621,
   ↪ 991.438649, 430.0, ORIENTATION=0.0,0.0,1.0/
&DEVC ID='Smf-A10', QUANTITY='MASS FRACTION', SPEC_ID='SOOT', XYZ=1052.0282,
   ↪ 1014.556623, 430.0, ORIENTATION=0.0,0.0,1.0/
&DEVC ID='Smf-A11', QUANTITY='MASS FRACTION', SPEC_ID='SOOT', XYZ=1052.0282,
   ↪ 1027.67672, 430.0, ORIENTATION=0.0,0.0,1.0/
&DEVC ID='Smf-A12', QUANTITY='MASS FRACTION', SPEC_ID='SOOT', XYZ=1054.46,
   ↪ 1038.45, 430.0, ORIENTATION=0.0,0.0,1.0/
&DEVC ID='Smf-A13', QUANTITY='MASS FRACTION', SPEC_ID='SOOT', XYZ=1037.840188,
   ↪  1046.060112, 430.0, ORIENTATION=0.0,0.0,1.0/
&DEVC ID='Smf-A14', QUANTITY='MASS FRACTION', SPEC_ID='SOOT', XYZ=1019.838194,
   ↪  1053.993194, 430.0, ORIENTATION=0.0,0.0,1.0/
&DEVC ID='Smf-A15', QUANTITY='MASS FRACTION', SPEC_ID='SOOT', XYZ=1008.96,
   ↪ 1063.95, 430.0, ORIENTATION=0.0,0.0,1.0/
&DEVC ID='Smf-A16', QUANTITY='MASS FRACTION', SPEC_ID='SOOT', XYZ=1000.96,
   ↪ 1073.45, 430.0, ORIENTATION=0.0,0.0,1.0/
&DEVC ID='Smf-A17', QUANTITY='MASS FRACTION', SPEC_ID='SOOT', XYZ=991.96,
   ↪ 1082.95, 430.0, ORIENTATION=0.0,0.0,1.0/
```

```
&DEVC ID='Smf-A18', QUANTITY='MASS FRACTION', SPEC_ID='SOOT', XYZ=983.96,
   ↪ 1091.95, 430.0, ORIENTATION=0.0,0.0,1.0/
&DEVC ID='Smf-A19', QUANTITY='MASS FRACTION', SPEC_ID='SOOT', XYZ=976.46,
   ↪ 1101.45, 430.0, ORIENTATION=0.0,0.0,1.0/
&DEVC ID='Smf-A20', QUANTITY='MASS FRACTION', SPEC_ID='SOOT', XYZ=964.96,
   ↪ 1106.45, 430.0, ORIENTATION=0.0,0.0,1.0/
&DEVC ID='Smf-A21', QUANTITY='MASS FRACTION', SPEC_ID='SOOT', XYZ=952.96,
   ↪ 1111.45, 430.0, ORIENTATION=0.0,0.0,1.0/
&DEVC ID='Smf-A22', QUANTITY='MASS FRACTION', SPEC_ID='SOOT', XYZ=945.96,
   ↪ 1114.45, 430.0, ORIENTATION=0.0,0.0,1.0/
&DEVC ID='Smf-A23', QUANTITY='MASS FRACTION', SPEC_ID='SOOT', XYZ=935.96,
   ↪ 1119.45, 430.0, ORIENTATION=0.0,0.0,1.0/
&DEVC ID='Smf-A24', QUANTITY='MASS FRACTION', SPEC_ID='SOOT', XYZ=927.96,
   ↪ 1127.45, 430.0, ORIENTATION=0.0,0.0,1.0/
&DEVC ID='Smf-A25', QUANTITY='MASS FRACTION', SPEC_ID='SOOT', XYZ=921.96,
   ↪ 1133.45, 430.0, ORIENTATION=0.0,0.0,1.0/
&DEVC ID='Smf-A26', QUANTITY='MASS FRACTION', SPEC_ID='SOOT', XYZ=915.96,
   ↪ 1139.45, 430.0, ORIENTATION=0.0,0.0,1.0/
&DEVC ID='Svf-A1', QUANTITY='VOLUME FRACTION', SPEC_ID='SOOT', XYZ=1106.46,
   ↪ 825.45, 430.0, ORIENTATION=0.0,0.0,1.0/
&DEVC ID='Svf-A2', QUANTITY='VOLUME FRACTION', SPEC_ID='SOOT', XYZ
   ↪ =1096.983191, 840.914324, 430.0, ORIENTATION=0.0,0.0,1.0/
&DEVC ID='Svf-A3', QUANTITY='VOLUME FRACTION', SPEC_ID='SOOT', XYZ=1086.46,
   ↪ 859.45, 430.0, ORIENTATION=0.0,0.0,1.0/
&DEVC ID='Svf-A4', QUANTITY='VOLUME FRACTION', SPEC_ID='SOOT', XYZ=1076.46,
   ↪ 876.45, 430.0, ORIENTATION=0.0,0.0,1.0/
&DEVC ID='Svf-A5', QUANTITY='VOLUME FRACTION', SPEC_ID='SOOT', XYZ=1062.96,
   ↪ 897.45, 430.0, ORIENTATION=0.0,0.0,1.0/
&DEVC ID='Svf-A6', QUANTITY='VOLUME FRACTION', SPEC_ID='SOOT', XYZ=1047.96,
   ↪ 919.95, 430.0, ORIENTATION=0.0,0.0,1.0/
&DEVC ID='Svf-A7', QUANTITY='VOLUME FRACTION', SPEC_ID='SOOT', XYZ=1046.96,
   ↪ 944.45, 430.0, ORIENTATION=0.0,0.0,1.0/
&DEVC ID='Svf-A8', QUANTITY='VOLUME FRACTION', SPEC_ID='SOOT', XYZ
   ↪ =1052.194368, 969.769196, 430.0, ORIENTATION=0.0,0.0,1.0/
&DEVC ID='Svf-A9', QUANTITY='VOLUME FRACTION', SPEC_ID='SOOT', XYZ
   ↪ =1052.383621, 991.438649, 430.0, ORIENTATION=0.0,0.0,1.0/
&DEVC ID='Svf-A10', QUANTITY='VOLUME FRACTION', SPEC_ID='SOOT', XYZ=1052.0282,
   ↪  1014.556623, 430.0, ORIENTATION=0.0,0.0,1.0/
&DEVC ID='Svf-A11', QUANTITY='VOLUME FRACTION', SPEC_ID='SOOT', XYZ=1052.0282,
   ↪  1027.67672, 430.0, ORIENTATION=0.0,0.0,1.0/
&DEVC ID='Svf-A12', QUANTITY='VOLUME FRACTION', SPEC_ID='SOOT', XYZ=1054.46,
   ↪ 1038.45, 430.0, ORIENTATION=0.0,0.0,1.0/
&DEVC ID='Svf-A13', QUANTITY='VOLUME FRACTION', SPEC_ID='SOOT', XYZ
   ↪ =1037.840188, 1046.060112, 430.0, ORIENTATION=0.0,0.0,1.0/
&DEVC ID='Svf-A14', QUANTITY='VOLUME FRACTION', SPEC_ID='SOOT', XYZ
   ↪ =1019.838194, 1053.993194, 430.0, ORIENTATION=0.0,0.0,1.0/
&DEVC ID='Svf-A15', QUANTITY='VOLUME FRACTION', SPEC_ID='SOOT', XYZ=1008.96,
   ↪ 1063.95, 430.0, ORIENTATION=0.0,0.0,1.0/
&DEVC ID='Svf-A16', QUANTITY='VOLUME FRACTION', SPEC_ID='SOOT', XYZ=1000.96,
   ↪ 1073.45, 430.0, ORIENTATION=0.0,0.0,1.0/
```

```
&DEVC ID='Svf-A17', QUANTITY='VOLUME FRACTION', SPEC_ID='SOOT', XYZ=991.96,
   ↪ 1082.95, 430.0, ORIENTATION=0.0,0.0,1.0/
&DEVC ID='Svf-A18', QUANTITY='VOLUME FRACTION', SPEC_ID='SOOT', XYZ=983.96,
   ↪ 1091.95, 430.0, ORIENTATION=0.0,0.0,1.0/
&DEVC ID='Svf-A19', QUANTITY='VOLUME FRACTION', SPEC_ID='SOOT', XYZ=976.46,
   ↪ 1101.45, 430.0, ORIENTATION=0.0,0.0,1.0/
&DEVC ID='Svf-A20', QUANTITY='VOLUME FRACTION', SPEC_ID='SOOT', XYZ=964.96,
   ↪ 1106.45, 430.0, ORIENTATION=0.0,0.0,1.0/
&DEVC ID='Svf-A21', QUANTITY='VOLUME FRACTION', SPEC_ID='SOOT', XYZ=952.96,
   ↪ 1111.45, 430.0, ORIENTATION=0.0,0.0,1.0/
&DEVC ID='Svf-A22', QUANTITY='VOLUME FRACTION', SPEC_ID='SOOT', XYZ=945.96,
   ↪ 1114.45, 430.0, ORIENTATION=0.0,0.0,1.0/
&DEVC ID='Svf-A23', QUANTITY='VOLUME FRACTION', SPEC_ID='SOOT', XYZ=935.96,
   ↪ 1119.45, 430.0, ORIENTATION=0.0,0.0,1.0/
&DEVC ID='Svf-A24', QUANTITY='VOLUME FRACTION', SPEC_ID='SOOT', XYZ=927.96,
   ↪ 1127.45, 430.0, ORIENTATION=0.0,0.0,1.0/
&DEVC ID='Svf-A25', QUANTITY='VOLUME FRACTION', SPEC_ID='SOOT', XYZ=921.96,
   ↪ 1133.45, 430.0, ORIENTATION=0.0,0.0,1.0/
&DEVC ID='Svf-A26', QUANTITY='VOLUME FRACTION', SPEC_ID='SOOT', XYZ=915.96,
   ↪ 1139.45, 430.0, ORIENTATION=0.0,0.0,1.0/
&DEVC ID='COmf-A1', QUANTITY='MASS FRACTION', SPEC_ID='CARBON MONOXIDE', XYZ
   ↪ =1106.46, 825.45, 430.0, ORIENTATION=0.0,0.0,1.0/
&DEVC ID='COmf-A2', QUANTITY='MASS FRACTION', SPEC_ID='CARBON MONOXIDE', XYZ
   ↪ =1096.983191, 840.914324, 430.0, ORIENTATION=0.0,0.0,1.0/
&DEVC ID='COmf-A3', QUANTITY='MASS FRACTION', SPEC_ID='CARBON MONOXIDE', XYZ
   ↪ =1086.46, 859.45, 430.0, ORIENTATION=0.0,0.0,1.0/
&DEVC ID='COmf-A4', QUANTITY='MASS FRACTION', SPEC_ID='CARBON MONOXIDE', XYZ
   ↪ =1076.46, 876.45, 430.0, ORIENTATION=0.0,0.0,1.0/
&DEVC ID='COmf-A5', QUANTITY='MASS FRACTION', SPEC_ID='CARBON MONOXIDE', XYZ
   ↪ =1062.96, 897.45, 430.0, ORIENTATION=0.0,0.0,1.0/
&DEVC ID='COmf-A6', QUANTITY='MASS FRACTION', SPEC_ID='CARBON MONOXIDE', XYZ
   ↪ =1047.96, 919.95, 430.0, ORIENTATION=0.0,0.0,1.0/
&DEVC ID='COmf-A7', QUANTITY='MASS FRACTION', SPEC_ID='CARBON MONOXIDE', XYZ
   ↪ =1046.96, 944.45, 430.0, ORIENTATION=0.0,0.0,1.0/
&DEVC ID='COmf-A8', QUANTITY='MASS FRACTION', SPEC_ID='CARBON MONOXIDE', XYZ
   ↪ =1052.194368, 969.769196, 430.0, ORIENTATION=0.0,0.0,1.0/
&DEVC ID='COmf-A9', QUANTITY='MASS FRACTION', SPEC_ID='CARBON MONOXIDE', XYZ
   ↪ =1052.383621, 991.438649, 430.0, ORIENTATION=0.0,0.0,1.0/
&DEVC ID='COmf-A10', QUANTITY='MASS FRACTION', SPEC_ID='CARBON MONOXIDE', XYZ
   ↪ =1052.0282, 1014.556623, 430.0, ORIENTATION=0.0,0.0,1.0/
&DEVC ID='COmf-A11', QUANTITY='MASS FRACTION', SPEC_ID='CARBON MONOXIDE', XYZ
   ↪ =1052.0282, 1027.67672, 430.0, ORIENTATION=0.0,0.0,1.0/
&DEVC ID='COmf-A12', QUANTITY='MASS FRACTION', SPEC_ID='CARBON MONOXIDE', XYZ
   ↪ =1054.46, 1038.45, 430.0, ORIENTATION=0.0,0.0,1.0/
&DEVC ID='COmf-A13', QUANTITY='MASS FRACTION', SPEC_ID='CARBON MONOXIDE', XYZ
   ↪ =1037.840188, 1046.060112, 430.0, ORIENTATION=0.0,0.0,1.0/
&DEVC ID='COmf-A14', QUANTITY='MASS FRACTION', SPEC_ID='CARBON MONOXIDE', XYZ
   ↪ =1019.838194, 1053.993194, 430.0, ORIENTATION=0.0,0.0,1.0/
&DEVC ID='COmf-A15', QUANTITY='MASS FRACTION', SPEC_ID='CARBON MONOXIDE', XYZ
   ↪ =1008.96, 1063.95, 430.0, ORIENTATION=0.0,0.0,1.0/
```

```
&DEVC ID='COmf-A16', QUANTITY='MASS FRACTION', SPEC_ID='CARBON MONOXIDE', XYZ
   ↪ =1000.96, 1073.45, 430.0, ORIENTATION=0.0,0.0,1.0/
&DEVC ID='COmf-A17', QUANTITY='MASS FRACTION', SPEC_ID='CARBON MONOXIDE', XYZ
   ↪ =991.96, 1082.95, 430.0, ORIENTATION=0.0,0.0,1.0/
&DEVC ID='COmf-A18', QUANTITY='MASS FRACTION', SPEC_ID='CARBON MONOXIDE', XYZ
   ↪ =983.96, 1091.95, 430.0, ORIENTATION=0.0,0.0,1.0/
&DEVC ID='COmf-A19', QUANTITY='MASS FRACTION', SPEC_ID='CARBON MONOXIDE', XYZ
   ↪ =976.46, 1101.45, 430.0, ORIENTATION=0.0,0.0,1.0/
&DEVC ID='COmf-A20', QUANTITY='MASS FRACTION', SPEC_ID='CARBON MONOXIDE', XYZ
   ↪ =964.96, 1106.45, 430.0, ORIENTATION=0.0,0.0,1.0/
&DEVC ID='COmf-A21', QUANTITY='MASS FRACTION', SPEC_ID='CARBON MONOXIDE', XYZ
   ↪ =952.96, 1111.45, 430.0, ORIENTATION=0.0,0.0,1.0/
&DEVC ID='COmf-A22', QUANTITY='MASS FRACTION', SPEC_ID='CARBON MONOXIDE', XYZ
   ↪ =945.96, 1114.45, 430.0, ORIENTATION=0.0,0.0,1.0/
&DEVC ID='COmf-A23', QUANTITY='MASS FRACTION', SPEC_ID='CARBON MONOXIDE', XYZ
   ↪ =935.96, 1119.45, 430.0, ORIENTATION=0.0,0.0,1.0/
&DEVC ID='COmf-A24', QUANTITY='MASS FRACTION', SPEC_ID='CARBON MONOXIDE', XYZ
   ↪ =927.96, 1127.45, 430.0, ORIENTATION=0.0,0.0,1.0/
&DEVC ID='COmf-A25', QUANTITY='MASS FRACTION', SPEC_ID='CARBON MONOXIDE', XYZ
   ↪ =921.96, 1133.45, 430.0, ORIENTATION=0.0,0.0,1.0/
&DEVC ID='COmf-A26', QUANTITY='MASS FRACTION', SPEC_ID='CARBON MONOXIDE', XYZ
   ↪ =915.96, 1139.45, 430.0, ORIENTATION=0.0,0.0,1.0/
&DEVC ID='COvf-A1', QUANTITY='VOLUME FRACTION', SPEC_ID='CARBON MONOXIDE', XYZ
   ↪ =1106.46, 825.45, 430.0, ORIENTATION=0.0,0.0,1.0/
&DEVC ID='COvf-A2', QUANTITY='VOLUME FRACTION', SPEC_ID='CARBON MONOXIDE', XYZ
   ↪ =1096.983191, 840.914324, 430.0, ORIENTATION=0.0,0.0,1.0/
&DEVC ID='COvf-A3', QUANTITY='VOLUME FRACTION', SPEC_ID='CARBON MONOXIDE', XYZ
   ↪ =1086.46, 859.45, 430.0, ORIENTATION=0.0,0.0,1.0/
&DEVC ID='COvf-A4', QUANTITY='VOLUME FRACTION', SPEC_ID='CARBON MONOXIDE', XYZ
   ↪ =1076.46, 876.45, 430.0, ORIENTATION=0.0,0.0,1.0/
&DEVC ID='COvf-A5', QUANTITY='VOLUME FRACTION', SPEC_ID='CARBON MONOXIDE', XYZ
   ↪ =1062.96, 897.45, 430.0, ORIENTATION=0.0,0.0,1.0/
&DEVC ID='COvf-A6', QUANTITY='VOLUME FRACTION', SPEC_ID='CARBON MONOXIDE', XYZ
   ↪ =1047.96, 919.95, 430.0, ORIENTATION=0.0,0.0,1.0/
&DEVC ID='COvf-A7', QUANTITY='VOLUME FRACTION', SPEC_ID='CARBON MONOXIDE', XYZ
   ↪ =1046.96, 944.45, 430.0, ORIENTATION=0.0,0.0,1.0/
&DEVC ID='COvf-A8', QUANTITY='VOLUME FRACTION', SPEC_ID='CARBON MONOXIDE', XYZ
   ↪ =1052.194368, 969.769196, 430.0, ORIENTATION=0.0,0.0,1.0/
&DEVC ID='COvf-A9', QUANTITY='VOLUME FRACTION', SPEC_ID='CARBON MONOXIDE', XYZ
   ↪ =1052.383621, 991.438649, 430.0, ORIENTATION=0.0,0.0,1.0/
&DEVC ID='COvf-A10', QUANTITY='VOLUME FRACTION', SPEC_ID='CARBON MONOXIDE',
   ↪ XYZ=1052.0282, 1014.556623, 430.0, ORIENTATION=0.0,0.0,1.0/
&DEVC ID='COvf-A11', QUANTITY='VOLUME FRACTION', SPEC_ID='CARBON MONOXIDE',
   ↪ XYZ=1052.0282, 1027.67672, 430.0, ORIENTATION=0.0,0.0,1.0/
&DEVC ID='COvf-A12', QUANTITY='VOLUME FRACTION', SPEC_ID='CARBON MONOXIDE',
   ↪ XYZ=1054.46, 1038.45, 430.0, ORIENTATION=0.0,0.0,1.0/
&DEVC ID='COvf-A13', QUANTITY='VOLUME FRACTION', SPEC_ID='CARBON MONOXIDE',
   ↪ XYZ=1037.840188, 1046.060112, 430.0, ORIENTATION=0.0,0.0,1.0/
&DEVC ID='COvf-A14', QUANTITY='VOLUME FRACTION', SPEC_ID='CARBON MONOXIDE',
   ↪ XYZ=1019.838194, 1053.993194, 430.0, ORIENTATION=0.0,0.0,1.0/
```

```
&DEVC ID='COvf-A15', QUANTITY='VOLUME FRACTION', SPEC_ID='CARBON MONOXIDE',
   ↪ XYZ=1008.96, 1063.95, 430.0, ORIENTATION=0.0,0.0,1.0/
&DEVC ID='COvf-A16', QUANTITY='VOLUME FRACTION', SPEC_ID='CARBON MONOXIDE',
   ↪ XYZ=1000.96, 1073.45, 430.0, ORIENTATION=0.0,0.0,1.0/
&DEVC ID='COvf-A17', QUANTITY='VOLUME FRACTION', SPEC_ID='CARBON MONOXIDE',
   ↪ XYZ=991.96, 1082.95, 430.0, ORIENTATION=0.0,0.0,1.0/
&DEVC ID='COvf-A18', QUANTITY='VOLUME FRACTION', SPEC_ID='CARBON MONOXIDE',
   ↪ XYZ=983.96, 1091.95, 430.0, ORIENTATION=0.0,0.0,1.0/
&DEVC ID='COvf-A19', QUANTITY='VOLUME FRACTION', SPEC_ID='CARBON MONOXIDE',
   ↪ XYZ=976.46, 1101.45, 430.0, ORIENTATION=0.0,0.0,1.0/
&DEVC ID='COvf-A20', QUANTITY='VOLUME FRACTION', SPEC_ID='CARBON MONOXIDE',
   ↪ XYZ=964.96, 1106.45, 430.0, ORIENTATION=0.0,0.0,1.0/
&DEVC ID='COvf-A21', QUANTITY='VOLUME FRACTION', SPEC_ID='CARBON MONOXIDE',
   ↪ XYZ=952.96, 1111.45, 430.0, ORIENTATION=0.0,0.0,1.0/
&DEVC ID='COvf-A22', QUANTITY='VOLUME FRACTION', SPEC_ID='CARBON MONOXIDE',
   ↪ XYZ=945.96, 1114.45, 430.0, ORIENTATION=0.0,0.0,1.0/
&DEVC ID='COvf-A23', QUANTITY='VOLUME FRACTION', SPEC_ID='CARBON MONOXIDE',
   ↪ XYZ=935.96, 1119.45, 430.0, ORIENTATION=0.0,0.0,1.0/
&DEVC ID='COvf-A24', QUANTITY='VOLUME FRACTION', SPEC_ID='CARBON MONOXIDE',
   ↪ XYZ=927.96, 1127.45, 430.0, ORIENTATION=0.0,0.0,1.0/
&DEVC ID='COvf-A25', QUANTITY='VOLUME FRACTION', SPEC_ID='CARBON MONOXIDE',
   ↪ XYZ=921.96, 1133.45, 430.0, ORIENTATION=0.0,0.0,1.0/
&DEVC ID='COvf-A26', QUANTITY='VOLUME FRACTION', SPEC_ID='CARBON MONOXIDE',
   ↪ XYZ=915.96, 1139.45, 430.0, ORIENTATION=0.0,0.0,1.0/
&DEVC ID='CO2mf-A1', QUANTITY='MASS FRACTION', SPEC_ID='CARBON DIOXIDE', XYZ
   ↪ =1106.46, 825.45, 430.0, ORIENTATION=0.0,0.0,1.0/
&DEVC ID='CO2mf-A2', QUANTITY='MASS FRACTION', SPEC_ID='CARBON DIOXIDE', XYZ
   ↪ =1096.983191, 840.914324, 430.0, ORIENTATION=0.0,0.0,1.0/
&DEVC ID='CO2mf-A3', QUANTITY='MASS FRACTION', SPEC_ID='CARBON DIOXIDE', XYZ
   ↪ =1086.46, 859.45, 430.0, ORIENTATION=0.0,0.0,1.0/
&DEVC ID='CO2mf-A4', QUANTITY='MASS FRACTION', SPEC_ID='CARBON DIOXIDE', XYZ
   ↪ =1076.46, 876.45, 430.0, ORIENTATION=0.0,0.0,1.0/
&DEVC ID='CO2mf-A5', QUANTITY='MASS FRACTION', SPEC_ID='CARBON DIOXIDE', XYZ
   ↪ =1062.96, 897.45, 430.0, ORIENTATION=0.0,0.0,1.0/
&DEVC ID='CO2mf-A6', QUANTITY='MASS FRACTION', SPEC_ID='CARBON DIOXIDE', XYZ
   ↪ =1047.96, 919.95, 430.0, ORIENTATION=0.0,0.0,1.0/
&DEVC ID='CO2mf-A7', QUANTITY='MASS FRACTION', SPEC_ID='CARBON DIOXIDE', XYZ
   ↪ =1046.96, 944.45, 430.0, ORIENTATION=0.0,0.0,1.0/
&DEVC ID='CO2mf-A8', QUANTITY='MASS FRACTION', SPEC_ID='CARBON DIOXIDE', XYZ
   ↪ =1052.194368, 969.769196, 430.0, ORIENTATION=0.0,0.0,1.0/
&DEVC ID='CO2mf-A9', QUANTITY='MASS FRACTION', SPEC_ID='CARBON DIOXIDE', XYZ
   ↪ =1052.383621, 991.438649, 430.0, ORIENTATION=0.0,0.0,1.0/
&DEVC ID='CO2mf-A10', QUANTITY='MASS FRACTION', SPEC_ID='CARBON DIOXIDE', XYZ
   ↪ =1052.0282, 1014.556623, 430.0, ORIENTATION=0.0,0.0,1.0/
&DEVC ID='CO2mf-A11', QUANTITY='MASS FRACTION', SPEC_ID='CARBON DIOXIDE', XYZ
   ↪ =1052.0282, 1027.67672, 430.0, ORIENTATION=0.0,0.0,1.0/
&DEVC ID='CO2mf-A12', QUANTITY='MASS FRACTION', SPEC_ID='CARBON DIOXIDE', XYZ
   ↪ =1054.46, 1038.45, 430.0, ORIENTATION=0.0,0.0,1.0/
&DEVC ID='CO2mf-A13', QUANTITY='MASS FRACTION', SPEC_ID='CARBON DIOXIDE', XYZ
   ↪ =1037.840188, 1046.060112, 430.0, ORIENTATION=0.0,0.0,1.0/
```

```
&DEVC ID='CO2mf-A14', QUANTITY='MASS FRACTION', SPEC_ID='CARBON DIOXIDE', XYZ
   ↪ =1019.838194, 1053.993194, 430.0, ORIENTATION=0.0,0.0,1.0/
&DEVC ID='CO2mf-A15', QUANTITY='MASS FRACTION', SPEC_ID='CARBON DIOXIDE', XYZ
   ↪ =1008.96, 1063.95, 430.0, ORIENTATION=0.0,0.0,1.0/
&DEVC ID='CO2mf-A16', QUANTITY='MASS FRACTION', SPEC_ID='CARBON DIOXIDE', XYZ
   ↪ =1000.96, 1073.45, 430.0, ORIENTATION=0.0,0.0,1.0/
&DEVC ID='CO2mf-A17', QUANTITY='MASS FRACTION', SPEC_ID='CARBON DIOXIDE', XYZ
   ↪ =991.96, 1082.95, 430.0, ORIENTATION=0.0,0.0,1.0/
&DEVC ID='CO2mf-A18', QUANTITY='MASS FRACTION', SPEC_ID='CARBON DIOXIDE', XYZ
   ↪ =983.96, 1091.95, 430.0, ORIENTATION=0.0,0.0,1.0/
&DEVC ID='CO2mf-A19', QUANTITY='MASS FRACTION', SPEC_ID='CARBON DIOXIDE', XYZ
   ↪ =976.46, 1101.45, 430.0, ORIENTATION=0.0,0.0,1.0/
&DEVC ID='CO2mf-A20', QUANTITY='MASS FRACTION', SPEC_ID='CARBON DIOXIDE', XYZ
   ↪ =964.96, 1106.45, 430.0, ORIENTATION=0.0,0.0,1.0/
&DEVC ID='CO2mf-A21', QUANTITY='MASS FRACTION', SPEC_ID='CARBON DIOXIDE', XYZ
   ↪ =952.96, 1111.45, 430.0, ORIENTATION=0.0,0.0,1.0/
&DEVC ID='CO2mf-A22', QUANTITY='MASS FRACTION', SPEC_ID='CARBON DIOXIDE', XYZ
   ↪ =945.96, 1114.45, 430.0, ORIENTATION=0.0,0.0,1.0/
&DEVC ID='CO2mf-A23', QUANTITY='MASS FRACTION', SPEC_ID='CARBON DIOXIDE', XYZ
   ↪ =935.96, 1119.45, 430.0, ORIENTATION=0.0,0.0,1.0/
&DEVC ID='CO2mf-A24', QUANTITY='MASS FRACTION', SPEC_ID='CARBON DIOXIDE', XYZ
   ↪ =927.96, 1127.45, 430.0, ORIENTATION=0.0,0.0,1.0/
&DEVC ID='CO2mf-A25', QUANTITY='MASS FRACTION', SPEC_ID='CARBON DIOXIDE', XYZ
   ↪ =921.96, 1133.45, 430.0, ORIENTATION=0.0,0.0,1.0/
&DEVC ID='CO2mf-A26', QUANTITY='MASS FRACTION', SPEC_ID='CARBON DIOXIDE', XYZ
   ↪ =915.96, 1139.45, 430.0, ORIENTATION=0.0,0.0,1.0/
&DEVC ID='CO2vf-A1', QUANTITY='VOLUME FRACTION', SPEC_ID='CARBON DIOXIDE', XYZ
   ↪ =1106.46, 825.45, 430.0, ORIENTATION=0.0,0.0,1.0/
&DEVC ID='CO2vf-A2', QUANTITY='VOLUME FRACTION', SPEC_ID='CARBON DIOXIDE', XYZ
   ↪ =1096.983191, 840.914324, 430.0, ORIENTATION=0.0,0.0,1.0/
&DEVC ID='CO2vf-A3', QUANTITY='VOLUME FRACTION', SPEC_ID='CARBON DIOXIDE', XYZ
   ↪ =1086.46, 859.45, 430.0, ORIENTATION=0.0,0.0,1.0/
&DEVC ID='CO2vf-A4', QUANTITY='VOLUME FRACTION', SPEC_ID='CARBON DIOXIDE', XYZ
   ↪ =1076.46, 876.45, 430.0, ORIENTATION=0.0,0.0,1.0/
&DEVC ID='CO2vf-A5', QUANTITY='VOLUME FRACTION', SPEC_ID='CARBON DIOXIDE', XYZ
   ↪ =1062.96, 897.45, 430.0, ORIENTATION=0.0,0.0,1.0/
&DEVC ID='CO2vf-A6', QUANTITY='VOLUME FRACTION', SPEC_ID='CARBON DIOXIDE', XYZ
   ↪ =1047.96, 919.95, 430.0, ORIENTATION=0.0,0.0,1.0/
&DEVC ID='CO2vf-A7', QUANTITY='VOLUME FRACTION', SPEC_ID='CARBON DIOXIDE', XYZ
   ↪ =1046.96, 944.45, 430.0, ORIENTATION=0.0,0.0,1.0/
&DEVC ID='CO2vf-A8', QUANTITY='VOLUME FRACTION', SPEC_ID='CARBON DIOXIDE', XYZ
   ↪ =1052.194368, 969.769196, 430.0, ORIENTATION=0.0,0.0,1.0/
&DEVC ID='CO2vf-A9', QUANTITY='VOLUME FRACTION', SPEC_ID='CARBON DIOXIDE', XYZ
   ↪ =1052.383621, 991.438649, 430.0, ORIENTATION=0.0,0.0,1.0/
&DEVC ID='CO2vf-A10', QUANTITY='VOLUME FRACTION', SPEC_ID='CARBON DIOXIDE',
   ↪ XYZ=1052.0282, 1014.556623, 430.0, ORIENTATION=0.0,0.0,1.0/
&DEVC ID='CO2vf-A11', QUANTITY='VOLUME FRACTION', SPEC_ID='CARBON DIOXIDE',
   ↪ XYZ=1052.0282, 1027.67672, 430.0, ORIENTATION=0.0,0.0,1.0/
&DEVC ID='CO2vf-A12', QUANTITY='VOLUME FRACTION', SPEC_ID='CARBON DIOXIDE',
   ↪ XYZ=1054.46, 1038.45, 430.0, ORIENTATION=0.0,0.0,1.0/
```

```
&DEVC ID='CO2vf-A13', QUANTITY='VOLUME FRACTION', SPEC_ID='CARBON DIOXIDE',
   ↪ XYZ=1037.840188, 1046.060112, 430.0, ORIENTATION=0.0,0.0,1.0/
&DEVC ID='CO2vf-A14', QUANTITY='VOLUME FRACTION', SPEC_ID='CARBON DIOXIDE',
   ↪ XYZ=1019.838194, 1053.993194, 430.0, ORIENTATION=0.0,0.0,1.0/
&DEVC ID='CO2vf-A15', QUANTITY='VOLUME FRACTION', SPEC_ID='CARBON DIOXIDE',
   ↪ XYZ=1008.96, 1063.95, 430.0, ORIENTATION=0.0,0.0,1.0/
&DEVC ID='CO2vf-A16', QUANTITY='VOLUME FRACTION', SPEC_ID='CARBON DIOXIDE',
   ↪ XYZ=1000.96, 1073.45, 430.0, ORIENTATION=0.0,0.0,1.0/
&DEVC ID='CO2vf-A17', QUANTITY='VOLUME FRACTION', SPEC_ID='CARBON DIOXIDE',
   ↪ XYZ=991.96, 1082.95, 430.0, ORIENTATION=0.0,0.0,1.0/
&DEVC ID='CO2vf-A18', QUANTITY='VOLUME FRACTION', SPEC_ID='CARBON DIOXIDE',
   ↪ XYZ=983.96, 1091.95, 430.0, ORIENTATION=0.0,0.0,1.0/
&DEVC ID='CO2vf-A19', QUANTITY='VOLUME FRACTION', SPEC_ID='CARBON DIOXIDE',
   ↪ XYZ=976.46, 1101.45, 430.0, ORIENTATION=0.0,0.0,1.0/
&DEVC ID='CO2vf-A20', QUANTITY='VOLUME FRACTION', SPEC_ID='CARBON DIOXIDE',
   ↪ XYZ=964.96, 1106.45, 430.0, ORIENTATION=0.0,0.0,1.0/
&DEVC ID='CO2vf-A21', QUANTITY='VOLUME FRACTION', SPEC_ID='CARBON DIOXIDE',
   ↪ XYZ=952.96, 1111.45, 430.0, ORIENTATION=0.0,0.0,1.0/
&DEVC ID='CO2vf-A22', QUANTITY='VOLUME FRACTION', SPEC_ID='CARBON DIOXIDE',
   ↪ XYZ=945.96, 1114.45, 430.0, ORIENTATION=0.0,0.0,1.0/
&DEVC ID='CO2vf-A23', QUANTITY='VOLUME FRACTION', SPEC_ID='CARBON DIOXIDE',
   ↪ XYZ=935.96, 1119.45, 430.0, ORIENTATION=0.0,0.0,1.0/
&DEVC ID='CO2vf-A24', QUANTITY='VOLUME FRACTION', SPEC_ID='CARBON DIOXIDE',
   ↪ XYZ=927.96, 1127.45, 430.0, ORIENTATION=0.0,0.0,1.0/
&DEVC ID='CO2vf-A25', QUANTITY='VOLUME FRACTION', SPEC_ID='CARBON DIOXIDE',
   ↪ XYZ=921.96, 1133.45, 430.0, ORIENTATION=0.0,0.0,1.0/
&DEVC ID='CO2vf-A26', QUANTITY='VOLUME FRACTION', SPEC_ID='CARBON DIOXIDE',
   ↪ XYZ=915.96, 1139.45, 430.0, ORIENTATION=0.0,0.0,1.0/
&DEVC ID='RHF-A1', QUANTITY='RADIATIVE HEAT FLUX GAS', XYZ=1106.46, 825.45,
   ↪ 430.0, ORIENTATION=0.0,0.0,1.0/
&DEVC ID='RHF-A2', QUANTITY='RADIATIVE HEAT FLUX GAS', XYZ=1096.983191,
   ↪ 840.914324, 430.0, ORIENTATION=0.0,0.0,1.0/
&DEVC ID='RHF-A3', QUANTITY='RADIATIVE HEAT FLUX GAS', XYZ=1086.46, 859.45,
   ↪ 430.0, ORIENTATION=0.0,0.0,1.0/
&DEVC ID='RHF-A4', QUANTITY='RADIATIVE HEAT FLUX GAS', XYZ=1076.46, 876.45,
   ↪ 430.0, ORIENTATION=0.0,0.0,1.0/
&DEVC ID='RHF-A5', QUANTITY='RADIATIVE HEAT FLUX GAS', XYZ=1062.96, 897.45,
   ↪ 430.0, ORIENTATION=0.0,0.0,1.0/
&DEVC ID='RHF-A6', QUANTITY='RADIATIVE HEAT FLUX GAS', XYZ=1047.96, 919.95,
   ↪ 430.0, ORIENTATION=0.0,0.0,1.0/
&DEVC ID='RHF-A7', QUANTITY='RADIATIVE HEAT FLUX GAS', XYZ=1046.96, 944.45,
   ↪ 430.0, ORIENTATION=0.0,0.0,1.0/
&DEVC ID='RHF-A8', QUANTITY='RADIATIVE HEAT FLUX GAS', XYZ=1052.194368,
   ↪ 969.769196, 430.0, ORIENTATION=0.0,0.0,1.0/
&DEVC ID='RHF-A9', QUANTITY='RADIATIVE HEAT FLUX GAS', XYZ=1052.383621,
   ↪ 991.438649, 430.0, ORIENTATION=0.0,0.0,1.0/
&DEVC ID='RHF-A10', QUANTITY='RADIATIVE HEAT FLUX GAS', XYZ=1052.0282,
   ↪ 1014.556623, 430.0, ORIENTATION=0.0,0.0,1.0/
&DEVC ID='RHF-A11', QUANTITY='RADIATIVE HEAT FLUX GAS', XYZ=1052.0282,
   ↪ 1027.67672, 430.0, ORIENTATION=0.0,0.0,1.0/
```

```
&DEVC ID='RHF-A12', QUANTITY='RADIATIVE HEAT FLUX GAS', XYZ=1054.46, 1038.45,
   ↪ 430.0, ORIENTATION=0.0,0.0,1.0/
&DEVC ID='RHF-A13', QUANTITY='RADIATIVE HEAT FLUX GAS', XYZ=1037.840188,
   ↪ 1046.060112, 430.0, ORIENTATION=0.0,0.0,1.0/
&DEVC ID='RHF-A14', QUANTITY='RADIATIVE HEAT FLUX GAS', XYZ=1019.838194,
   ↪ 1053.993194, 430.0, ORIENTATION=0.0,0.0,1.0/
&DEVC ID='RHF-A15', QUANTITY='RADIATIVE HEAT FLUX GAS', XYZ=1008.96, 1063.95,
   ↪ 430.0, ORIENTATION=0.0,0.0,1.0/
&DEVC ID='RHF-A16', QUANTITY='RADIATIVE HEAT FLUX GAS', XYZ=1000.96, 1073.45,
   ↪ 430.0, ORIENTATION=0.0,0.0,1.0/
&DEVC ID='RHF-A17', QUANTITY='RADIATIVE HEAT FLUX GAS', XYZ=991.96, 1082.95,
   ↪ 430.0, ORIENTATION=0.0,0.0,1.0/
&DEVC ID='RHF-A18', QUANTITY='RADIATIVE HEAT FLUX GAS', XYZ=983.96, 1091.95,
   ↪ 430.0, ORIENTATION=0.0,0.0,1.0/
&DEVC ID='RHF-A19', QUANTITY='RADIATIVE HEAT FLUX GAS', XYZ=976.46, 1101.45,
   ↪ 430.0, ORIENTATION=0.0,0.0,1.0/
&DEVC ID='RHF-A20', QUANTITY='RADIATIVE HEAT FLUX GAS', XYZ=964.96, 1106.45,
   ↪ 430.0, ORIENTATION=0.0,0.0,1.0/
&DEVC ID='RHF-A21', QUANTITY='RADIATIVE HEAT FLUX GAS', XYZ=952.96, 1111.45,
   ↪ 430.0, ORIENTATION=0.0,0.0,1.0/
&DEVC ID='RHF-A22', QUANTITY='RADIATIVE HEAT FLUX GAS', XYZ=945.96, 1114.45,
   ↪ 430.0, ORIENTATION=0.0,0.0,1.0/
&DEVC ID='RHF-A23', QUANTITY='RADIATIVE HEAT FLUX GAS', XYZ=935.96, 1119.45,
   ↪ 430.0, ORIENTATION=0.0,0.0,1.0/
&DEVC ID='RHF-A24', QUANTITY='RADIATIVE HEAT FLUX GAS', XYZ=927.96, 1127.45,
   ↪ 430.0, ORIENTATION=0.0,0.0,1.0/
&DEVC ID='RHF-A25', QUANTITY='RADIATIVE HEAT FLUX GAS', XYZ=921.96, 1133.45,
   ↪ 430.0, ORIENTATION=0.0,0.0,1.0/
&DEVC ID='RHF-A26', QUANTITY='RADIATIVE HEAT FLUX GAS', XYZ=915.96, 1139.45,
   ↪ 430.0, ORIENTATION=0.0,0.0,1.0/
&DEVC ID='Vis-A1', QUANTITY='VISIBILITY', XYZ=1106.46, 825.45, 430.0,
   ↪ ORIENTATION=0.0,0.0,1.0/
&DEVC ID='Vis-A2', QUANTITY='VISIBILITY', XYZ=1096.983191, 840.914324, 430.0,
   ↪ ORIENTATION=0.0,0.0,1.0/
&DEVC ID='Vis-A3', QUANTITY='VISIBILITY', XYZ=1086.46, 859.45, 430.0,
   ↪ ORIENTATION=0.0,0.0,1.0/
&DEVC ID='Vis-A4', QUANTITY='VISIBILITY', XYZ=1076.46, 876.45, 430.0,
   ↪ ORIENTATION=0.0,0.0,1.0/
&DEVC ID='Vis-A5', QUANTITY='VISIBILITY', XYZ=1062.96, 897.45, 430.0,
   ↪ ORIENTATION=0.0,0.0,1.0/
&DEVC ID='Vis-A6', QUANTITY='VISIBILITY', XYZ=1047.96, 919.95, 430.0,
   ↪ ORIENTATION=0.0,0.0,1.0/
&DEVC ID='Vis-A7', QUANTITY='VISIBILITY', XYZ=1046.96, 944.45, 430.0,
   ↪ ORIENTATION=0.0,0.0,1.0/
&DEVC ID='Vis-A8', QUANTITY='VISIBILITY', XYZ=1052.194368, 969.769196, 430.0,
   ↪ ORIENTATION=0.0,0.0,1.0/
&DEVC ID='Vis-A9', QUANTITY='VISIBILITY', XYZ=1052.383621, 991.438649, 430.0,
   ↪ ORIENTATION=0.0,0.0,1.0/
&DEVC ID='Vis-A10', QUANTITY='VISIBILITY', XYZ=1052.0282, 1014.556623, 430.0,
   ↪ ORIENTATION=0.0,0.0,1.0/
```

```
&DEVC ID='Vis-A11', QUANTITY='VISIBILITY', XYZ=1052.0282, 1027.67672, 430.0,
   ↪ ORIENTATION=0.0,0.0,1.0/
&DEVC ID='Vis-A12', QUANTITY='VISIBILITY', XYZ=1054.46, 1038.45, 430.0,
   ↪ ORIENTATION=0.0,0.0,1.0/
&DEVC ID='Vis-A13', QUANTITY='VISIBILITY', XYZ=1037.840188, 1046.060112,
   ↪ 430.0, ORIENTATION=0.0,0.0,1.0/
&DEVC ID='Vis-A14', QUANTITY='VISIBILITY', XYZ=1019.838194, 1053.993194,
   ↪ 430.0, ORIENTATION=0.0,0.0,1.0/
&DEVC ID='Vis-A15', QUANTITY='VISIBILITY', XYZ=1008.96, 1063.95, 430.0,
   ↪ ORIENTATION=0.0,0.0,1.0/
&DEVC ID='Vis-A16', QUANTITY='VISIBILITY', XYZ=1000.96, 1073.45, 430.0,
   ↪ ORIENTATION=0.0,0.0,1.0/
&DEVC ID='Vis-A17', QUANTITY='VISIBILITY', XYZ=991.96, 1082.95, 430.0,
   ↪ ORIENTATION=0.0,0.0,1.0/
&DEVC ID='Vis-A18', QUANTITY='VISIBILITY', XYZ=983.96, 1091.95, 430.0,
   ↪ ORIENTATION=0.0,0.0,1.0/
&DEVC ID='Vis-A19', QUANTITY='VISIBILITY', XYZ=976.46, 1101.45, 430.0,
   ↪ ORIENTATION=0.0,0.0,1.0/
&DEVC ID='Vis-A20', QUANTITY='VISIBILITY', XYZ=964.96, 1106.45, 430.0,
   ↪ ORIENTATION=0.0,0.0,1.0/
&DEVC ID='Vis-A21', QUANTITY='VISIBILITY', XYZ=952.96, 1111.45, 430.0,
   ↪ ORIENTATION=0.0,0.0,1.0/
&DEVC ID='Vis-A22', QUANTITY='VISIBILITY', XYZ=945.96, 1114.45, 430.0,
   ↪ ORIENTATION=0.0,0.0,1.0/
&DEVC ID='Vis-A23', QUANTITY='VISIBILITY', XYZ=935.96, 1119.45, 430.0,
   ↪ ORIENTATION=0.0,0.0,1.0/
&DEVC ID='Vis-A24', QUANTITY='VISIBILITY', XYZ=927.96, 1127.45, 430.0,
   ↪ ORIENTATION=0.0,0.0,1.0/
&DEVC ID='Vis-A25', QUANTITY='VISIBILITY', XYZ=921.96, 1133.45, 430.0,
   ↪ ORIENTATION=0.0,0.0,1.0/
&DEVC ID='Vis-A26', QUANTITY='VISIBILITY', XYZ=915.96, 1139.45, 430.0,
   ↪ ORIENTATION=0.0,0.0,1.0/
&DEVC ID='FED-A1', QUANTITY='FED', XYZ=1106.46, 825.45, 430.0, ORIENTATION
   ↪ =0.0,0.0,1.0/
&DEVC ID='FED-A2', QUANTITY='FED', XYZ=1096.983191, 840.914324, 430.0,
   ↪ ORIENTATION=0.0,0.0,1.0/
&DEVC ID='FED-A3', QUANTITY='FED', XYZ=1086.46, 859.45, 430.0, ORIENTATION
   ↪ =0.0,0.0,1.0/
&DEVC ID='FED-A4', QUANTITY='FED', XYZ=1076.46, 876.45, 430.0, ORIENTATION
   ↪ =0.0,0.0,1.0/
&DEVC ID='FED-A5', QUANTITY='FED', XYZ=1062.96, 897.45, 430.0, ORIENTATION
   ↪ =0.0,0.0,1.0/
&DEVC ID='FED-A6', QUANTITY='FED', XYZ=1047.96, 919.95, 430.0, ORIENTATION
   ↪ =0.0,0.0,1.0/
&DEVC ID='FED-A7', QUANTITY='FED', XYZ=1046.96, 944.45, 430.0, ORIENTATION
   ↪ =0.0,0.0,1.0/
&DEVC ID='FED-A8', QUANTITY='FED', XYZ=1052.194368, 969.769196, 430.0,
   ↪ ORIENTATION=0.0,0.0,1.0/
&DEVC ID='FED-A9', QUANTITY='FED', XYZ=1052.383621, 991.438649, 430.0,
   ↪ ORIENTATION=0.0,0.0,1.0/
```

```
&DEVC ID='FED-A10', QUANTITY='FED', XYZ=1052.0282, 1014.556623, 430.0,
   ↪ ORIENTATION=0.0,0.0,1.0/
&DEVC ID='FED-A11', QUANTITY='FED', XYZ=1052.0282, 1027.67672, 430.0,
   ↪ ORIENTATION=0.0,0.0,1.0/
&DEVC ID='FED-A12', QUANTITY='FED', XYZ=1054.46, 1038.45, 430.0, ORIENTATION
   ↪ =0.0,0.0,1.0/
&DEVC ID='FED-A13', QUANTITY='FED', XYZ=1037.840188, 1046.060112, 430.0,
   ↪ ORIENTATION=0.0,0.0,1.0/
&DEVC ID='FED-A14', QUANTITY='FED', XYZ=1019.838194, 1053.993194, 430.0,
   ↪ ORIENTATION=0.0,0.0,1.0/
&DEVC ID='FED-A15', QUANTITY='FED', XYZ=1008.96, 1063.95, 430.0, ORIENTATION
   ↪ =0.0,0.0,1.0/
&DEVC ID='FED-A16', QUANTITY='FED', XYZ=1000.96, 1073.45, 430.0, ORIENTATION
   ↪ =0.0,0.0,1.0/
&DEVC ID='FED-A17', QUANTITY='FED', XYZ=991.96, 1082.95, 430.0, ORIENTATION
   ↪ =0.0,0.0,1.0/
&DEVC ID='FED-A18', QUANTITY='FED', XYZ=983.96, 1091.95, 430.0, ORIENTATION
   ↪ =0.0,0.0,1.0/
&DEVC ID='FED-A19', QUANTITY='FED', XYZ=976.46, 1101.45, 430.0, ORIENTATION
   ↪ =0.0,0.0,1.0/
&DEVC ID='FED-A20', QUANTITY='FED', XYZ=964.96, 1106.45, 430.0, ORIENTATION
   ↪ =0.0,0.0,1.0/
&DEVC ID='FED-A21', QUANTITY='FED', XYZ=952.96, 1111.45, 430.0, ORIENTATION
   ↪ =0.0,0.0,1.0/
&DEVC ID='FED-A22', QUANTITY='FED', XYZ=945.96, 1114.45, 430.0, ORIENTATION
   ↪ =0.0,0.0,1.0/
&DEVC ID='FED-A23', QUANTITY='FED', XYZ=935.96, 1119.45, 430.0, ORIENTATION
   ↪ =0.0,0.0,1.0/
&DEVC ID='FED-A24', QUANTITY='FED', XYZ=927.96, 1127.45, 430.0, ORIENTATION
   ↪ =0.0,0.0,1.0/
&DEVC ID='FED-A25', QUANTITY='FED', XYZ=921.96, 1133.45, 430.0, ORIENTATION
   ↪ =0.0,0.0,1.0/
&DEVC ID='FED-A26', QUANTITY='FED', XYZ=915.96, 1139.45, 430.0, ORIENTATION
   ↪ =0.0,0.0,1.0/


Landuse boundary conditions
&SURF ID='NA' RGB=255,255,255 /
&SURF ID='A01' RGB=255,254,212 VEG_LSET_FUEL_INDEX=1 /
&SURF ID='A02' RGB=255,253,102 VEG_LSET_FUEL_INDEX=2 /
&SURF ID='A03' RGB=236,212,99 VEG_LSET_FUEL_INDEX=3 /
&SURF ID='A04' RGB=254,193,119 VEG_LSET_FUEL_INDEX=4 /
&SURF ID='A05' RGB=249,197,92 VEG_LSET_FUEL_INDEX=5 /
&SURF ID='A06' RGB=217,196,152 VEG_LSET_FUEL_INDEX=6 /
&SURF ID='A07' RGB=170,155,127 VEG_LSET_FUEL_INDEX=7 /
&SURF ID='A08' RGB=229,253,214 VEG_LSET_FUEL_INDEX=8 /
&SURF ID='A09' RGB=162,191,90 VEG_LSET_FUEL_INDEX=9 /
&SURF ID='A10' RGB=114,154,85 VEG_LSET_FUEL_INDEX=10 /
&SURF ID='A11' RGB=235,212,253 VEG_LSET_FUEL_INDEX=11 /
&SURF ID='A12' RGB=163,177,243 VEG_LSET_FUEL_INDEX=12 /
```

```
&SURF ID='A13' RGB=0,0,0 VEG_LSET_FUEL_INDEX=13 /
&SURF ID='Urban' RGB=186,119,80 /
&SURF ID='Snow-Ice' RGB=234,234,234 /
&SURF ID='Agricolture' RGB=253,242,242 /
&SURF ID='Water' RGB=137,183,221 /
&SURF ID='Barren' RGB=133,153,156 /
&SURF ID='Ignition' VEG_LSET_IGNITE_TIME=0. COLOR='RED' /
&SURF ID='Burned' RGB=20,20,20 /


Output quantities
&SLCF AGL_SLICE=5. QUANTITY='LEVEL SET VALUE' /
&SLCF AGL_SLICE=5. QUANTITY='TEMPERATURE' VECTOR=T /
&SLCF PBX=0.00 QUANTITY='TEMPERATURE' VECTOR=T /
&SLCF PBY=0.00 QUANTITY='TEMPERATURE' VECTOR=T /


Wind
&WIND SPEED= 10.0, DIRECTION= 180 /


(Obstacles here)


&TAIL /
```

B.2. Small scale cases

```
&HEAD CHID='smallcase_south_300m', TITLE='smallcase_south_300m'/


&MISC TMPA=37.0/


&TIME T_BEGIN=0, T_END=1000/


&DUMP DT_RESTART=300.0/


Wind
&WIND SPEED=10.0 DIRECTION=180 /


&REAC ID='SFPE WOOD_OAK',
       FYI='SFPE Handbook, 5th Ed, Tables A.38 and A.39 "Red oak"',
       FUEL='REAC_FUEL',
       C=1.0,
       H=1.7,
       O=0.72,
       N=1.0E-3,
       CO_YIELD=4.0E-3,
       SOOT_YIELD=0.015,
       HEAT_OF_COMBUSTION=1.71E+4,
       RADIATIVE_FRACTION=0.371 /


Meshes
&MESH ID='MESH', IJK=550, 766, 37, XB=200.0, 750.0, 2.0, 768.0, -2.0, 35.0,
   ↪ MPI_PROCESS=0/


Vents
&VENT ID='Mesh Vent: MESH [XMIN]', SURF_ID='OPEN', XB
   ↪ =200.0,200.0,2.0,768.0,-2.0,35.0/
&VENT ID='Mesh Vent: MESH [XMAX]', SURF_ID='OPEN', XB
   ↪ =750.0,750.0,2.0,768.0,-2.0,35.0/
&VENT ID='Mesh Vent: MESH [YMIN]', SURF_ID='OPEN', XB
   ↪ =200.0,750.0,2.0,2.0,-2.0,35.0/
&VENT ID='Mesh Vent: MESH [YMAX]', SURF_ID='OPEN', XB
   ↪ =200.0,750.0,768.0,768.0,-2.0,35.0/
&VENT ID='Mesh Vent: MESH [ZMAX]', SURF_ID='OPEN', XB
   ↪ =200.0,750.0,2.0,768.0,35.0,35.0/


Slices
```

```
&SLCF QUANTITY='TEMPERATURE', ID='SliceTemp01', PBZ=1.0/
&SLCF QUANTITY='PRESSURE', ID='SlicePressure01', PBZ=1.0/
&SLCF QUANTITY='DENSITY', SPEC_ID='SOOT', ID='SliceSootDensity01', PBZ=1.0/
&SLCF QUANTITY='MASS FRACTION', SPEC_ID='SOOT', ID='SliceSootMF01', PBZ=1.0/
&SLCF QUANTITY='VISIBILITY', ID='SliceVis01', PBZ=1.0/


&SURF ID='Burner',
      COLOR='RED',
      HRRPUA=120,
      TAU_Q=-60.0,
      TMP_FRONT=300.0/


Obstacles
&OBST ID='Burner', XB=215.0,735.0,9.0,89.0,0.0,2.75, SURF_ID='Burner'/
&OBST ID='Terrain', XB=0.0,956.13,0.0,768.64,-10.0,0.0, RGB=160,239,151,
   ↪ TRANSPARENCY=0.309804/


Devices
&DEVC ID='Origin_UV', QUANTITY='U-VELOCITY', XYZ=478.04,384.3,30.0/
&DEVC ID='Origin_VV', QUANTITY='V-VELOCITY', XYZ=478.04,384.3,30.0/
&DEVC ID='Origin_WV', QUANTITY='W-VELOCITY', XYZ=478.04,384.3,30.0/
&DEVC ID='Temp-A1', QUANTITY='TEMPERATURE', XYZ=358.0, 727.5, 1.0, ORIENTATION
   ↪ =0.0,0.0,1.0/
&DEVC ID='Temp-A2', QUANTITY='TEMPERATURE', XYZ=364.0, 721.5, 1.0, ORIENTATION
   ↪ =0.0,0.0,1.0/
&DEVC ID='Temp-A3', QUANTITY='TEMPERATURE', XYZ=370.0, 715.5, 1.0, ORIENTATION
   ↪ =0.0,0.0,1.0/
&DEVC ID='Temp-A4', QUANTITY='TEMPERATURE', XYZ=378.0, 707.5, 1.0, ORIENTATION
   ↪ =0.0,0.0,1.0/
&DEVC ID='Temp-A5', QUANTITY='TEMPERATURE', XYZ=388.0, 702.5, 1.0, ORIENTATION
   ↪ =0.0,0.0,1.0/
&DEVC ID='Temp-A6', QUANTITY='TEMPERATURE', XYZ=395.0, 699.5, 1.0, ORIENTATION
   ↪ =0.0,0.0,1.0/
&DEVC ID='Temp-A7', QUANTITY='TEMPERATURE', XYZ=407.0, 694.5, 1.0, ORIENTATION
   ↪ =0.0,0.0,1.0/
&DEVC ID='Temp-A8', QUANTITY='TEMPERATURE', XYZ=418.5, 689.5, 1.0, ORIENTATION
   ↪ =0.0,0.0,1.0/
&DEVC ID='Temp-A9', QUANTITY='TEMPERATURE', XYZ=426.0, 680.0, 1.0, ORIENTATION
   ↪ =0.0,0.0,1.0/
&DEVC ID='Temp-A10', QUANTITY='TEMPERATURE', XYZ=434.0, 671.0, 1.0,
   ↪ ORIENTATION=0.0,0.0,1.0/
&DEVC ID='Temp-A11', QUANTITY='TEMPERATURE', XYZ=443.0, 661.5, 1.0,
   ↪ ORIENTATION=0.0,0.0,1.0/
&DEVC ID='Temp-A12', QUANTITY='TEMPERATURE', XYZ=451.0, 652.0, 1.0,
   ↪ ORIENTATION=0.0,0.0,1.0/
&DEVC ID='Temp-A13', QUANTITY='TEMPERATURE', XYZ=461.878194, 642.043194, 1.0,
   ↪ ORIENTATION=0.0,0.0,1.0/
```

```
&DEVC ID='Temp-A14', QUANTITY='TEMPERATURE', XYZ=479.880188, 634.110112, 1.0,
   ↪ ORIENTATION=0.0,0.0,1.0/
&DEVC ID='Temp-A15', QUANTITY='TEMPERATURE', XYZ=496.5, 626.5, 1.0,
   ↪ ORIENTATION=0.0,0.0,1.0/
&DEVC ID='Temp-A16', QUANTITY='TEMPERATURE', XYZ=494.0682, 615.72672, 1.0,
   ↪ ORIENTATION=0.0,0.0,1.0/
&DEVC ID='Temp-A17', QUANTITY='TEMPERATURE', XYZ=494.0682, 602.606623, 1.0,
   ↪ ORIENTATION=0.0,0.0,1.0/
&DEVC ID='Temp-A18', QUANTITY='TEMPERATURE', XYZ=494.423621, 579.488649, 1.0,
   ↪ ORIENTATION=0.0,0.0,1.0/
&DEVC ID='Temp-A19', QUANTITY='TEMPERATURE', XYZ=494.234368, 557.819196, 1.0,
   ↪ ORIENTATION=0.0,0.0,1.0/
&DEVC ID='Temp-A20', QUANTITY='TEMPERATURE', XYZ=489.0, 532.5, 1.0,
   ↪ ORIENTATION=0.0,0.0,1.0/
&DEVC ID='Temp-A21', QUANTITY='TEMPERATURE', XYZ=490.0, 508.0, 1.0,
   ↪ ORIENTATION=0.0,0.0,1.0/
&DEVC ID='Temp-A22', QUANTITY='TEMPERATURE', XYZ=505.0, 485.5, 1.0,
   ↪ ORIENTATION=0.0,0.0,1.0/
&DEVC ID='Temp-A23', QUANTITY='TEMPERATURE', XYZ=518.5, 464.5, 1.0,
   ↪ ORIENTATION=0.0,0.0,1.0/
&DEVC ID='Temp-A24', QUANTITY='TEMPERATURE', XYZ=528.5, 447.5, 1.0,
   ↪ ORIENTATION=0.0,0.0,1.0/
&DEVC ID='Temp-A25', QUANTITY='TEMPERATURE', XYZ=539.023191, 428.964324, 1.0,
   ↪ ORIENTATION=0.0,0.0,1.0/
&DEVC ID='Temp-A26', QUANTITY='TEMPERATURE', XYZ=548.5, 413.5, 1.0,
   ↪ ORIENTATION=0.0,0.0,1.0/
&DEVC ID='Smf-A1', QUANTITY='MASS FRACTION', SPEC_ID='SOOT', XYZ=358.0, 727.5,
   ↪  1.0, ORIENTATION=0.0,0.0,1.0/
&DEVC ID='Smf-A2', QUANTITY='MASS FRACTION', SPEC_ID='SOOT', XYZ=364.0, 721.5,
   ↪  1.0, ORIENTATION=0.0,0.0,1.0/
&DEVC ID='Smf-A3', QUANTITY='MASS FRACTION', SPEC_ID='SOOT', XYZ=370.0, 715.5,
   ↪  1.0, ORIENTATION=0.0,0.0,1.0/
&DEVC ID='Smf-A4', QUANTITY='MASS FRACTION', SPEC_ID='SOOT', XYZ=378.0, 707.5,
   ↪  1.0, ORIENTATION=0.0,0.0,1.0/
&DEVC ID='Smf-A5', QUANTITY='MASS FRACTION', SPEC_ID='SOOT', XYZ=388.0, 702.5,
   ↪  1.0, ORIENTATION=0.0,0.0,1.0/
&DEVC ID='Smf-A6', QUANTITY='MASS FRACTION', SPEC_ID='SOOT', XYZ=395.0, 699.5,
   ↪  1.0, ORIENTATION=0.0,0.0,1.0/
&DEVC ID='Smf-A7', QUANTITY='MASS FRACTION', SPEC_ID='SOOT', XYZ=407.0, 694.5,
   ↪  1.0, ORIENTATION=0.0,0.0,1.0/
&DEVC ID='Smf-A8', QUANTITY='MASS FRACTION', SPEC_ID='SOOT', XYZ=418.5, 689.5,
   ↪  1.0, ORIENTATION=0.0,0.0,1.0/
&DEVC ID='Smf-A9', QUANTITY='MASS FRACTION', SPEC_ID='SOOT', XYZ=426.0, 680.0,
   ↪  1.0, ORIENTATION=0.0,0.0,1.0/
&DEVC ID='Smf-A10', QUANTITY='MASS FRACTION', SPEC_ID='SOOT', XYZ=434.0,
   ↪ 671.0, 1.0, ORIENTATION=0.0,0.0,1.0/
&DEVC ID='Smf-A11', QUANTITY='MASS FRACTION', SPEC_ID='SOOT', XYZ=443.0,
   ↪ 661.5, 1.0, ORIENTATION=0.0,0.0,1.0/
&DEVC ID='Smf-A12', QUANTITY='MASS FRACTION', SPEC_ID='SOOT', XYZ=451.0,
   ↪ 652.0, 1.0, ORIENTATION=0.0,0.0,1.0/
```

```
&DEVC ID='Smf-A13', QUANTITY='MASS FRACTION', SPEC_ID='SOOT', XYZ=461.878194,
   ↪ 642.043194, 1.0, ORIENTATION=0.0,0.0,1.0/
&DEVC ID='Smf-A14', QUANTITY='MASS FRACTION', SPEC_ID='SOOT', XYZ=479.880188,
   ↪ 634.110112, 1.0, ORIENTATION=0.0,0.0,1.0/
&DEVC ID='Smf-A15', QUANTITY='MASS FRACTION', SPEC_ID='SOOT', XYZ=496.5,
   ↪ 626.5, 1.0, ORIENTATION=0.0,0.0,1.0/
&DEVC ID='Smf-A16', QUANTITY='MASS FRACTION', SPEC_ID='SOOT', XYZ=494.0682,
   ↪ 615.72672, 1.0, ORIENTATION=0.0,0.0,1.0/
&DEVC ID='Smf-A17', QUANTITY='MASS FRACTION', SPEC_ID='SOOT', XYZ=494.0682,
   ↪ 602.606623, 1.0, ORIENTATION=0.0,0.0,1.0/
&DEVC ID='Smf-A18', QUANTITY='MASS FRACTION', SPEC_ID='SOOT', XYZ=494.423621,
   ↪ 579.488649, 1.0, ORIENTATION=0.0,0.0,1.0/
&DEVC ID='Smf-A19', QUANTITY='MASS FRACTION', SPEC_ID='SOOT', XYZ=494.234368,
   ↪ 557.819196, 1.0, ORIENTATION=0.0,0.0,1.0/
&DEVC ID='Smf-A20', QUANTITY='MASS FRACTION', SPEC_ID='SOOT', XYZ=489.0,
   ↪ 532.5, 1.0, ORIENTATION=0.0,0.0,1.0/
&DEVC ID='Smf-A21', QUANTITY='MASS FRACTION', SPEC_ID='SOOT', XYZ=490.0,
   ↪ 508.0, 1.0, ORIENTATION=0.0,0.0,1.0/
&DEVC ID='Smf-A22', QUANTITY='MASS FRACTION', SPEC_ID='SOOT', XYZ=505.0,
   ↪ 485.5, 1.0, ORIENTATION=0.0,0.0,1.0/
&DEVC ID='Smf-A23', QUANTITY='MASS FRACTION', SPEC_ID='SOOT', XYZ=518.5,
   ↪ 464.5, 1.0, ORIENTATION=0.0,0.0,1.0/
&DEVC ID='Smf-A24', QUANTITY='MASS FRACTION', SPEC_ID='SOOT', XYZ=528.5,
   ↪ 447.5, 1.0, ORIENTATION=0.0,0.0,1.0/
&DEVC ID='Smf-A25', QUANTITY='MASS FRACTION', SPEC_ID='SOOT', XYZ=539.023191,
   ↪ 428.964324, 1.0, ORIENTATION=0.0,0.0,1.0/
&DEVC ID='Smf-A26', QUANTITY='MASS FRACTION', SPEC_ID='SOOT', XYZ=548.5,
   ↪ 413.5, 1.0, ORIENTATION=0.0,0.0,1.0/
&DEVC ID='Svf-A1', QUANTITY='VOLUME FRACTION', SPEC_ID='SOOT', XYZ=358.0,
   ↪ 727.5, 1.0, ORIENTATION=0.0,0.0,1.0/
&DEVC ID='Svf-A2', QUANTITY='VOLUME FRACTION', SPEC_ID='SOOT', XYZ=364.0,
   ↪ 721.5, 1.0, ORIENTATION=0.0,0.0,1.0/
&DEVC ID='Svf-A3', QUANTITY='VOLUME FRACTION', SPEC_ID='SOOT', XYZ=370.0,
   ↪ 715.5, 1.0, ORIENTATION=0.0,0.0,1.0/
&DEVC ID='Svf-A4', QUANTITY='VOLUME FRACTION', SPEC_ID='SOOT', XYZ=378.0,
   ↪ 707.5, 1.0, ORIENTATION=0.0,0.0,1.0/
&DEVC ID='Svf-A5', QUANTITY='VOLUME FRACTION', SPEC_ID='SOOT', XYZ=388.0,
   ↪ 702.5, 1.0, ORIENTATION=0.0,0.0,1.0/
&DEVC ID='Svf-A6', QUANTITY='VOLUME FRACTION', SPEC_ID='SOOT', XYZ=395.0,
   ↪ 699.5, 1.0, ORIENTATION=0.0,0.0,1.0/
&DEVC ID='Svf-A7', QUANTITY='VOLUME FRACTION', SPEC_ID='SOOT', XYZ=407.0,
   ↪ 694.5, 1.0, ORIENTATION=0.0,0.0,1.0/
&DEVC ID='Svf-A8', QUANTITY='VOLUME FRACTION', SPEC_ID='SOOT', XYZ=418.5,
   ↪ 689.5, 1.0, ORIENTATION=0.0,0.0,1.0/
&DEVC ID='Svf-A9', QUANTITY='VOLUME FRACTION', SPEC_ID='SOOT', XYZ=426.0,
   ↪ 680.0, 1.0, ORIENTATION=0.0,0.0,1.0/
&DEVC ID='Svf-A10', QUANTITY='VOLUME FRACTION', SPEC_ID='SOOT', XYZ=434.0,
   ↪ 671.0, 1.0, ORIENTATION=0.0,0.0,1.0/
&DEVC ID='Svf-A11', QUANTITY='VOLUME FRACTION', SPEC_ID='SOOT', XYZ=443.0,
   ↪ 661.5, 1.0, ORIENTATION=0.0,0.0,1.0/
```

```
&DEVC ID='Svf-A12', QUANTITY='VOLUME FRACTION', SPEC_ID='SOOT', XYZ=451.0,
   ↪ 652.0, 1.0, ORIENTATION=0.0,0.0,1.0/
&DEVC ID='Svf-A13', QUANTITY='VOLUME FRACTION', SPEC_ID='SOOT', XYZ
   ↪ =461.878194, 642.043194, 1.0, ORIENTATION=0.0,0.0,1.0/
&DEVC ID='Svf-A14', QUANTITY='VOLUME FRACTION', SPEC_ID='SOOT', XYZ
   ↪ =479.880188, 634.110112, 1.0, ORIENTATION=0.0,0.0,1.0/
&DEVC ID='Svf-A15', QUANTITY='VOLUME FRACTION', SPEC_ID='SOOT', XYZ=496.5,
   ↪ 626.5, 1.0, ORIENTATION=0.0,0.0,1.0/
&DEVC ID='Svf-A16', QUANTITY='VOLUME FRACTION', SPEC_ID='SOOT', XYZ=494.0682,
   ↪ 615.72672, 1.0, ORIENTATION=0.0,0.0,1.0/
&DEVC ID='Svf-A17', QUANTITY='VOLUME FRACTION', SPEC_ID='SOOT', XYZ=494.0682,
   ↪ 602.606623, 1.0, ORIENTATION=0.0,0.0,1.0/
&DEVC ID='Svf-A18', QUANTITY='VOLUME FRACTION', SPEC_ID='SOOT', XYZ
   ↪ =494.423621, 579.488649, 1.0, ORIENTATION=0.0,0.0,1.0/
&DEVC ID='Svf-A19', QUANTITY='VOLUME FRACTION', SPEC_ID='SOOT', XYZ
   ↪ =494.234368, 557.819196, 1.0, ORIENTATION=0.0,0.0,1.0/
&DEVC ID='Svf-A20', QUANTITY='VOLUME FRACTION', SPEC_ID='SOOT', XYZ=489.0,
   ↪ 532.5, 1.0, ORIENTATION=0.0,0.0,1.0/
&DEVC ID='Svf-A21', QUANTITY='VOLUME FRACTION', SPEC_ID='SOOT', XYZ=490.0,
   ↪ 508.0, 1.0, ORIENTATION=0.0,0.0,1.0/
&DEVC ID='Svf-A22', QUANTITY='VOLUME FRACTION', SPEC_ID='SOOT', XYZ=505.0,
   ↪ 485.5, 1.0, ORIENTATION=0.0,0.0,1.0/
&DEVC ID='Svf-A23', QUANTITY='VOLUME FRACTION', SPEC_ID='SOOT', XYZ=518.5,
   ↪ 464.5, 1.0, ORIENTATION=0.0,0.0,1.0/
&DEVC ID='Svf-A24', QUANTITY='VOLUME FRACTION', SPEC_ID='SOOT', XYZ=528.5,
   ↪ 447.5, 1.0, ORIENTATION=0.0,0.0,1.0/
&DEVC ID='Svf-A25', QUANTITY='VOLUME FRACTION', SPEC_ID='SOOT', XYZ
   ↪ =539.023191, 428.964324, 1.0, ORIENTATION=0.0,0.0,1.0/
&DEVC ID='Svf-A26', QUANTITY='VOLUME FRACTION', SPEC_ID='SOOT', XYZ=548.5,
   ↪ 413.5, 1.0, ORIENTATION=0.0,0.0,1.0/
&DEVC ID='COmf-A1', QUANTITY='MASS FRACTION', SPEC_ID='CARBON MONOXIDE', XYZ
   ↪ =358.0, 727.5, 1.0, ORIENTATION=0.0,0.0,1.0/
&DEVC ID='COmf-A2', QUANTITY='MASS FRACTION', SPEC_ID='CARBON MONOXIDE', XYZ
   ↪ =364.0, 721.5, 1.0, ORIENTATION=0.0,0.0,1.0/
&DEVC ID='COmf-A3', QUANTITY='MASS FRACTION', SPEC_ID='CARBON MONOXIDE', XYZ
   ↪ =370.0, 715.5, 1.0, ORIENTATION=0.0,0.0,1.0/
&DEVC ID='COmf-A4', QUANTITY='MASS FRACTION', SPEC_ID='CARBON MONOXIDE', XYZ
   ↪ =378.0, 707.5, 1.0, ORIENTATION=0.0,0.0,1.0/
&DEVC ID='COmf-A5', QUANTITY='MASS FRACTION', SPEC_ID='CARBON MONOXIDE', XYZ
   ↪ =388.0, 702.5, 1.0, ORIENTATION=0.0,0.0,1.0/
&DEVC ID='COmf-A6', QUANTITY='MASS FRACTION', SPEC_ID='CARBON MONOXIDE', XYZ
   ↪ =395.0, 699.5, 1.0, ORIENTATION=0.0,0.0,1.0/
&DEVC ID='COmf-A7', QUANTITY='MASS FRACTION', SPEC_ID='CARBON MONOXIDE', XYZ
   ↪ =407.0, 694.5, 1.0, ORIENTATION=0.0,0.0,1.0/
&DEVC ID='COmf-A8', QUANTITY='MASS FRACTION', SPEC_ID='CARBON MONOXIDE', XYZ
   ↪ =418.5, 689.5, 1.0, ORIENTATION=0.0,0.0,1.0/
&DEVC ID='COmf-A9', QUANTITY='MASS FRACTION', SPEC_ID='CARBON MONOXIDE', XYZ
   ↪ =426.0, 680.0, 1.0, ORIENTATION=0.0,0.0,1.0/
&DEVC ID='COmf-A10', QUANTITY='MASS FRACTION', SPEC_ID='CARBON MONOXIDE', XYZ
   ↪ =434.0, 671.0, 1.0, ORIENTATION=0.0,0.0,1.0/
```

```
&DEVC ID='COmf-A11', QUANTITY='MASS FRACTION', SPEC_ID='CARBON MONOXIDE', XYZ
   ↪ =443.0, 661.5, 1.0, ORIENTATION=0.0,0.0,1.0/
&DEVC ID='COmf-A12', QUANTITY='MASS FRACTION', SPEC_ID='CARBON MONOXIDE', XYZ
   ↪ =451.0, 652.0, 1.0, ORIENTATION=0.0,0.0,1.0/
&DEVC ID='COmf-A13', QUANTITY='MASS FRACTION', SPEC_ID='CARBON MONOXIDE', XYZ
   ↪ =461.878194, 642.043194, 1.0, ORIENTATION=0.0,0.0,1.0/
&DEVC ID='COmf-A14', QUANTITY='MASS FRACTION', SPEC_ID='CARBON MONOXIDE', XYZ
   ↪ =479.880188, 634.110112, 1.0, ORIENTATION=0.0,0.0,1.0/
&DEVC ID='COmf-A15', QUANTITY='MASS FRACTION', SPEC_ID='CARBON MONOXIDE', XYZ
   ↪ =496.5, 626.5, 1.0, ORIENTATION=0.0,0.0,1.0/
&DEVC ID='COmf-A16', QUANTITY='MASS FRACTION', SPEC_ID='CARBON MONOXIDE', XYZ
   ↪ =494.0682, 615.72672, 1.0, ORIENTATION=0.0,0.0,1.0/
&DEVC ID='COmf-A17', QUANTITY='MASS FRACTION', SPEC_ID='CARBON MONOXIDE', XYZ
   ↪ =494.0682, 602.606623, 1.0, ORIENTATION=0.0,0.0,1.0/
&DEVC ID='COmf-A18', QUANTITY='MASS FRACTION', SPEC_ID='CARBON MONOXIDE', XYZ
   ↪ =494.423621, 579.488649, 1.0, ORIENTATION=0.0,0.0,1.0/
&DEVC ID='COmf-A19', QUANTITY='MASS FRACTION', SPEC_ID='CARBON MONOXIDE', XYZ
   ↪ =494.234368, 557.819196, 1.0, ORIENTATION=0.0,0.0,1.0/
&DEVC ID='COmf-A20', QUANTITY='MASS FRACTION', SPEC_ID='CARBON MONOXIDE', XYZ
   ↪ =489.0, 532.5, 1.0, ORIENTATION=0.0,0.0,1.0/
&DEVC ID='COmf-A21', QUANTITY='MASS FRACTION', SPEC_ID='CARBON MONOXIDE', XYZ
   ↪ =490.0, 508.0, 1.0, ORIENTATION=0.0,0.0,1.0/
&DEVC ID='COmf-A22', QUANTITY='MASS FRACTION', SPEC_ID='CARBON MONOXIDE', XYZ
   ↪ =505.0, 485.5, 1.0, ORIENTATION=0.0,0.0,1.0/
&DEVC ID='COmf-A23', QUANTITY='MASS FRACTION', SPEC_ID='CARBON MONOXIDE', XYZ
   ↪ =518.5, 464.5, 1.0, ORIENTATION=0.0,0.0,1.0/
&DEVC ID='COmf-A24', QUANTITY='MASS FRACTION', SPEC_ID='CARBON MONOXIDE', XYZ
   ↪ =528.5, 447.5, 1.0, ORIENTATION=0.0,0.0,1.0/
&DEVC ID='COmf-A25', QUANTITY='MASS FRACTION', SPEC_ID='CARBON MONOXIDE', XYZ
   ↪ =539.023191, 428.964324, 1.0, ORIENTATION=0.0,0.0,1.0/
&DEVC ID='COmf-A26', QUANTITY='MASS FRACTION', SPEC_ID='CARBON MONOXIDE', XYZ
   ↪ =548.5, 413.5, 1.0, ORIENTATION=0.0,0.0,1.0/
&DEVC ID='COvf-A1', QUANTITY='VOLUME FRACTION', SPEC_ID='CARBON MONOXIDE', XYZ
   ↪ =358.0, 727.5, 1.0, ORIENTATION=0.0,0.0,1.0/
&DEVC ID='COvf-A2', QUANTITY='VOLUME FRACTION', SPEC_ID='CARBON MONOXIDE', XYZ
   ↪ =364.0, 721.5, 1.0, ORIENTATION=0.0,0.0,1.0/
&DEVC ID='COvf-A3', QUANTITY='VOLUME FRACTION', SPEC_ID='CARBON MONOXIDE', XYZ
   ↪ =370.0, 715.5, 1.0, ORIENTATION=0.0,0.0,1.0/
&DEVC ID='COvf-A4', QUANTITY='VOLUME FRACTION', SPEC_ID='CARBON MONOXIDE', XYZ
   ↪ =378.0, 707.5, 1.0, ORIENTATION=0.0,0.0,1.0/
&DEVC ID='COvf-A5', QUANTITY='VOLUME FRACTION', SPEC_ID='CARBON MONOXIDE', XYZ
   ↪ =388.0, 702.5, 1.0, ORIENTATION=0.0,0.0,1.0/
&DEVC ID='COvf-A6', QUANTITY='VOLUME FRACTION', SPEC_ID='CARBON MONOXIDE', XYZ
   ↪ =395.0, 699.5, 1.0, ORIENTATION=0.0,0.0,1.0/
&DEVC ID='COvf-A7', QUANTITY='VOLUME FRACTION', SPEC_ID='CARBON MONOXIDE', XYZ
   ↪ =407.0, 694.5, 1.0, ORIENTATION=0.0,0.0,1.0/
&DEVC ID='COvf-A8', QUANTITY='VOLUME FRACTION', SPEC_ID='CARBON MONOXIDE', XYZ
   ↪ =418.5, 689.5, 1.0, ORIENTATION=0.0,0.0,1.0/
&DEVC ID='COvf-A9', QUANTITY='VOLUME FRACTION', SPEC_ID='CARBON MONOXIDE', XYZ
   ↪ =426.0, 680.0, 1.0, ORIENTATION=0.0,0.0,1.0/
```

```
&DEVC ID='COvf-A10', QUANTITY='VOLUME FRACTION', SPEC_ID='CARBON MONOXIDE',
   ↪ XYZ=434.0, 671.0, 1.0, ORIENTATION=0.0,0.0,1.0/
&DEVC ID='COvf-A11', QUANTITY='VOLUME FRACTION', SPEC_ID='CARBON MONOXIDE',
   ↪ XYZ=443.0, 661.5, 1.0, ORIENTATION=0.0,0.0,1.0/
&DEVC ID='COvf-A12', QUANTITY='VOLUME FRACTION', SPEC_ID='CARBON MONOXIDE',
   ↪ XYZ=451.0, 652.0, 1.0, ORIENTATION=0.0,0.0,1.0/
&DEVC ID='COvf-A13', QUANTITY='VOLUME FRACTION', SPEC_ID='CARBON MONOXIDE',
   ↪ XYZ=461.878194, 642.043194, 1.0, ORIENTATION=0.0,0.0,1.0/
&DEVC ID='COvf-A14', QUANTITY='VOLUME FRACTION', SPEC_ID='CARBON MONOXIDE',
   ↪ XYZ=479.880188, 634.110112, 1.0, ORIENTATION=0.0,0.0,1.0/
&DEVC ID='COvf-A15', QUANTITY='VOLUME FRACTION', SPEC_ID='CARBON MONOXIDE',
   ↪ XYZ=496.5, 626.5, 1.0, ORIENTATION=0.0,0.0,1.0/
&DEVC ID='COvf-A16', QUANTITY='VOLUME FRACTION', SPEC_ID='CARBON MONOXIDE',
   ↪ XYZ=494.0682, 615.72672, 1.0, ORIENTATION=0.0,0.0,1.0/
&DEVC ID='COvf-A17', QUANTITY='VOLUME FRACTION', SPEC_ID='CARBON MONOXIDE',
   ↪ XYZ=494.0682, 602.606623, 1.0, ORIENTATION=0.0,0.0,1.0/
&DEVC ID='COvf-A18', QUANTITY='VOLUME FRACTION', SPEC_ID='CARBON MONOXIDE',
   ↪ XYZ=494.423621, 579.488649, 1.0, ORIENTATION=0.0,0.0,1.0/
&DEVC ID='COvf-A19', QUANTITY='VOLUME FRACTION', SPEC_ID='CARBON MONOXIDE',
   ↪ XYZ=494.234368, 557.819196, 1.0, ORIENTATION=0.0,0.0,1.0/
&DEVC ID='COvf-A20', QUANTITY='VOLUME FRACTION', SPEC_ID='CARBON MONOXIDE',
   ↪ XYZ=489.0, 532.5, 1.0, ORIENTATION=0.0,0.0,1.0/
&DEVC ID='COvf-A21', QUANTITY='VOLUME FRACTION', SPEC_ID='CARBON MONOXIDE',
   ↪ XYZ=490.0, 508.0, 1.0, ORIENTATION=0.0,0.0,1.0/
&DEVC ID='COvf-A22', QUANTITY='VOLUME FRACTION', SPEC_ID='CARBON MONOXIDE',
   ↪ XYZ=505.0, 485.5, 1.0, ORIENTATION=0.0,0.0,1.0/
&DEVC ID='COvf-A23', QUANTITY='VOLUME FRACTION', SPEC_ID='CARBON MONOXIDE',
   ↪ XYZ=518.5, 464.5, 1.0, ORIENTATION=0.0,0.0,1.0/
&DEVC ID='COvf-A24', QUANTITY='VOLUME FRACTION', SPEC_ID='CARBON MONOXIDE',
   ↪ XYZ=528.5, 447.5, 1.0, ORIENTATION=0.0,0.0,1.0/
&DEVC ID='COvf-A25', QUANTITY='VOLUME FRACTION', SPEC_ID='CARBON MONOXIDE',
   ↪ XYZ=539.023191, 428.964324, 1.0, ORIENTATION=0.0,0.0,1.0/
&DEVC ID='COvf-A26', QUANTITY='VOLUME FRACTION', SPEC_ID='CARBON MONOXIDE',
   ↪ XYZ=548.5, 413.5, 1.0, ORIENTATION=0.0,0.0,1.0/
&DEVC ID='CO2mf-A1', QUANTITY='MASS FRACTION', SPEC_ID='CARBON DIOXIDE', XYZ
   ↪ =358.0, 727.5, 1.0, ORIENTATION=0.0,0.0,1.0/
&DEVC ID='CO2mf-A2', QUANTITY='MASS FRACTION', SPEC_ID='CARBON DIOXIDE', XYZ
   ↪ =364.0, 721.5, 1.0, ORIENTATION=0.0,0.0,1.0/
&DEVC ID='CO2mf-A3', QUANTITY='MASS FRACTION', SPEC_ID='CARBON DIOXIDE', XYZ
   ↪ =370.0, 715.5, 1.0, ORIENTATION=0.0,0.0,1.0/
&DEVC ID='CO2mf-A4', QUANTITY='MASS FRACTION', SPEC_ID='CARBON DIOXIDE', XYZ
   ↪ =378.0, 707.5, 1.0, ORIENTATION=0.0,0.0,1.0/
&DEVC ID='CO2mf-A5', QUANTITY='MASS FRACTION', SPEC_ID='CARBON DIOXIDE', XYZ
   ↪ =388.0, 702.5, 1.0, ORIENTATION=0.0,0.0,1.0/
&DEVC ID='CO2mf-A6', QUANTITY='MASS FRACTION', SPEC_ID='CARBON DIOXIDE', XYZ
   ↪ =395.0, 699.5, 1.0, ORIENTATION=0.0,0.0,1.0/
&DEVC ID='CO2mf-A7', QUANTITY='MASS FRACTION', SPEC_ID='CARBON DIOXIDE', XYZ
   ↪ =407.0, 694.5, 1.0, ORIENTATION=0.0,0.0,1.0/
&DEVC ID='CO2mf-A8', QUANTITY='MASS FRACTION', SPEC_ID='CARBON DIOXIDE', XYZ
   ↪ =418.5, 689.5, 1.0, ORIENTATION=0.0,0.0,1.0/
```

```
&DEVC ID='CO2mf-A9', QUANTITY='MASS FRACTION', SPEC_ID='CARBON DIOXIDE', XYZ
   ↪ =426.0, 680.0, 1.0, ORIENTATION=0.0,0.0,1.0/
&DEVC ID='CO2mf-A10', QUANTITY='MASS FRACTION', SPEC_ID='CARBON DIOXIDE', XYZ
   ↪ =434.0, 671.0, 1.0, ORIENTATION=0.0,0.0,1.0/
&DEVC ID='CO2mf-A11', QUANTITY='MASS FRACTION', SPEC_ID='CARBON DIOXIDE', XYZ
   ↪ =443.0, 661.5, 1.0, ORIENTATION=0.0,0.0,1.0/
&DEVC ID='CO2mf-A12', QUANTITY='MASS FRACTION', SPEC_ID='CARBON DIOXIDE', XYZ
   ↪ =451.0, 652.0, 1.0, ORIENTATION=0.0,0.0,1.0/
&DEVC ID='CO2mf-A13', QUANTITY='MASS FRACTION', SPEC_ID='CARBON DIOXIDE', XYZ
   ↪ =461.878194, 642.043194, 1.0, ORIENTATION=0.0,0.0,1.0/
&DEVC ID='CO2mf-A14', QUANTITY='MASS FRACTION', SPEC_ID='CARBON DIOXIDE', XYZ
   ↪ =479.880188, 634.110112, 1.0, ORIENTATION=0.0,0.0,1.0/
&DEVC ID='CO2mf-A15', QUANTITY='MASS FRACTION', SPEC_ID='CARBON DIOXIDE', XYZ
   ↪ =496.5, 626.5, 1.0, ORIENTATION=0.0,0.0,1.0/
&DEVC ID='CO2mf-A16', QUANTITY='MASS FRACTION', SPEC_ID='CARBON DIOXIDE', XYZ
   ↪ =494.0682, 615.72672, 1.0, ORIENTATION=0.0,0.0,1.0/
&DEVC ID='CO2mf-A17', QUANTITY='MASS FRACTION', SPEC_ID='CARBON DIOXIDE', XYZ
   ↪ =494.0682, 602.606623, 1.0, ORIENTATION=0.0,0.0,1.0/
&DEVC ID='CO2mf-A18', QUANTITY='MASS FRACTION', SPEC_ID='CARBON DIOXIDE', XYZ
   ↪ =494.423621, 579.488649, 1.0, ORIENTATION=0.0,0.0,1.0/
&DEVC ID='CO2mf-A19', QUANTITY='MASS FRACTION', SPEC_ID='CARBON DIOXIDE', XYZ
   ↪ =494.234368, 557.819196, 1.0, ORIENTATION=0.0,0.0,1.0/
&DEVC ID='CO2mf-A20', QUANTITY='MASS FRACTION', SPEC_ID='CARBON DIOXIDE', XYZ
   ↪ =489.0, 532.5, 1.0, ORIENTATION=0.0,0.0,1.0/
&DEVC ID='CO2mf-A21', QUANTITY='MASS FRACTION', SPEC_ID='CARBON DIOXIDE', XYZ
   ↪ =490.0, 508.0, 1.0, ORIENTATION=0.0,0.0,1.0/
&DEVC ID='CO2mf-A22', QUANTITY='MASS FRACTION', SPEC_ID='CARBON DIOXIDE', XYZ
   ↪ =505.0, 485.5, 1.0, ORIENTATION=0.0,0.0,1.0/
&DEVC ID='CO2mf-A23', QUANTITY='MASS FRACTION', SPEC_ID='CARBON DIOXIDE', XYZ
   ↪ =518.5, 464.5, 1.0, ORIENTATION=0.0,0.0,1.0/
&DEVC ID='CO2mf-A24', QUANTITY='MASS FRACTION', SPEC_ID='CARBON DIOXIDE', XYZ
   ↪ =528.5, 447.5, 1.0, ORIENTATION=0.0,0.0,1.0/
&DEVC ID='CO2mf-A25', QUANTITY='MASS FRACTION', SPEC_ID='CARBON DIOXIDE', XYZ
   ↪ =539.023191, 428.964324, 1.0, ORIENTATION=0.0,0.0,1.0/
&DEVC ID='CO2mf-A26', QUANTITY='MASS FRACTION', SPEC_ID='CARBON DIOXIDE', XYZ
   ↪ =548.5, 413.5, 1.0, ORIENTATION=0.0,0.0,1.0/
&DEVC ID='CO2vf-A1', QUANTITY='VOLUME FRACTION', SPEC_ID='CARBON DIOXIDE', XYZ
   ↪ =358.0, 727.5, 1.0, ORIENTATION=0.0,0.0,1.0/
&DEVC ID='CO2vf-A2', QUANTITY='VOLUME FRACTION', SPEC_ID='CARBON DIOXIDE', XYZ
   ↪ =364.0, 721.5, 1.0, ORIENTATION=0.0,0.0,1.0/
&DEVC ID='CO2vf-A3', QUANTITY='VOLUME FRACTION', SPEC_ID='CARBON DIOXIDE', XYZ
   ↪ =370.0, 715.5, 1.0, ORIENTATION=0.0,0.0,1.0/
&DEVC ID='CO2vf-A4', QUANTITY='VOLUME FRACTION', SPEC_ID='CARBON DIOXIDE', XYZ
   ↪ =378.0, 707.5, 1.0, ORIENTATION=0.0,0.0,1.0/
&DEVC ID='CO2vf-A5', QUANTITY='VOLUME FRACTION', SPEC_ID='CARBON DIOXIDE', XYZ
   ↪ =388.0, 702.5, 1.0, ORIENTATION=0.0,0.0,1.0/
&DEVC ID='CO2vf-A6', QUANTITY='VOLUME FRACTION', SPEC_ID='CARBON DIOXIDE', XYZ
   ↪ =395.0, 699.5, 1.0, ORIENTATION=0.0,0.0,1.0/
&DEVC ID='CO2vf-A7', QUANTITY='VOLUME FRACTION', SPEC_ID='CARBON DIOXIDE', XYZ
   ↪ =407.0, 694.5, 1.0, ORIENTATION=0.0,0.0,1.0/
```

```
&DEVC ID='CO2vf-A8', QUANTITY='VOLUME FRACTION', SPEC_ID='CARBON DIOXIDE', XYZ
   ↪ =418.5, 689.5, 1.0, ORIENTATION=0.0,0.0,1.0/
&DEVC ID='CO2vf-A9', QUANTITY='VOLUME FRACTION', SPEC_ID='CARBON DIOXIDE', XYZ
   ↪ =426.0, 680.0, 1.0, ORIENTATION=0.0,0.0,1.0/
&DEVC ID='CO2vf-A10', QUANTITY='VOLUME FRACTION', SPEC_ID='CARBON DIOXIDE',
   ↪ XYZ=434.0, 671.0, 1.0, ORIENTATION=0.0,0.0,1.0/
&DEVC ID='CO2vf-A11', QUANTITY='VOLUME FRACTION', SPEC_ID='CARBON DIOXIDE',
   ↪ XYZ=443.0, 661.5, 1.0, ORIENTATION=0.0,0.0,1.0/
&DEVC ID='CO2vf-A12', QUANTITY='VOLUME FRACTION', SPEC_ID='CARBON DIOXIDE',
   ↪ XYZ=451.0, 652.0, 1.0, ORIENTATION=0.0,0.0,1.0/
&DEVC ID='CO2vf-A13', QUANTITY='VOLUME FRACTION', SPEC_ID='CARBON DIOXIDE',
   ↪ XYZ=461.878194, 642.043194, 1.0, ORIENTATION=0.0,0.0,1.0/
&DEVC ID='CO2vf-A14', QUANTITY='VOLUME FRACTION', SPEC_ID='CARBON DIOXIDE',
   ↪ XYZ=479.880188, 634.110112, 1.0, ORIENTATION=0.0,0.0,1.0/
&DEVC ID='CO2vf-A15', QUANTITY='VOLUME FRACTION', SPEC_ID='CARBON DIOXIDE',
   ↪ XYZ=496.5, 626.5, 1.0, ORIENTATION=0.0,0.0,1.0/
&DEVC ID='CO2vf-A16', QUANTITY='VOLUME FRACTION', SPEC_ID='CARBON DIOXIDE',
   ↪ XYZ=494.0682, 615.72672, 1.0, ORIENTATION=0.0,0.0,1.0/
&DEVC ID='CO2vf-A17', QUANTITY='VOLUME FRACTION', SPEC_ID='CARBON DIOXIDE',
   ↪ XYZ=494.0682, 602.606623, 1.0, ORIENTATION=0.0,0.0,1.0/
&DEVC ID='CO2vf-A18', QUANTITY='VOLUME FRACTION', SPEC_ID='CARBON DIOXIDE',
   ↪ XYZ=494.423621, 579.488649, 1.0, ORIENTATION=0.0,0.0,1.0/
&DEVC ID='CO2vf-A19', QUANTITY='VOLUME FRACTION', SPEC_ID='CARBON DIOXIDE',
   ↪ XYZ=494.234368, 557.819196, 1.0, ORIENTATION=0.0,0.0,1.0/
&DEVC ID='CO2vf-A20', QUANTITY='VOLUME FRACTION', SPEC_ID='CARBON DIOXIDE',
   ↪ XYZ=489.0, 532.5, 1.0, ORIENTATION=0.0,0.0,1.0/
&DEVC ID='CO2vf-A21', QUANTITY='VOLUME FRACTION', SPEC_ID='CARBON DIOXIDE',
   ↪ XYZ=490.0, 508.0, 1.0, ORIENTATION=0.0,0.0,1.0/
&DEVC ID='CO2vf-A22', QUANTITY='VOLUME FRACTION', SPEC_ID='CARBON DIOXIDE',
   ↪ XYZ=505.0, 485.5, 1.0, ORIENTATION=0.0,0.0,1.0/
&DEVC ID='CO2vf-A23', QUANTITY='VOLUME FRACTION', SPEC_ID='CARBON DIOXIDE',
   ↪ XYZ=518.5, 464.5, 1.0, ORIENTATION=0.0,0.0,1.0/
&DEVC ID='CO2vf-A24', QUANTITY='VOLUME FRACTION', SPEC_ID='CARBON DIOXIDE',
   ↪ XYZ=528.5, 447.5, 1.0, ORIENTATION=0.0,0.0,1.0/
&DEVC ID='CO2vf-A25', QUANTITY='VOLUME FRACTION', SPEC_ID='CARBON DIOXIDE',
   ↪ XYZ=539.023191, 428.964324, 1.0, ORIENTATION=0.0,0.0,1.0/
&DEVC ID='CO2vf-A26', QUANTITY='VOLUME FRACTION', SPEC_ID='CARBON DIOXIDE',
   ↪ XYZ=548.5, 413.5, 1.0, ORIENTATION=0.0,0.0,1.0/
&DEVC ID='RHF-A1', QUANTITY='RADIATIVE HEAT FLUX GAS', XYZ=358.0, 727.5, 1.0,
   ↪ ORIENTATION=0.0,0.0,1.0/
&DEVC ID='RHF-A2', QUANTITY='RADIATIVE HEAT FLUX GAS', XYZ=364.0, 721.5, 1.0,
   ↪ ORIENTATION=0.0,0.0,1.0/
&DEVC ID='RHF-A3', QUANTITY='RADIATIVE HEAT FLUX GAS', XYZ=370.0, 715.5, 1.0,
   ↪ ORIENTATION=0.0,0.0,1.0/
&DEVC ID='RHF-A4', QUANTITY='RADIATIVE HEAT FLUX GAS', XYZ=378.0, 707.5, 1.0,
   ↪ ORIENTATION=0.0,0.0,1.0/
&DEVC ID='RHF-A5', QUANTITY='RADIATIVE HEAT FLUX GAS', XYZ=388.0, 702.5, 1.0,
   ↪ ORIENTATION=0.0,0.0,1.0/
&DEVC ID='RHF-A6', QUANTITY='RADIATIVE HEAT FLUX GAS', XYZ=395.0, 699.5, 1.0,
   ↪ ORIENTATION=0.0,0.0,1.0/
```

```
&DEVC ID='RHF-A7', QUANTITY='RADIATIVE HEAT FLUX GAS', XYZ=407.0, 694.5, 1.0,
   ↪ ORIENTATION=0.0,0.0,1.0/
&DEVC ID='RHF-A8', QUANTITY='RADIATIVE HEAT FLUX GAS', XYZ=418.5, 689.5, 1.0,
   ↪ ORIENTATION=0.0,0.0,1.0/
&DEVC ID='RHF-A9', QUANTITY='RADIATIVE HEAT FLUX GAS', XYZ=426.0, 680.0, 1.0,
   ↪ ORIENTATION=0.0,0.0,1.0/
&DEVC ID='RHF-A10', QUANTITY='RADIATIVE HEAT FLUX GAS', XYZ=434.0, 671.0, 1.0,
   ↪  ORIENTATION=0.0,0.0,1.0/
&DEVC ID='RHF-A11', QUANTITY='RADIATIVE HEAT FLUX GAS', XYZ=443.0, 661.5, 1.0,
   ↪  ORIENTATION=0.0,0.0,1.0/
&DEVC ID='RHF-A12', QUANTITY='RADIATIVE HEAT FLUX GAS', XYZ=451.0, 652.0, 1.0,
   ↪  ORIENTATION=0.0,0.0,1.0/
&DEVC ID='RHF-A13', QUANTITY='RADIATIVE HEAT FLUX GAS', XYZ=461.878194,
   ↪ 642.043194, 1.0, ORIENTATION=0.0,0.0,1.0/
&DEVC ID='RHF-A14', QUANTITY='RADIATIVE HEAT FLUX GAS', XYZ=479.880188,
   ↪ 634.110112, 1.0, ORIENTATION=0.0,0.0,1.0/
&DEVC ID='RHF-A15', QUANTITY='RADIATIVE HEAT FLUX GAS', XYZ=496.5, 626.5, 1.0,
   ↪  ORIENTATION=0.0,0.0,1.0/
&DEVC ID='RHF-A16', QUANTITY='RADIATIVE HEAT FLUX GAS', XYZ=494.0682,
   ↪ 615.72672, 1.0, ORIENTATION=0.0,0.0,1.0/
&DEVC ID='RHF-A17', QUANTITY='RADIATIVE HEAT FLUX GAS', XYZ=494.0682,
   ↪ 602.606623, 1.0, ORIENTATION=0.0,0.0,1.0/
&DEVC ID='RHF-A18', QUANTITY='RADIATIVE HEAT FLUX GAS', XYZ=494.423621,
   ↪ 579.488649, 1.0, ORIENTATION=0.0,0.0,1.0/
&DEVC ID='RHF-A19', QUANTITY='RADIATIVE HEAT FLUX GAS', XYZ=494.234368,
   ↪ 557.819196, 1.0, ORIENTATION=0.0,0.0,1.0/
&DEVC ID='RHF-A20', QUANTITY='RADIATIVE HEAT FLUX GAS', XYZ=489.0, 532.5, 1.0,
   ↪  ORIENTATION=0.0,0.0,1.0/
&DEVC ID='RHF-A21', QUANTITY='RADIATIVE HEAT FLUX GAS', XYZ=490.0, 508.0, 1.0,
   ↪  ORIENTATION=0.0,0.0,1.0/
&DEVC ID='RHF-A22', QUANTITY='RADIATIVE HEAT FLUX GAS', XYZ=505.0, 485.5, 1.0,
   ↪  ORIENTATION=0.0,0.0,1.0/
&DEVC ID='RHF-A23', QUANTITY='RADIATIVE HEAT FLUX GAS', XYZ=518.5, 464.5, 1.0,
   ↪  ORIENTATION=0.0,0.0,1.0/
&DEVC ID='RHF-A24', QUANTITY='RADIATIVE HEAT FLUX GAS', XYZ=528.5, 447.5, 1.0,
   ↪  ORIENTATION=0.0,0.0,1.0/
&DEVC ID='RHF-A25', QUANTITY='RADIATIVE HEAT FLUX GAS', XYZ=539.023191,
   ↪ 428.964324, 1.0, ORIENTATION=0.0,0.0,1.0/
&DEVC ID='RHF-A26', QUANTITY='RADIATIVE HEAT FLUX GAS', XYZ=548.5, 413.5, 1.0,
   ↪  ORIENTATION=0.0,0.0,1.0/
&DEVC ID='Vis-A1', QUANTITY='VISIBILITY', XYZ=358.0, 727.5, 1.0, ORIENTATION
   ↪ =0.0,0.0,1.0/
&DEVC ID='Vis-A2', QUANTITY='VISIBILITY', XYZ=364.0, 721.5, 1.0, ORIENTATION
   ↪ =0.0,0.0,1.0/
&DEVC ID='Vis-A3', QUANTITY='VISIBILITY', XYZ=370.0, 715.5, 1.0, ORIENTATION
   ↪ =0.0,0.0,1.0/
&DEVC ID='Vis-A4', QUANTITY='VISIBILITY', XYZ=378.0, 707.5, 1.0, ORIENTATION
   ↪ =0.0,0.0,1.0/
&DEVC ID='Vis-A5', QUANTITY='VISIBILITY', XYZ=388.0, 702.5, 1.0, ORIENTATION
   ↪ =0.0,0.0,1.0/
```

```
&DEVC ID='Vis-A6', QUANTITY='VISIBILITY', XYZ=395.0, 699.5, 1.0, ORIENTATION
   ↪ =0.0,0.0,1.0/
&DEVC ID='Vis-A7', QUANTITY='VISIBILITY', XYZ=407.0, 694.5, 1.0, ORIENTATION
   ↪ =0.0,0.0,1.0/
&DEVC ID='Vis-A8', QUANTITY='VISIBILITY', XYZ=418.5, 689.5, 1.0, ORIENTATION
   ↪ =0.0,0.0,1.0/
&DEVC ID='Vis-A9', QUANTITY='VISIBILITY', XYZ=426.0, 680.0, 1.0, ORIENTATION
   ↪ =0.0,0.0,1.0/
&DEVC ID='Vis-A10', QUANTITY='VISIBILITY', XYZ=434.0, 671.0, 1.0, ORIENTATION
   ↪ =0.0,0.0,1.0/
&DEVC ID='Vis-A11', QUANTITY='VISIBILITY', XYZ=443.0, 661.5, 1.0, ORIENTATION
   ↪ =0.0,0.0,1.0/
&DEVC ID='Vis-A12', QUANTITY='VISIBILITY', XYZ=451.0, 652.0, 1.0, ORIENTATION
   ↪ =0.0,0.0,1.0/
&DEVC ID='Vis-A13', QUANTITY='VISIBILITY', XYZ=461.878194, 642.043194, 1.0,
   ↪ ORIENTATION=0.0,0.0,1.0/
&DEVC ID='Vis-A14', QUANTITY='VISIBILITY', XYZ=479.880188, 634.110112, 1.0,
   ↪ ORIENTATION=0.0,0.0,1.0/
&DEVC ID='Vis-A15', QUANTITY='VISIBILITY', XYZ=496.5, 626.5, 1.0, ORIENTATION
   ↪ =0.0,0.0,1.0/
&DEVC ID='Vis-A16', QUANTITY='VISIBILITY', XYZ=494.0682, 615.72672, 1.0,
   ↪ ORIENTATION=0.0,0.0,1.0/
&DEVC ID='Vis-A17', QUANTITY='VISIBILITY', XYZ=494.0682, 602.606623, 1.0,
   ↪ ORIENTATION=0.0,0.0,1.0/
&DEVC ID='Vis-A18', QUANTITY='VISIBILITY', XYZ=494.423621, 579.488649, 1.0,
   ↪ ORIENTATION=0.0,0.0,1.0/
&DEVC ID='Vis-A19', QUANTITY='VISIBILITY', XYZ=494.234368, 557.819196, 1.0,
   ↪ ORIENTATION=0.0,0.0,1.0/
&DEVC ID='Vis-A20', QUANTITY='VISIBILITY', XYZ=489.0, 532.5, 1.0, ORIENTATION
   ↪ =0.0,0.0,1.0/
&DEVC ID='Vis-A21', QUANTITY='VISIBILITY', XYZ=490.0, 508.0, 1.0, ORIENTATION
   ↪ =0.0,0.0,1.0/
&DEVC ID='Vis-A22', QUANTITY='VISIBILITY', XYZ=505.0, 485.5, 1.0, ORIENTATION
   ↪ =0.0,0.0,1.0/
&DEVC ID='Vis-A23', QUANTITY='VISIBILITY', XYZ=518.5, 464.5, 1.0, ORIENTATION
   ↪ =0.0,0.0,1.0/
&DEVC ID='Vis-A24', QUANTITY='VISIBILITY', XYZ=528.5, 447.5, 1.0, ORIENTATION
   ↪ =0.0,0.0,1.0/
&DEVC ID='Vis-A25', QUANTITY='VISIBILITY', XYZ=539.023191, 428.964324, 1.0,
   ↪ ORIENTATION=0.0,0.0,1.0/
&DEVC ID='Vis-A26', QUANTITY='VISIBILITY', XYZ=548.5, 413.5, 1.0, ORIENTATION
   ↪ =0.0,0.0,1.0/
&DEVC ID='FED-A1', QUANTITY='FED', XYZ=358.0, 727.5, 1.0, ORIENTATION
   ↪ =0.0,0.0,1.0/
&DEVC ID='FED-A2', QUANTITY='FED', XYZ=364.0, 721.5, 1.0, ORIENTATION
   ↪ =0.0,0.0,1.0/
&DEVC ID='FED-A3', QUANTITY='FED', XYZ=370.0, 715.5, 1.0, ORIENTATION
   ↪ =0.0,0.0,1.0/
&DEVC ID='FED-A4', QUANTITY='FED', XYZ=378.0, 707.5, 1.0, ORIENTATION
   ↪ =0.0,0.0,1.0/
```

```
&DEVC ID='FED-A5', QUANTITY='FED', XYZ=388.0, 702.5, 1.0, ORIENTATION
   ↪ =0.0,0.0,1.0/
&DEVC ID='FED-A6', QUANTITY='FED', XYZ=395.0, 699.5, 1.0, ORIENTATION
   ↪ =0.0,0.0,1.0/
&DEVC ID='FED-A7', QUANTITY='FED', XYZ=407.0, 694.5, 1.0, ORIENTATION
   ↪ =0.0,0.0,1.0/
&DEVC ID='FED-A8', QUANTITY='FED', XYZ=418.5, 689.5, 1.0, ORIENTATION
   ↪ =0.0,0.0,1.0/
&DEVC ID='FED-A9', QUANTITY='FED', XYZ=426.0, 680.0, 1.0, ORIENTATION
   ↪ =0.0,0.0,1.0/
&DEVC ID='FED-A10', QUANTITY='FED', XYZ=434.0, 671.0, 1.0, ORIENTATION
   ↪ =0.0,0.0,1.0/
&DEVC ID='FED-A11', QUANTITY='FED', XYZ=443.0, 661.5, 1.0, ORIENTATION
   ↪ =0.0,0.0,1.0/
&DEVC ID='FED-A12', QUANTITY='FED', XYZ=451.0, 652.0, 1.0, ORIENTATION
   ↪ =0.0,0.0,1.0/
&DEVC ID='FED-A13', QUANTITY='FED', XYZ=461.878194, 642.043194, 1.0,
   ↪ ORIENTATION=0.0,0.0,1.0/
&DEVC ID='FED-A14', QUANTITY='FED', XYZ=479.880188, 634.110112, 1.0,
   ↪ ORIENTATION=0.0,0.0,1.0/
&DEVC ID='FED-A15', QUANTITY='FED', XYZ=496.5, 626.5, 1.0, ORIENTATION
   ↪ =0.0,0.0,1.0/
&DEVC ID='FED-A16', QUANTITY='FED', XYZ=494.0682, 615.72672, 1.0, ORIENTATION
   ↪ =0.0,0.0,1.0/
&DEVC ID='FED-A17', QUANTITY='FED', XYZ=494.0682, 602.606623, 1.0, ORIENTATION
   ↪ =0.0,0.0,1.0/
&DEVC ID='FED-A18', QUANTITY='FED', XYZ=494.423621, 579.488649, 1.0,
   ↪ ORIENTATION=0.0,0.0,1.0/
&DEVC ID='FED-A19', QUANTITY='FED', XYZ=494.234368, 557.819196, 1.0,
   ↪ ORIENTATION=0.0,0.0,1.0/
&DEVC ID='FED-A20', QUANTITY='FED', XYZ=489.0, 532.5, 1.0, ORIENTATION
   ↪ =0.0,0.0,1.0/
&DEVC ID='FED-A21', QUANTITY='FED', XYZ=490.0, 508.0, 1.0, ORIENTATION
   ↪ =0.0,0.0,1.0/
&DEVC ID='FED-A22', QUANTITY='FED', XYZ=505.0, 485.5, 1.0, ORIENTATION
   ↪ =0.0,0.0,1.0/
&DEVC ID='FED-A23', QUANTITY='FED', XYZ=518.5, 464.5, 1.0, ORIENTATION
   ↪ =0.0,0.0,1.0/
&DEVC ID='FED-A24', QUANTITY='FED', XYZ=528.5, 447.5, 1.0, ORIENTATION
   ↪ =0.0,0.0,1.0/
&DEVC ID='FED-A25', QUANTITY='FED', XYZ=539.023191, 428.964324, 1.0,
   ↪ ORIENTATION=0.0,0.0,1.0/
&DEVC ID='FED-A26', QUANTITY='FED', XYZ=548.5, 413.5, 1.0, ORIENTATION
   ↪ =0.0,0.0,1.0/


&TAIL /
```